Abstract

Ceramic bone cements, mainly calcium phosphate based, represent an alternative to the polymeric cements used in Vertebroplasty. Unfortunately, calcium phosphate bone cements, which are made from mixing solid powder and liquid phase, can be affected by press-filtering. This favours liquid phase migration out of the syringe during the cement injection and, consequently, the liquid-to-powder ratio of the remaining cement in the syringe increases. This finally led to unavailable higher injection extrusion pressure.

The objectives of the present project were: a) to review the state of the art; and b) to compute the problem of press-filtering. Two models have been implemented. The first, in MATLAB®, was treated as a convection-diffusion problem adapted to the flow of liquid phase in the cement and solved by finite volume differences. The second, in COMSOL®, was an Euler-Euler particle/fluid flow approach. The project ends with a survey of possible methods that could be used in the laboratory to obtain the different coefficients which are needed for the computation; other suitable tests to investigate the cement behaviour during its extrusion are also referred.

Introduction

Vertebral compression fracture (VCF), mainly caused by osteoporosis for old person and by extreme activities for younger person is a worldwide problem causing pain, loss of quality of life and dependence. As a treatment, Vertebroplasty (VP) and Kyphoplasty (KP) are relatively modern minimally invasive technique consisting in the injection of polymeric cement in the damaged vertebra.

The use of these techniques present several advantages, the main being the ability for the patient to be independent and the total or partial removal of the pain. However recent studies and review [1-2] have reported that polymeric cement despites their advantages present several inconveniences such as highly exothermic polymerization (necrosis of the surrounding tissues), monomer residues (Toxicity), high stiffness after polymerization causing fracture of the adjacent vertebrae. Moreover, polymeric cements lack of bone-tissue regeneration capacity and in-vivo bioactivity make them a bad option for the treatment of burst fractures for young patient.

On the other hand ceramic bone cement (mostly apatitic calcium phosphate cements) are bioactive, non-toxic, can be formulated to increase osteointegration and bone-tissue regeneration, are not exothermic while hardening and once hardened are less stiff than polymeric cements.

Based on the hypothesis that ceramic cements could be an alternative or a better option to the use of polymeric cements in Vertebroplasty and Kyphoplasty many papers have been

published in the last years on the improvement of such kind of injectable biocements. Another key feature for the development of this generation of bone substitutes is related to their injectability. Meaning their ability to be injected (extrusion force needed) but also the ability of the cement to remain homogeneous during its injection. Indeed one of the main reported problem with ceramic biocements as material for VP and KP is their injectability, it has been reported [3-4], that while injecting the cement several undesired phenomena could occur including, drying out of the paste, cyclic dewatering, stress build-up, droplet formation at die exit, flow blockage. All of these phenomenon results in poor injectability of ceramic cement paste and a special effort is needed to understand the parameters to take into account in the injection process.

Thus, the specific objectives of the present work were formulated to understand the physical phenomena responsible for this liquid phase migration, propose and associated theoretical background describing it (Chapter I), try to model the phenomena using COMSOL© and MATLAB©(Chapter II), finally chapter III present a survey of possible methods that could be used in the laboratory to obtain the different coefficients which are needed for the computation; other suitable tests to investigate the cement behaviour during its extrusion are also referred.

[1] "New developments in calcium phosphate bone cements: Approaching spinal applications", Maria Daniela Vlad, PhD Thesis, UPC, 2008

[2] "Calcium phosphates and ceramic bone cements versus acrylic cements", Driessens F.C.M, Fernandez E, Ginebra M.P, Boltong M.G, Planell J.A, Anales de quimica, vol 93, 1997

[3]"Extrusion of pastes with a piston extruder for the determination of the local solid and fluid concentration, the local porosity and saturation and displacement profiles by means of NMR imaging",J. Götz, W. Kreibich, M.Peciar, Rheol Acta , p134-143, 2002

[4]"Mortar physical properties evolution in extrusion flow", A. Perrot, C. Lanos, Y. Melinge, P. Estellé,, Rheol. Acta 46, 8 , p1065-1073, 2007

1. Literature study on liquid phase migration and jamming phenomenon

1.1. Description of the injection stage Vertebroplasty and Kyphoplasty

Vertebroplasty and Kyphoplasty are minimally invasive techniques treating vertebrae that have experienced compression fracture by injecting bone cement in it. Both aim to stop pain and to stabilize the spine. The two methods are pretty similar, while for Vertebroplasty the bone cement is injected into the broken areas of bones directly, for Kyphoplasty a balloon is inserted in the vertebral body and gently inflated to restore shape and height of the fractured bone, balloon is then removed and the cement is injected. Since the only difference between VP and KP is the use of a balloon in the vertebrae the injection material is similar in both techniques. And his composed by a syringe (where cement is stored) mounted on a canula (inserted in the bone).

During most of the VP and KP the following steps are observed:

1. The needle (canula) is inserted in the vertebra (rotating and percussion movement).
2. Insert inner sleeve, the inner sleeve with side-opening is inserted in order to close off the front-opening of the outer needle.
3. Cement is pumped with the syringe from the cement mixing unit.
4. Syringe is plugged to the canula.
5. Cement is injected in the vertebra.

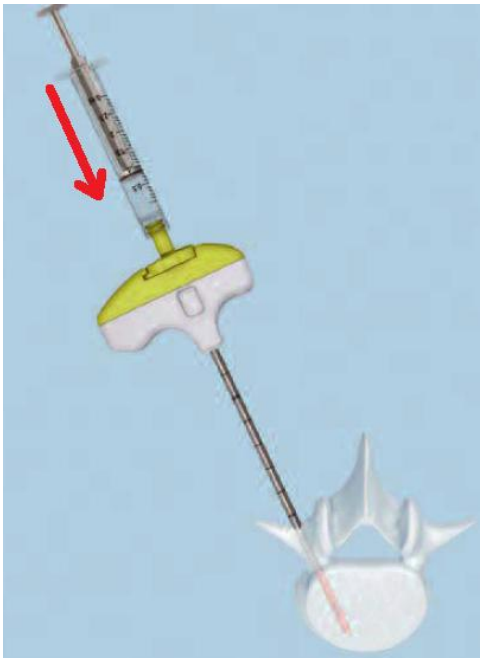

Figure 1: Schematic representation of the configuration during VP and KP. The canula is inserted in the vertebrae and a syringe is mounted on it.

The syringe design remains more or less the same from one company to another, distinction are made on devices such as a mixing unit integrated to the syringe, the plug movement activated by a manual screw instead of a simple pressure, or an injection gun (Osteoject^{TM}, EZflow^{TM}) allowing the surgeon to inject at higher pressure without making too much useless efforts. Lately patent has been proposed to include an helix mixing the cement during the injection in order to homogenised the paste and prevent LPM. Our work will focus on a standard syringe, meaning a circular barrel, ended by a die (conical) and mounted on a canula which will be inserted in the vertebrae (see fig.2)

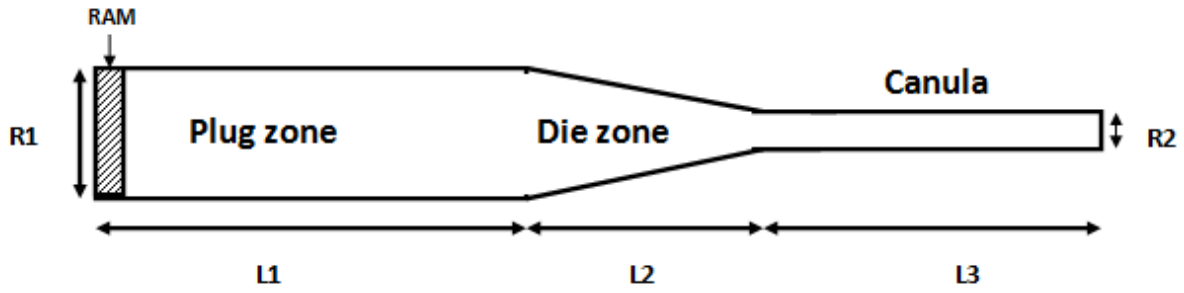

Figure 2: Simple representation of the injection system used in VP and KP.

1.2. Filler materials

Vertebrae is a bone located in a load-bearing environment, hence the material that will be injected to stabilises it must be able to withstand complex loading statically and cyclically. Moreover the material has to be biocompatible, easy to prepare, to present proper flow and settling time characteristics. Other specificities can be needed such as the ability of the material to release antibiotics or to be viewed on radiography allowing a better control of the filling process of the vertebra. Historically the first material used for Vertebroplasty were a mixture of PMMA and a contrast agent [1], since then PMMA has been widely used modifying the formulation of its additives mixtures. Its success rely on the fact that a majority of patient suffering from vertebral fracture are old and that the clinical operation's first objective is to relief pain and increase patient mobility and independence. Nevertheless those are relatively short term effects that could be used for elderly patient. The use of PMMA as filler material with young patient is not an optimal choice, indeed PMMA presents no potential to remodel or integrate the surrounding bone, its relatively high stiffness would

with time and cyclic loading damage the surrounding vertebrae, its high polymerization temperature is suspected (as well as unreacted monomer) to induce thermal and chemical necrosis of the bone tissues and nerve ends [2]. For their low settling temperature and osteoconductive properties, ceramic bone cement has received from the surgeon community a significant interest. Indeed the resorption potential and the biological bone replacement process that this kind of cement present is of great interest in the healing of young patient traumatic fracture. Moreover ceramic cement presented bones like mechanical properties reducing the risk of damaging surrounding vertebrae with time. Despite their higher price and more complicated handling characteristics ceramic cements appear to be the most interesting kind of materials (after further optimization) to reinforce and reconstruct vertebrae.

Table 1: Desirable properties of an injectable bone cement for use in VP and/or KP [3]

• Easy preparation	• Injection time 6-10min	• Setting time ~15min
• Low cost	• High radiopacity	• Low curing temperature
• No toxicity	• Excellent biocompatibility	• Mechanical properties of a healthy vertebral body
• Excellent bioactivity	• Excellent osteoconduction	• Good injectability

1.3. Injectability problems

However, it has been observed that ceramic cement present poor injectability [4], with a definition of injectability varying from one author to another, for R.Alves [5] injectability is defined as in terms of the residual mass of cement retained into the syringe after loading with a constant force, nevertheless if a small amount of cement remains in the syringe the problem would be only economical but since surgery is not considered as a process where benefit has to be made we cannot consider it as a fundamental problem. What appeared to be more problematic concern the composition of the paste injected itself, it has been reported that cement concentration could vary during the injection leading to phenomenon

such as a drying out of the paste, cyclic dewatering, stress Build up, and droplet formation at die head [6]. Thus, for Bohner [7] injectability should be defined by the paste capacity to stay homogeneous during injection, independently of injection force.

Even if the physic of the process is not fully understood, it is suspected that particulate pastes (such as biocement) when extrudate can exhibit a difference between the velocity of the solid and the liquid phase, this is generally called liquid phase migration (LPM) in extreme cases LPM is such that solid particles concentration increase and can cause particle jamming in the syringe constriction, it is possible to know if LPM occurs, indeed a characteristic of it is the raise of injection pressure that could go up to a factor 15 [8] and makes the injection process impossible to complete for the surgeon [9] . Jamming of the particle also have to be avoided, since the vertebrae must be completely filled without removing the canula and/or changing the syringe.

It is difficult to understand what is truly happening in the syringe during the injection, indeed it is impossible for the naked eye to see particles and fluid movement during injection of the paste, added to the fact that most of the syringes wall are opaque. Nevertheless the need of food, pharmaceutical, building, aerospace, and biomedical industry to understand this phenomena and counter it leads scientific to develop study methods that helped writing theories on LPM and jamming phenomenon. The first part of this work will summarize the different existing observations and theories investigated to describe cement behaviour during injection.

1.4. Liquid phase migration

LPM can have several origins including paste consolidation, dilatation of the solid undergoing extension [10]and drainage phenomena in the die land [11].

The framework and problems encountered for our study are pretty similar to extrusion process of pastes (pharmaceutical industry, food industry), cement (building industry), or ceramics (Aerospace industry), indeed ceramic cement presents rheological behaviour close to the one of extruded materials previously cited and extrusion process consisting in plugging the paste/ cement out of a cylindrical barrel through a dye of given geometry is

similar to the one of injection by the use of a syringe. As mentioned previously it has been reported [12] [13] that during injection of an initially homogenised cement paste variation in concentration occurred within the barrel leading to phenomenon such as a drying out of the paste, cyclic dewatering, stress Build up, and droplet formation at die head [6]. Those phenomenon have been reported principally for industrial extrusion of paste but they are the same for VP and KP. Their origins even if not fully understood have been studied by the scientific community and it is admitted [14] [10] [15] that liquid phase migration, or drainage is at the root of the problem.

It is generally admitted that water migration in the paste solely occur in the barrel or the syringe (extruder) and is influenced by the stress distribution arising from compaction and deformation of the paste [16]. The main mechanisms cited to explain LPM are drainage/compaction which correspond to a simple consolidation model widely used in soil mechanics [17] and pore suction resulting from extensional flow in the die land entry. This pore suction effect is also responsible of the formation of stiffer static zones in the die land [10].

Even if liquid phase migration correspond to a global phenomena occurring in the whole cement paste, its effects on the paste are known and cartography of water content in pastes have been made [18] [19] [20] from those observation we know that when LPM occurs a drier zone appears near the ram that could take the form of an arc at the wall opposed to the flow [18], the water migrate from this dry zone to the centre of the barrel forming a wetter area in the middle of the barrel and finally a dewatered "dead zone" near the exit forming a dry conical shape at the syringe exit, if this zone is too big jamming will occur and block the injection process. Those zone can be seen on fig.3 for a square die extruder and a conical die syringe.

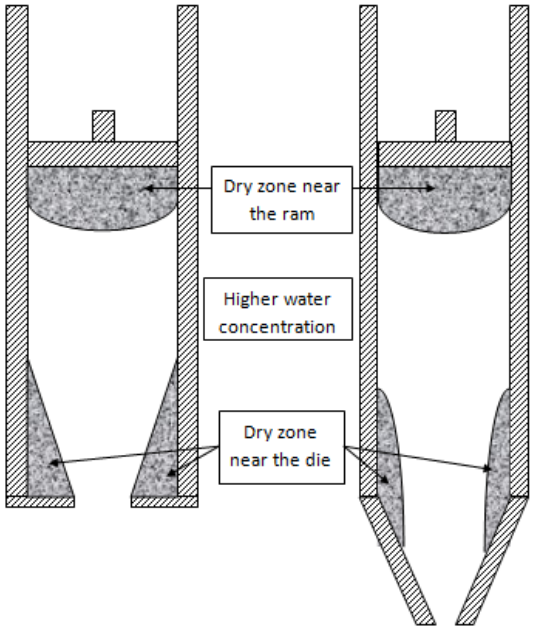

Figure 3: Schematic representation of the location of dried cement zone for two extruder geometries.

Different approaches have been used by the scientific in order to investigate the phenomena. While one part of the community focused on the formulation of the cement pastes [21] [22] [6] the other believed LPM could be controlled by process parameters such as the syringe design or the velocity of the ram during injection [23] [6] [24] [16] We will see that LPM is in fact controlled by both which give to the problem a lot of variables. Firstly we will discuss the influence of the paste formulation (Particle size, shape, size distribution, roughness, interstitial liquid viscosity) and secondly discuss the influence of injection parameters (ram velocity, syringe and die design) on LPM.

1.4.1. Cement formulation influence on LPM

Liquid phase migration occurs within the cement paste, it seems legitimate to think that the cement formulation and microstructure study represent the most suitable way to control the injectability of a CaP bone cement [21]. We can consider ceramic cement as a suspension of particles in a liquid (generally water), the mix could be aggregated of some plasticizer or drugs helping bone reconstruction but we will not discuss their influence on liquid phase migration. A literature study helps us to determine the crucial factor controlling LPM at the

paste level. We propose to sum-up the different observations made, point by points and to illustrate them with scheme capturing their basic physic.

For facility purpose and because it is impossible to capture all the physics occurring a cement paste. We will consider cement as a paste made by two principal constituents being the cement particles (unregarding their nature) and a liquid which will fill the particle matrix.

1.4.1.1. Interstitial liquid viscosity

Considering the nature and more specifically the viscosity of the liquid filling the interstitial space between cement particles, it is easy to understand that a more viscous liquid will have more difficulties to filtrate through to particle matrix, in the mean time, the particles being surrounded by this more viscous fluid won't be able to move easily in the paste. Nevertheless it has been noticed [6] that cement presenting higher viscosity needs higher extrusion pressure, hence higher pore pressure differences and are more subjected to LPM. However, using a liquid having a low viscosity expose the surgeon to two problems being the injection of a high water content cement at the beginning of the injection [25] and possible leakage of the cement out of the vertebrae [9] during the injection (for VP). Thus liquid viscosity should be kept relatively low to avoid LPM and sufficiently high for the surgeon to control it to stay in the vertebrae.

1.4.1.2. Particle size distribution

It is quasi impossible to obtain a cement having a centred particle size distribution, indeed we cannot expect our cement particles to have the same size. Moreover, the use of a wide particle size distribution has been shown to decrease extrusion pressure and restraining occurrence of drainage phenomenon [22].

1.4.1.3. Particle roughness

Surface roughness of particles is a key parameter that can prevent drainage of interstitial liquid out of the paste [22]. Indeed for particle with smooth surfaces if pressure is applied the particles can be easily moved and fill the pore initially filled with water, while for particle with rough surfaces friction forces between particles will prevent the pore closing fig.4.

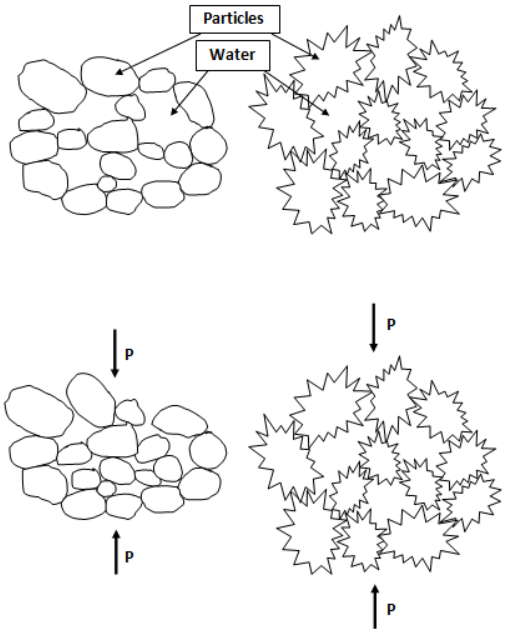

Figure 4: Schematic representation of the role of particle roughness in LPM phenomena.

1.4.1.4. Interparticle forces

If we consider a process where rocks or beads had to be extruded, even if it doesn't exists we would be in right to consider that no forces other than collision and frictional forces would play a role in the behaviour of the material. This consideration is not true for materials such as cement. Indeed even if their effect on cement rheological behaviour are not fully understood, interparticle forces play a determining role in the formation of a particle network more or less easy to break and deform. Thus interparticle forces such as Van Der Walls, electrostatic or capillary forces (forming neck shaped bridge between particles) are radically influencing the ability of the paste to stand LPM [22]. Those forces also play a role on the physical properties of the cement such as its shearing resistance, bulk modulus or its viscosity. Those forces can be controlled via additives, or by varying the pH of the cement but the understanding of their influence on LPM requires more advanced techniques and it might be easier to access cement having better injectability controlling other properties than those.

1.4.1.5. Solid content

It will be explain more in detail in the injection process parameters that extrusion velocity play a determining role in the apparition of LPM or not [23]. However it has been observed that the threshold velocity at which LPM appears increase with solid content of the paste [10]. Meaning that for a same extrusion velocity (ram velocity) paste having a higher solid content are more likely to undergo LPM than paste presenting low solid content. Supposition are made to assign this observation to the higher extrusion pressure (more frictional forces in between particles to counter) or pore suction role (smaller pore due to higher solid content).

1.4.2. Injection process influence on LPM

Based on recent studies [23] [6] [24] [16] scientifics have found that occurrence of LPM were not only sensitive to the paste formulation but also to the injection parameters.

1.4.2.1. Ram velocity

It appeared that liquid concentration in the cement paste remain constant if extrusion speed is sufficiently high. Therefore that it exist a threshold of ram velocity under which LPM occurs and over which does not occurs. Based on this observation Perrot [23] described LPM as a competition between filtration of the interstitial liquid through the granular skeleton and ram speed. This is confirmed by the behaviour of cement paste, at high deformation rate cement's behaviour is plastic while it becomes frictional plastic at low deformation rate [23], meaning that a structural change (local change in composition), appears in the paste.

In order to understand what could be at the origin of extrusion velocity effect on liquid filtration in the paste we have to take an insight in the paste microstructure as it is done in fig.5. The interaction of polar water molecules, active polymeric agent and electro-charged cement particles. The electrical interaction of these three gives a structure where the cement particle are wrapped by a thin film of water which are linked to each other by neck-

like bridges to form a network structure in between particles. The remaining water is free to fill in the pore among particles.

At the beginning of the injection of cement, the particles are compacted and shear stresses between them increase gradually. In order to see the paste beginning to flow induced shear stress has to exceeds the yield stress of the paste. Particle compaction stops when a balance is reached between pressure in the paste and paste flow at a specific extrusion velocity. During all the compaction stage the paste remains relatively homogeneous and pressure is steady.

The injection process gives rise to a pressure difference in the pores of the network allowing the free-water molecules to easily move. Generally free water particles move faster than solid particles due to the difficulty of particles to overcome the resistance of network destruction.

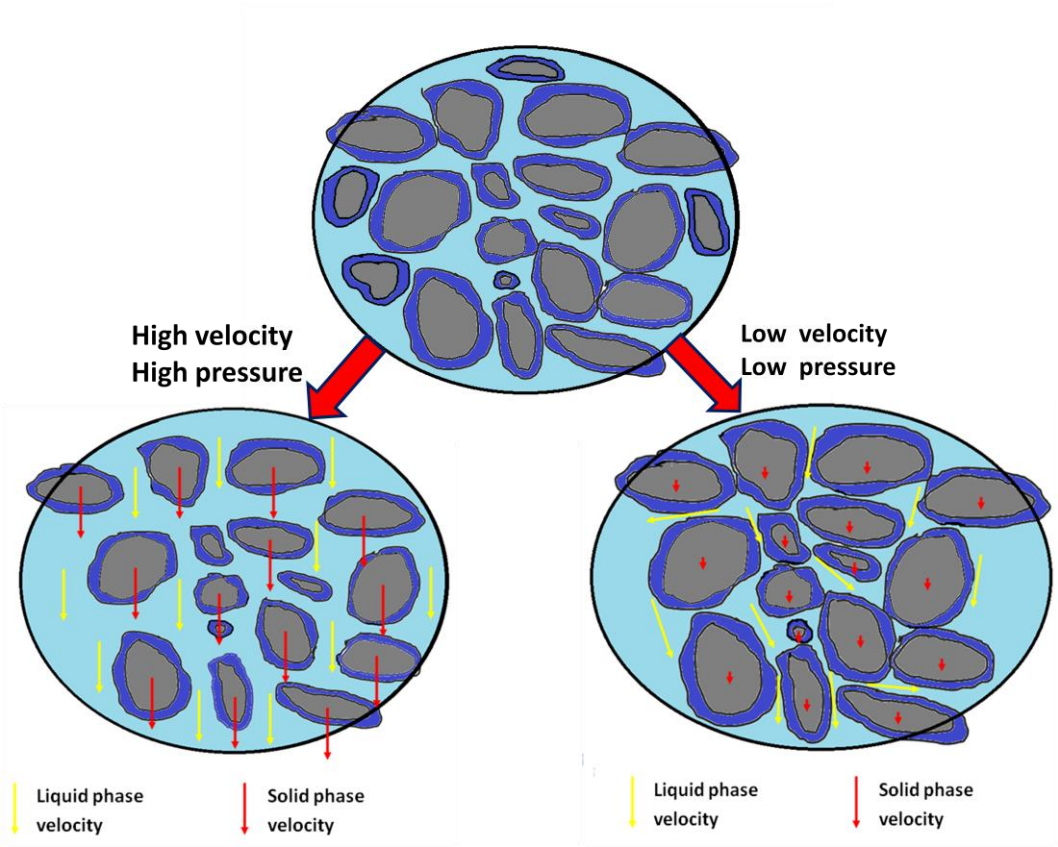

Figure 5: Schematic representation of the ram velocity influence on LPM. Comparison between "high" and "low" ram velocities.

When injection speed is high (high ram velocity) pressure in the paste is also really high, sufficiently high to "destroy" the network, hence cement particles are not connected anymore making their movement easier, they can almost synchronously move with free-water molecules, the paste remains homogeneous and no LPM is observed.

When injection speed is low (low ram velocity), the pressure is also low and deformation of network is slow and breaking of links among particles occurs less frequently. Some particles stay dynamically linked and cannot move freely while free-water and free-particles can move in the network, a wetter extrudate should be collected at the die and a drier paste observed near the ram.

Nevertheless, for the surgeon ram velocity does not have to be too high in order to control the filling process of the vertebrae, an adequate velocity has to be found in between velocity threshold for LPM or cement settling and an acceptable velocity allowing the surgeon to keep under control the filling process.

1.4.2.2. Die geometry

Previously we mentioned the fact that LPM occurred principally in the plug flow area of the syringe and not in the die land [16]. However it has been shown that die geometry influence LPM [6] . Indeed LPM is reduced when bigger die land diameter are used, this is due to the fact that smaller die involve higher pressure required to shape the material through the die, hence bigger pore pressure differences leading to water flow in the pores. Added to the exit diameter of the die, its geometry play an important role too since conical shaped die are more likely to prevent extrudate heterogeneity and static zone formation [10]. Thus, the use of a smooth change in cross section reduce inner pressure needed to shape the material resulting in less chance to see heterogeneity in the cement.

1.4.2.3. Wall roughness

One of the main effect of LPM, beside heterogeneity of the injected cement is the relatively high increase of injection pressure due to the formation of a drier, more frictional paste near the ram during extrusion. Indeed the pressure needed to extrudate the cement need to overcome several forces such as the shaping force required to plastically form the material (due to the die geometry) and friction force acting at the syringe walls. Giving a higher roughness to the wall would result in higher frictional forces to overcome and by continuity higher extrusion pressure, giving rise to all the phenomenon explained before. Even if as proposed by Bridgwater [10] and proved by [26] a small amount of LPM exists at the wall. Which form a very thin layer of liquid (considered to be of a thickness of one particle diameter [27]), supposed to lubricate the paste flow and cause apparent slip. This very thin layer cannot counter the wall roughness of the syringe. A syringe having smooth and polished wall will present less probability induce cement heterogeneity during its injection in a vertebrae.

Conclusion Liquid Phase Migration

We have seen that in order to avoid as much as possible LPM, the scientist must:

- Find an appropriate solid content of the cement in order to get desired mechanical properties.
- Use a cement having a broad particle size distribution (Naturally the case)
- Keep particle roughness low.
- Keep wall of the syringe roughness low.
- Find an appropriate liquid viscosity in order to obtain the desired paste rheology.
- Use die having a smooth change in cross section.
- Keep die diameter has high as possible.
- Find velocity threshold above which LPM does not occurs.

1.5. Jamming phenomenon

Added to the liquid phase migration occurring in the barrel another phenomenon corresponding to the blockage of the cement in the syringe as been observed and is known as jamming. Everyone has experimented jamming particulate jamming in a constriction, from the sand in an hourglass, to your car in a traffic jam it all remains on the same yet not fully understood physics. Jamming could be described as the transition between a liquid state (normal car or sand flow) to a blocked system (traffic jam or stuck sand).

Let's consider a granular material constituted of individual particles ranging from the size of icing sugar to the size of trucks. A dynamical states (flow) of a great number of particles needs energy which could be of different nature (gravity, kinetic energy, wish to go from a point A to a point B). Nevertheless collisions between particle or human anticipation dissipate this energy, sometimes energy is totally dissipated and the system remains blocked (jammed) and could be unjammed by an exterior contribution. In some cases the jammed state is such that even an extra amount of energy will not change its configuration. Both cases are problematic for KP and VP, indeed if we consider the two situations:

- The cement particle are jammed in the syringe constriction but can be unjammed by an exterior amount of energy. In this configuration we can imagine that water will flow out of the cement by filter pressing and a variation of water concentration in the cement will be observed. Added to this, if the system gets unjammed by an extra-pressure applied by the surgeon it could lead to a bad control of the process and hurt the patient. Hence jamming even if "reversible" is not desired.

- The second case where the system is jammed and cannot be unjammed won't be accepted either, first of all because the same filter pressing phenomena will occur and second of all because it would lead to a bad, incomplete filling of the vertebrae. An extreme solution would be to change the syringe, but it includes an economical cost and a setting time problem (cement would settle in the canula).

Thus, jamming of our cementitious paste has to be strictly avoided and ceramic cement as well as injection unit has to be conjointly designed in order to continuously inject the cement in the vertebra.

During the injection process, particles are pushed out of the syringe though a constriction, the cement paste is thus compacted and undergo compression and shear forces. The particles get closer one to each other and when volume fraction of the particle is high enough the gaps between particles collapse and elongated clusters are formed along the compression axis [29] [30].The volume fraction of particles could then increase till a jammed state of the suspension. We can draw a similarity with the force chains which sustain the compression stress in the case of granular flows. However, the complex particle shape and size distribution of cement as well of its chemically reactive nature makes the study of jamming transition hard to understand. Moreover, in the case of fluid driven particle flow, fluid and particle are intimately connected [31] which make the injection of cement more difficult to study than discharge of grain silos which were the main area of application to jamming research.

Even if purely mechanical (force chains and higher solid volume fraction) correspond to what our physical sense easily understand as the main reason of jamming. It has been reported that other phenomena are responsible, or play a determining role in the fully comprehension of jamming transition. Those phenomena are associated to the shear thickening behaviour of granular material such as cements, and they are mentioned on fig.6.

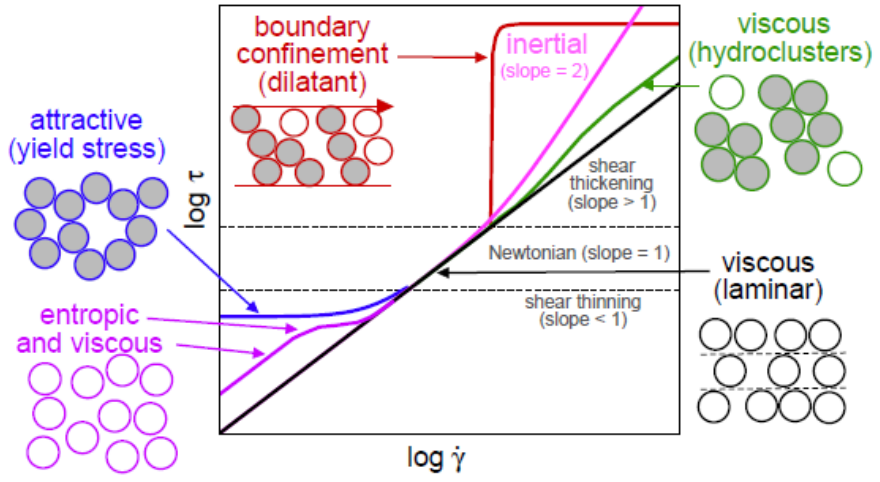

Figure 6: Different regime of shear stress τ vs. shear rate $\dot{\gamma}$ and influences on the paste rheology.

In order to better understand and make the link with jammed state we will describe and explain the different phenomena responsible for shear thickening of granular materials.

- ***Shear thickening***

The property of shear thickening of granular paste is considered Non-Newtonian. It correspond to an effective viscosity increase with shear rate. This phenomena is characterized by different features and it exists different types of shear thickening showed on fig.6 [32].

-Dilatancy

Often used as a synonym for shear thickening in early literature, it has been shown that dilantancy could occurs without observing any shear thickening of the granular material [33] meaning that dilatancy should not be directly related to shear thickening. Reynolds [34] explain the dilatant character of dense granular flow by the particle trying to go around each other when subject to stress but cannot take direct path so their packing volume expand (dilates). It is assumed that dilatancy occurs when solid volume fraction exceed a critical value [35].

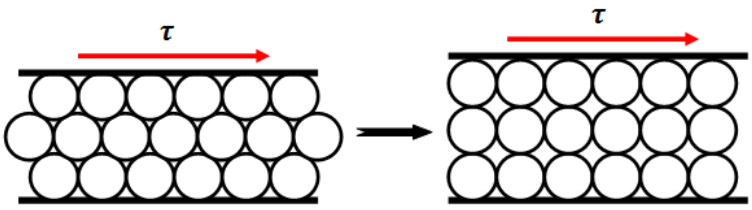

Figure 7: Representation of the dilatant character of granular material under shear stress.

-Hydroclustering

The basic concept supporting hydrocluster mechanism stipulate that particles are pushed into each other by shear, then they stick one to each other due to the small lubrication gaps existing between particles. Thus to move away from each other they must overcome the viscous drag forces keeping them grouped. Large clusters results in larger effective viscosity [36] and lead to jamming.

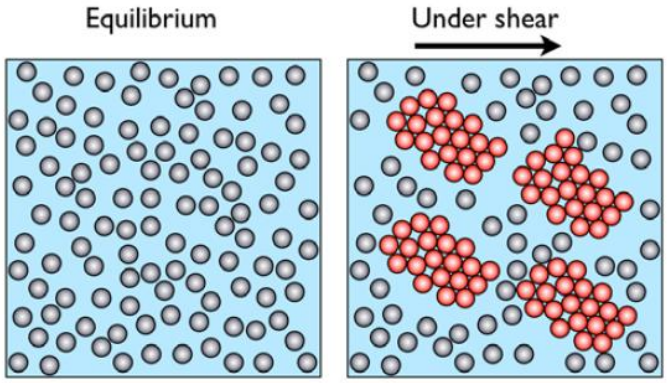

Figure 8: Schematic representation of the hydroclustering phenomena occurring during shearing of particle suspensions.

Calculation and simulations based on modelisation of hydrocluster produced an increase in viscosity of order 2 which is far-less than what have been observed in experiments. Unfortunately due to the relative calculation cost and simulation difficulties close to close packing, no simulations were run near the jamming transition.

-Inertial effects

At sufficiently high shear rate one type of apparent shear thickening can be observed. However it cannot be attributed to a granular material behaviour since it has been observed in pure Newtonian liquids (no particles) at high shear rate. Moreover, we cannot consider the injection process to be of high shear rate since the injection last between 4 and 8 minutes. Finally in our case inertial effects are not considered to be of importance on jamming of cement during injection.

Solutions

In order to avoid jamming phenomena, scientific community start to investigate the influence of different parameters on the probability for a paste to clog the die or the exit. In the same way as for LPM two approach have been used to tackle to problem, and they are pretty similar to the one used for LPM. Indeed the first approach consist in studying the paste formulation and particle properties (shape, size, roughness) and the second one rely more on the design of the syringe itself (wall roughness, die shape and exit diameter. We propose to sum-up the different observations made by points and to illustrate them with scheme capturing the basic physic of them.

1.5.1. Paste formulation influence on jamming

Once again paste formulation play an important role in the probability for a paste to jam or not. Even if the initial solid particles concentration is easily seen as the main parameter which control jamming, we will see that it exists other material dependent parameters which foster or not jamming of the cement paste in the die zone.

During elastic or plastic shear pastes may dilate, compact, or shear at constant volume, and this material behaviour under shear is supposed to be one possible reason of jamming at die entry. It mainly depends on the internal angle friction (depend on the particle concentration) of the particles and Poisson's ratio of the solid skeleton [37].

1.5.1.1. Particle size

A basic and easy to understand concept is that constriction can be blocked by large particle at lower concentration than for small ones [38]. Indeed if we take 3 "big" particles and 300 "small" particles and we extrude them through a die having the same dimension in both case, the three big particles have more probability to form an arc blocking the constriction than 300 ones flowing through the die. In the mean time particle of larger density and dimensions are more likely to collide with the walls and between each other's leading to greater chance of jamming [38]. It is then really important to prepare the mix that has to be injected with a finely crushed cement in order to obtain the desired rheology of the paste.

1.5.1.2. Particle shape

Even if it is not interesting nor possible to act on cement particle shape in our case, the study of particle shape influence on jamming probability has been studied in the case of injection of polymer microparticles [39] in this study it has been found that semi-spheres are more likely to block a constriction for equivalent surface area than spheres. It has been noticed that contact angle of the particles play a determining role in constriction clogging.

1.5.1.3. Particle hardness

A characteristic more linked to the physical properties of the particle itself is its hardness. It has been observed that hard particles are more likely to jam than deformable ones [38] [29] .Indeed hard particles when they come to contact cannot be deformed making the unjamming process more difficult than for smooth deformable particles which when they come to close packing can deform to avoid blockage of the flow.

1.5.1.4. Particle roughness

Rough particle will have more difficulties to pass through a constriction due to the higher friction force acting between them, hence sliding and rearrangement between them have less probability than for smooth particle. Force chains between the particles will have more chance to be formed increasing probability of jamming.

1.5.1.5. Interparticle forces

As explained for LPM interparticle forces are responsible for the formation of a particle network making the material cohesive. The main forces making cement a cohesive materials are capillary forces (neck-like bridge of water between particles), and electrostatic forces (polar water molecules and charges cement particle), they are both considered to have a decisive role for the agglomeration of granular materials [40] [41], and by extension jamming of pastes. Adjunction of additive to the cement mix could act as fluidizer as well as the modification of the cement pH. But once again we should not forget that the cement we are using is injected in the human body and product used have to be in accordance with the international reglementation in terms of biocompability.

1.5.2. Syringe geometry and features influence on LPM

1.5.2.1. Wall roughness

If wall roughness was a problem in the plug flow area for the control of LPM it is now a problem for particle jamming in the die zone. Indeed wall roughness induce more frictional force at the wall of the die [42] [43], particles have then a tendency to agglomerate more at the wall than for smooth walls, agglomeration increase solid volume fraction locally at the die, thus increasing probability of formation of forces chains that will clog the exit.

1.5.2.2. *Syringe geometry*

Once again scientific have studied the influence of the syringe geometry on the jamming propensity of cement during injection. We will see that the conclusion drawn from their observation are in a certain way linked to the one done for LPM. Nevertheless while LPM occurred in the plug flow area, jamming occurs in the constricting zone (die area).

1.5.2.3. Critical exit size

Of course one could think that a wide exit size would be a certainty for no jamming to occur, and even if a wide exit aperture is possible to achieve at the syringe level, it is problematic at the canula's level for the patient comfort. Nowadays medical profession try to keep surgery as less invasive and painful as possible for the patient. Hence canula diameter is kept as small as possible, but we know that small exit are more easy to jam by particles. A solution seems to have been found by Zuriguel et al. [44] which They assign that no jamming occur for an orifice aperture larger than a certain number of times the diameter of one particle. Nevertheless this properties can only be verified for 3D die, it is not possible to find a relation between exit size and particle size to prevent jamming for 2D systems [45]

1.5.2.4. Shape of the die

We explained in the LPM section that smooth change in cross section area were preferable to avoid migration of the liquid in the cement. Unfortunately it is not true for jamming, indeed it has been observed [38] that ramp constriction block particles more likely than rectangular constrictions, rectangular constrictions let more space for the particle to disperse laterally and rearrange. Thus a compromise in the shape of the constriction as to be found in order to avoid both jamming and LPM.

Conclusion jamming

We have seen that in order to avoid as much as possible jamming, the scientist must:

- Limit the size of the particles.
- Prefer square shaped die to ramp shaped ones.
- Use particles as spherical as possible.
- Find an adapted diameter large enough to avoid jamming and keep the surgery as less invasive as possible.
- A relation between an adequate particle size and minimal die aperture avoiding jamming has to be found.
- Make the wall of the syringe as smooth as possible.

1.6. Theories developed

In the first part of this chapter we have seen thanks to a literature study the role of different parameters on LPM and jamming occurring during cement injection. From this we drawn different recommendation to avoid them. Nevertheless, the different conclusion given don't establish an approved easy to apply recipe, moreover injection test are time consuming and includes cost in persons, and material. Thus model needed to be developed in order to access data on extrusion easily. We will in this part propose an overview of the existing theories developed to model LPM and jamming. Those theories are still being investigated and developed they cannot be taken as fundamentally true. They should be discussed and compared with experimental results. We will present common test that helped to develop those theory in the third chapter dedicated to the future strategy that should be adopted to develop easy to inject cement and adapted syringe to VP and KP.

The rheological behaviour of cementitious pastes regroup three, apparently distinct, fields which consider different kind of materials under various conditions. Indeed cement materials can be seen as a meeting between the rheology of a suspension, the physics of granular matter and soil mechanics . Scientific community state different approach in order to model liquid phase migration in paste. These models take their origins from soil mechanic (cam-clay, poroelasticity, Therzaghi) as well as polymer rheology. The main goal of this section is to present an review of what have been done in terms of modelisation for LPM and justify the approach taken in chapter 2.

1.6.1. Theory and modelisation methods developed for LPM

The problem we are trying to tackle does not correspond to a simple fluid mechanics problem where the fluid behaviour is well defined and were the study focus on the syringe geometry or fluid viscosity influence on injectability. The problem that has to be modelled concern the migration the liquid phase through a granular paste under extrusion force. Meaning that the behaviour of the material will change in time and space making the problem hard to model. Previous work [46] focused on the modelisation of ceramic cement pastes considering this material as a Newtonian fluid passing through a die, nevertheless this

approach, even if useful to understand the evolution of parameters such as velocity or pressure in the syringe, does not simulate the main encountered problems known as jamming and LPM. It has to be kept in mind that simulations are useful and can be compared to experimental results only if they incorporate the physical behaviour of the materials. According to this, even if simple law describing rheological behaviour of cement pastes exists (Bingham model [47] [48],Herschel Bulkey model), have been widely used [49] and gave results in accordance with experimental observations, they cannot represent the problems we are facing and trying to model. Hence the need to study the flow developed during injection of cement in order to develop models including water migration in the paste and its influence on the paste rheology.

Two mains groups of simulation exists if one wants to study LPM in cement during injection. The first one is based on the stress state in the cement material, stress on the liquid (pore pressure) and on the solid (granular network stress), as well as on the matrix permeability. This method has been used by Rough et al. [50] [16] and by Perrot et Al. [51-53] The second one is more soil mechanic related and consist in modelling the injection of the cement paste via FEM by means of Cam-Clay [54] [55] or poroelasticity models. We will start by quickly describing the ideas behind the methodology used by Rough and Perrot, and then give an insight in the modelisation of cement extrusion using FEA codes and existing soil mechanic theories.

1.6.1.1. Methodology

If one wants to model paste extrusion including liquid phase migration the physic of LPM should be understood. When a cement is compacted and extruded the total stress applied is the sum of the stresses imposed on the solid matrix and on the liquid phase. The stress acting on the granular matrix is responsible for its deformation while the stress acting on liquid (pore pressure) is considered as the driving force for the flow of the liquid phase. Nevertheless liquid flow in between the cement grain is controlled by the permeability of the solid matrix which depends on the porosity of the granular media.

Methods developed to study LPM during extrusion are based on the separation of the stresses (solid and liquid) in order to study the flow of liquid relative to solid. This way water

distribution in space and time could be computed by incorporating a material model with water dependent characteristics.

For computation purpose our domain has to be discretized, we consider that LPM occurs only in the extrusion direction. Hence no radial LPM occurs, this is of an approximation which could give raise to further improvement of the method. The domain is then discretized in slices of equal height in the extrusion direction. The computational process will follow the water content, and stress state evolution of the paste, spatially and temporally.

1.6.1.2. Mathematical approach

As explained previously the domain is discretized in slices the methodology used Rough et al. [50] [16] and by Perrot et Al. [51-53] are similar on their forms and only differs on the equation used.

The backbone of this kind of approach is the filtration velocity of water (Q) described by Darcy law eq.[1.1]

$$Q = \frac{k}{\rho_w g}\frac{\Delta u}{\Delta z} \qquad [1.1]$$

$\boldsymbol{k}$: permeability coefficients	$\boldsymbol{\rho_w}$:interstitial fluid density
$\frac{\boldsymbol{\Delta u}}{\boldsymbol{\Delta z}}$ pressure difference between two faces of a slices.	$\mathbf{g}$: gravity constant

In this law we can see that water filtration is influenced by the permeability coefficient and the pressure differences between two faces and it is on these definitions that the mathematical model differs. We will present two tables (tab.2 and tab.3) explaining the differences found between the two approaches.

Table 2: Coefficient of permeability choose by Rough and Perrot in their work.

Rough	Perrot
In his approach Rough use a coefficient of permeability derived from previous work. The permeability is defined as a function of the porosity of the paste ($\boldsymbol{\theta}$) [56]. $$K(\theta) = K_{sat}\left(\frac{\theta - \theta_r}{\theta_{sat} - \theta_r}\right)^{\eta}$$ With $\boldsymbol{K_{sat}}$ being the saturated permeability coefficient defined as: $$K_{sat} = exp\left(\frac{\varepsilon - 1}{0.0185}\right)$$ And $\boldsymbol{\eta}$ an index found from soil-water retention curve. $\boldsymbol{\varepsilon}$ is the porosity of the paste sample $\boldsymbol{\theta}$ is the volumetric fraction of water content. $\boldsymbol{\theta_{sat}}$ saturated volumetric fraction of water content.	Depending on its work, Perrot choose to define permeability from the Taylor model widely used in soil mechanics and more easy to use than Kozeny-Carman equations of permeability. $$K(e) = 10^{\frac{e-e_0}{C_k}} + K_0$$ With K_0 being the initial permeability and C_k being the Taylor fitting parameter.

Table 3: **Methods to compute stress state evolution along the syringe. Comparison of Rough and Perrot approach**

Rough	Perrot
In order to access pressure differences between two faces of a slices Rough derived his work from experimental data, recording the total stress acting as a function of the cement height in the barrel. If we consider cement at die end, we consider that the total stress acting is equal to the solid stress $\boldsymbol{\sigma}'$ and pore pressure is equal to zero. Then a simple Janssen-Walker analysis is used to iteratively determine the solid stress on the top of each slice from the stress acting on the slices underneath. $$\sigma'_{(z)} = \sigma'_{(z-1)}\, exp\left(\frac{4\mu K \boldsymbol{\Delta} z}{R_1}\right)$$ K: Active Rankine active coefficient of earth pressure. R1: inner diameter of the barrel The paste-wall friction coefficient $\boldsymbol{\mu}$ is determined from the same kind of Janssen-Walker analysis. $$\mu = exp\left[-\left(\frac{W + 0.137}{0.149}\right)\right]$$ W: Mass fraction water content. Thanks to the experimental data it was possible to obtain the total stress as a function of cement height. $$\sigma_z = exp\left[\frac{\rho_{z=0} + \left(\frac{\rho_{z=0} - \rho_{z=0}}{h}\right) - B}{A}\right]$$ A and B are experimental coefficient. Pore pressure differences $\boldsymbol{\Delta u}$ can be accessed at the face of each slices by substituting the solid stress at the face of each slices from the total acting stress.	For Perrot when the ram move down a friction appear at the wall cement/syringe. The friction force create a pressure gradient responsible for the filtration of the liquid through the granular skeleton. An equilibrium of force is written on a cylindrical slice between z and z+dz. $$\frac{\pi D^2}{4}[-\sigma(z + dz) + \sigma(z)] + \pi D K_W(z) dz = 0$$ $K_W(z)$ is the friction stress at the syringe wall at position z. Solving this equation with adapted boundary and initial conditions permits to access pressure differences acting in Darcy laws. NB: It can be written with different more or less complex models but has to include a water content dependence in order to account for lubrication effect. Chapter 2 will explain with further detail the methodology used.

Linking the permeability of the paste and the pore pressure at a given height via the Darcy law of water flow, one can access the flow rate of water, thus the new water distribution in the paste, the new paste density, permeability, stress, pore pressure... The process described in fig.10 is iterated for each ram displacement and allow the scientific to follow spatially and temporally the evolution of water content in the paste as well as the extrusion pressure. One of the main process parameters has been found to be the ram velocity, motivating Perrot [52] to find a criterion for homogeneous extrusion of cement paste.

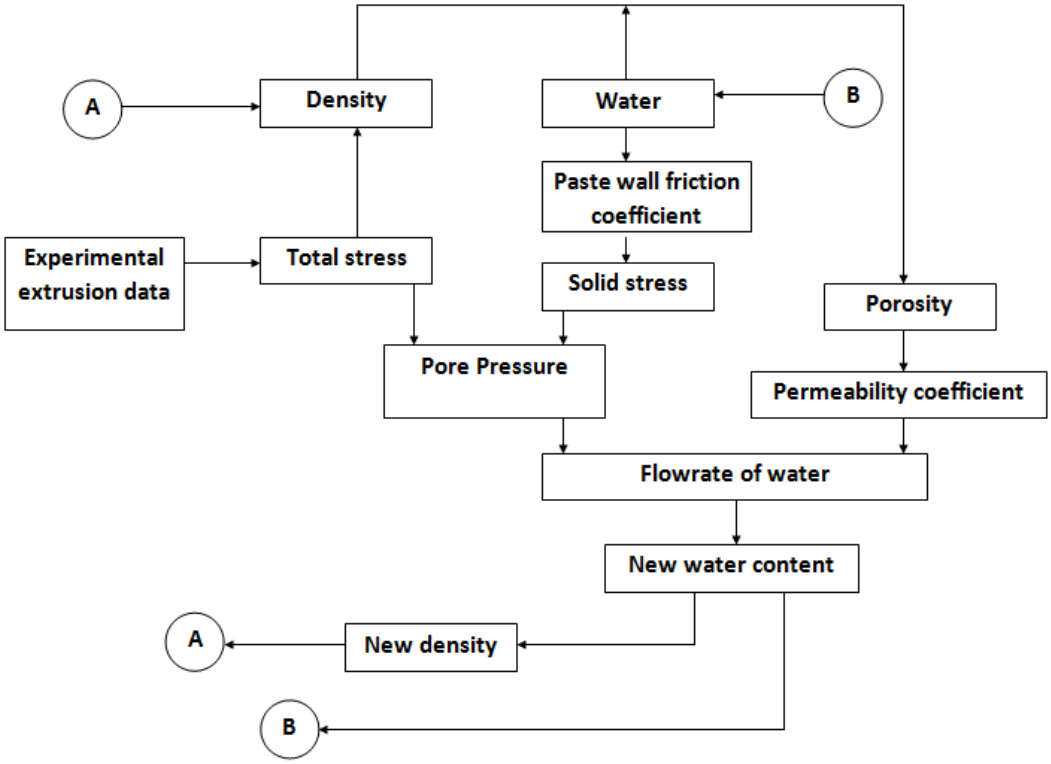

Figure 9: Summary of the procedure used to compute extrusion force and liquid phase migration.

This model developed by rough is not complete neither is the one proposed by Perrot in his latest work [51], but they represents a study of the fundamental features of the stresses developing within an extruding paste. The models predictions are in good agreement with the obtained results. Nevertheless, these model have been developed for square entry die extruder, they does not take into account radial LPM neither suction effects, it is also assumed that velocity distribution is constant (plug flow).

Even if the latest work presented by Perrot [51] seems the most developed and accurate in terms of extrusion pressure prediction (see fig.11), in regards of the evolution of void ratio in the extrusion barrel we cannot tell that it represents what happen in the extruder in terms of liquid phase migration (fig.12)

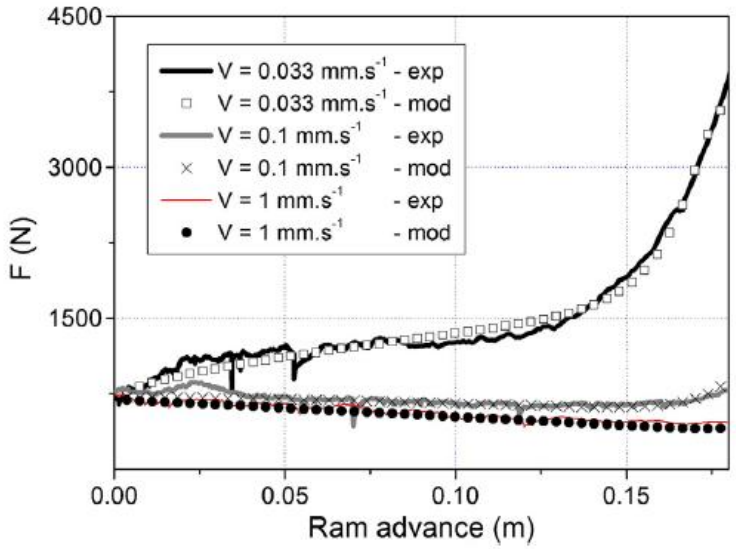

Figure 10: Comparison between experimental (line)and modelled (dotted line) force vs Ram advance for three different ram velocities. (From Perrot [1])

We can see on fig.11 that at low extrusion velocity (0.033mm.s^{-1}), as the ram advance extrusion force increase importantly in a first time, corresponding to the compaction stage, then steadily corresponding to the formation of a dry area near the ram, and finally exponentially corresponding to the meeting of the dry zone located at the ram and the dead zone near the die exit. At high velocity the extrusion pressure diminish, which is associated to the capacity of the paste to remain homogeneous during extrusion, extrusion force even decrease slightly, this could be explained by the smaller cement/wall frictional interface as the ram advance.

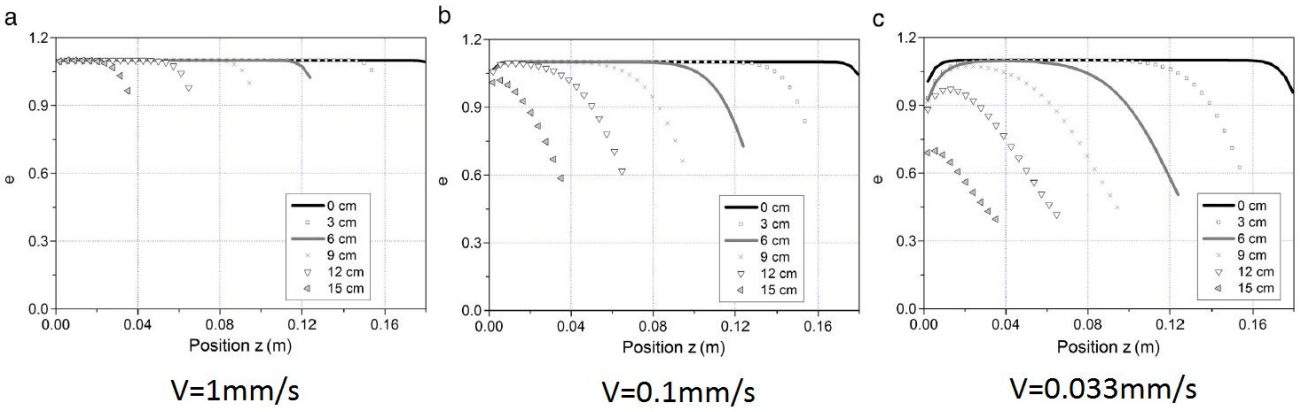

Figure 11: Void ratio content at different ram velocities (a) V=1mm/s, (b) V=0.1mm/s, (c) V=0.033mm/s, and for different ram displacement (0cm, 3cm, 6cm, 9cm, 12cm, 15 cm) (From Perrot [1])

However, if we take a look at the evolution of void ratio within the extruder it does not reflect what has been observed experimentally. We can see that at high ram velocity ($1mm.s^{-1}$) the void ratio remain constant during extrusion, only a small area near the ram is subjected to a small decrease of void ratio (drying out of the paste). When ram velocity is low we can see that the paste dries out dramatically near the ram (forming a cork) and even near the ram exit (corresponding to the dead zone). Nevertheless, even if the drying out of the paste is well observed, no central zone having higher water content can be seen. Meaning that water flows out of the zone near the ram, but this water does not move to the middle of the barrel as it has been observed experimentally in plug flow extrusion, or cement injection.

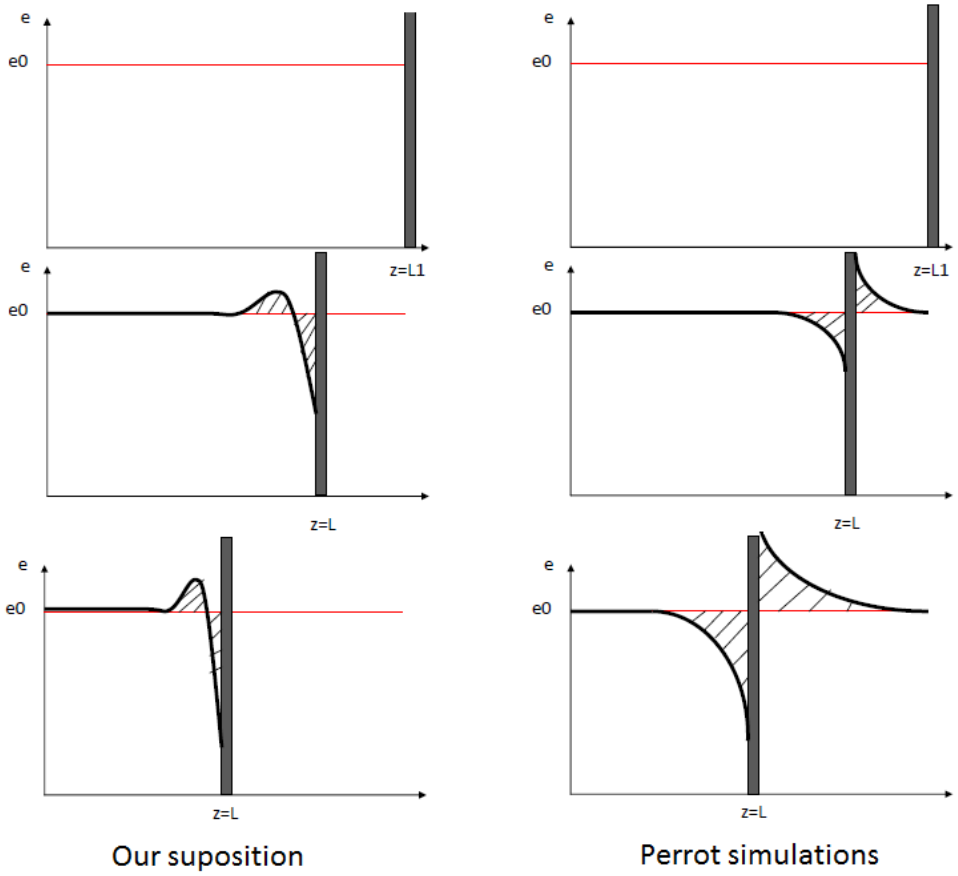

Figure 12: Representation of our thoughts on how should the void ratio evolution in the barrel extruder be. Comparison with what has been modelled in Perrot's work [1]

Fig.13 summarize our think on what should be the results of void ratio evolution during cement injection on the left, where water when moving out of zones near the ram goes downstream to the ram. We also model what is happening in the simulation done by Perrot. Indeed he used fitting coefficient materializing liquid flowing through the ram because in its experiments he observed the ram not to be waterproof. Nevertheless, the dry zone should play the role of clog and keep the ram waterproof at low velocity. In order to obtain results in accordance with experimental observation, we tried to modify his theory and the process is explained in chapter 2.

1.6.1.3. Cam -clay model

We have seen that mathematical models for paste flow incorporating LPM for pastes being injected exists. Nevertheless it has been shown that based on soil mechanics, 1D paste extrusion flows could be accurately modelled [54] [57], including effects of LPM. Indeed soil mechanic is appropriate to describe cement extrusion. Soil mechanics is defined by three major components:

- **A Yield surface:** Similar to the one encountered in plasticity theory, the soil behaviour is divided in two regions. Inside the surface where soil behave as an elastic material, and on the surface where soil deform plastically.
- **Flow rule:** Stipulate that the direction of the plastic strain increment is normal to the yield surface. This flow rule is independent of the stress increment.
- **Hardening function:** Variation of the yield surface with plastic deformation.

The cam clay model for its simplicity and ease to code gain popularity in soil mechanic and is now the most influential soil model. The required material properties could be easily obtained from hydrostatic compression, drained and undrained shearing tests as well as permeability measurements.

A diagram similar to the Mohr coulomb diagram could be draw from the three presented components defining the cam clay model (see fig.14). This diagram permits to represent the stress state in the p'-q space (p' being the mean effective stress and q the deviatoric stress or Yield stress). Associated volumetric change, hardening, softening and flowing rules are defined in terms of stress, strains and materials properties.

The critical state line correspond to a state where the soil is continuously sheared with no changes in effective stresses or volume.

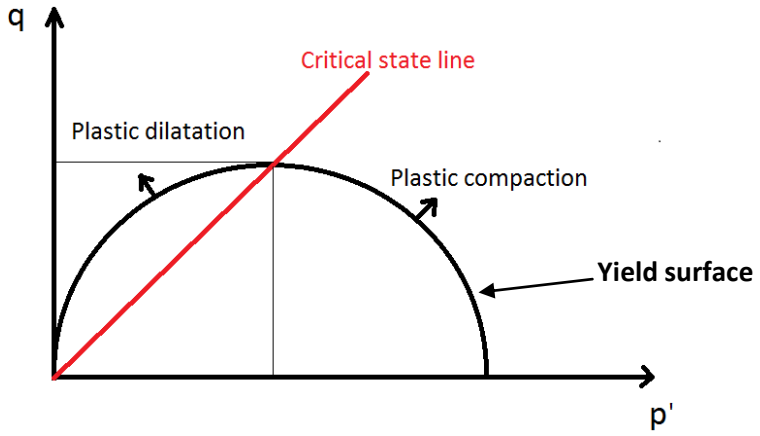

Figure 13: Representation of the Yield function and critical state line for a soil in p'- q space. The Yield function correspond to the one of a modified Cam-Clay model.

On the diagram presented on fig.14, one can read the Yield function represented by an semi-ellipsoid shape, in this surface the granular materials deforms elastically following hooks law, on the yield surface materials deform plastically and an irreversible hardening function is associated to this deformation. The granular material can compact plastically if its stress state is located on the right of the critical state line, and undergoes plastic dilatation if stress state correspond to a zone on the left of the critical state line.

If one wants to draw the current stress state of its granular material in terms of principal stress it is possible using eq.[1.2] and eq.[1.3].

$$p' = -\frac{1}{3}(\sigma_1 + \sigma_2 + \sigma_3) \qquad [1.2]$$

$$q = \frac{1}{\sqrt{2}}\sqrt{(\sigma_1 - \sigma_2)^2 + (\sigma_2 - \sigma_3)^2 + (\sigma_1 - \sigma_3)^2} \qquad [1.3]$$

Cam-Clay model does not only model an elasto-plastic deformation of the granular material. Indeed the model include a void ratio dependence of its properties, thus in a Cam-Clay model material is assumed to compact elastically and then plastically under an isotropic effective pressure stress. Following eq.4 and eq.5 one can access the current void ratio of the paste as a function of the stress state.

Elastically $$d[e] = -\kappa d\left[ln\left(\frac{p}{p_0}\right)\right] \qquad [1.4]$$

Plastically $$d[e] = -\lambda d\left[ln\left(\frac{p}{p_0}\right)\right] \qquad [1.5]$$

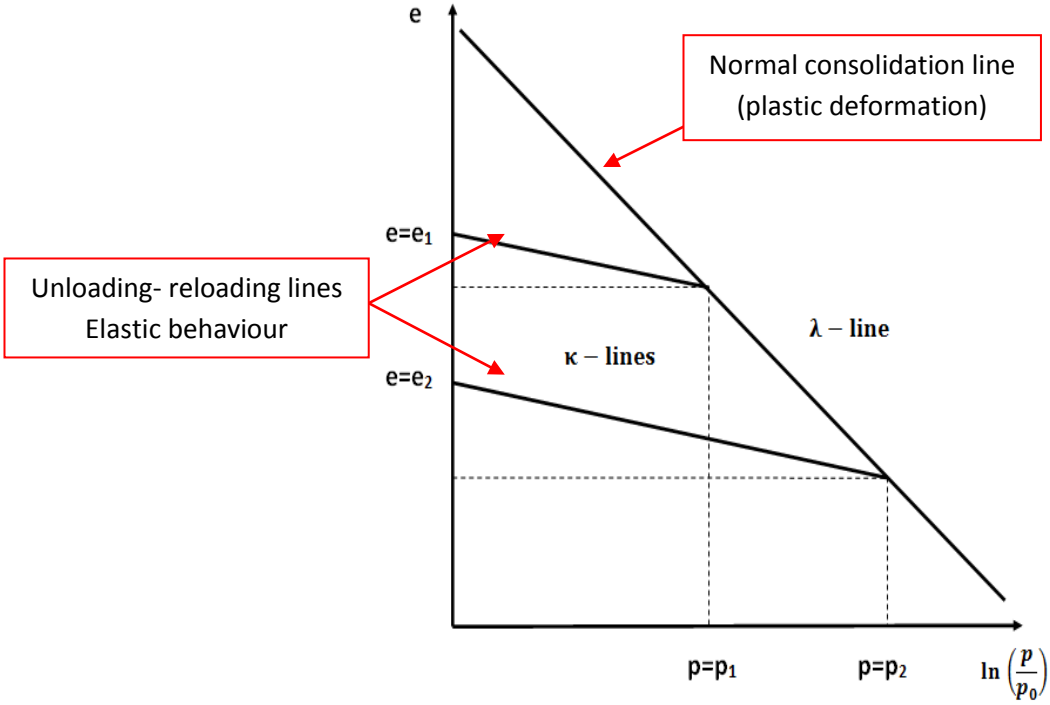

Figure 14: Evolution of the void ratio with applied pressure.

Visualisation of the compaction of a granular material.

Hence the void ratio depends on the stress state applied to the paste, it is possible to follow void ratio evolution as a function of the stress state (LPM by extension). It also means that the yield function, the hardening function and the flow rules depends on the void ratio of the cement. From this one can draw in a (p',q,e) space the evolution of the Yield surface, and granular material behaviour as a function of the void ratio (fig.16). For example the material can flow more easily at high void ratio, or present a larger elastic zone at low void ratio.

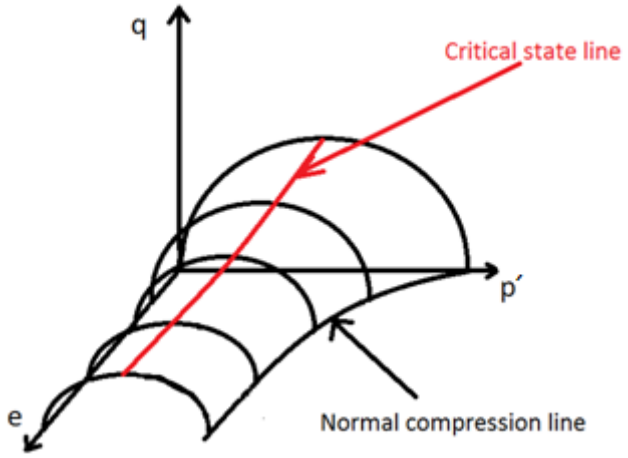

Figure 15: Visualisation of the Yield function and the critical state line in the (p´,q,e) space.

We did not developed the whole Cam-clay theory in order to keep it simple to understand. From a computational point of view if one use a FEM code and access to each element of his material the behaviour described by the Cam-Clay model. Allowing the operator to access the current void ratio, the current stress state (p',q), the stress history and the soil structure at anytime of the extrusion.

For all its sophistification, only five parameters are required.

Table.4 : Needed constants for Cam-Clay model.

κ	Elastic modulus (slope of the reloading-unloading line)
G	Shear modulus of the granular media
λ	Slope of the normal compression line
p_0	The preconsolidation pressure
M	Slope of the critical state line

Modified Cam-Clay model can be implemented in a finite element code in order to study the LPM occurring during extrusion. The solver used to solve the problem with modified Cam-Clay is Langrangian [54] [55] [37], meaning that the mesh is attached to the material, resulting in severe distortion of elements in the die land. To overcome this problem adaptive remeshing is employed.

NB: *Two Cam-Clay model exist, the simple one (SCC) and the modified one (MCC). The only difference between the two being the shape of the Yield surfaces. The MCC present a semi-ellipsoid surface while the SCC has a logarithmic spiral shape.*

1.6.2. Theory and modelisation methods developed for jamming

We made it clear that jamming phenomena has to be studied not only for the process of cement injection in vertebrae but also in extrusion or transportation process of any kind of granular materials (cement, grout, persons taking an emergency exit). Jamming has been described as the transition from a fluid like to a solid like material for granular mater [58].

Due to the large variation of size, shape and mechanical properties of particles no theory has been developed to describe the behaviour of any kind of granular material in a given process.

This part of this work focus on the existing methodologies developed to described and study jamming phenomena occurring when a granular material pass through a constriction. We will see that two approach are used in this case, a microscopic one which focus on the interparticle forces and particle packing and a global one assigning to the material a mathematical law describing its behaviour under a given stress state.

1.6.2.1. Microscopic description - Molecular dynamic

Microscopic phenomena simulations of a granular material consist in defining the geometry of the problem, assign to the particle a mass, a size a shape and a driving force. Added to that one can assign interparticle forces as well as a collision model including friction forces. Thus this kind of modelisation is multi-parameters and need to be well defined. In addition it has to capture the basic physic of jamming, that is to say:

- Use algorithm to generate ordered (crystalline) and disordered (glassy) packing of grains.
- Use test algorithm in order to say whether a packing is jammed.
- Give statistical information of the generated jammed packing.

For this purpose, molecular dynamic (MD) seems to be one of the most adapted to study nearly jammed packing of hard spherical particles.

It exists different degree of difficulties in the description of granular material by molecular dynamic, the easiest one being a fully Newtonian description of the granular flow considering that each particles is subjected to a force balance which define its motion in the system, this force balance include free motion force and the sum of all interactions with other particles. Collision between particles could be considered elastic or dissipative. And interactions between particles can be considered frictionless or not.

Another more advanced MD method consist in describing particles as having a hard central core (the particle itself), and a surrounding layer possessing attractive or repulsive potential forces. As particles would come into contact their interactional behaviour would change, and one particle could be able to be attracted or repulsed from another one depending on the attributed law to the surrounding layer, this could take into account interparticle attraction forces to model necking phenomena, or hydroclustering.

Nevertheless even if those simulations can be run for a small amount of particle, the numerical costs limit the number of particles that could be submitted to such simulations. Molecular dynamic cannot be applied to large system containing a lot of particles, and should be reserved to study local phenomena such as hydroclustering formation, or interparticle forces role in jamming.

1.6.2.2. Rheology of Non-Newtonian fluids

Granular matter can be considered as a specific class of plastic fluids showing a relation between yield stress and viscosity [59]. It exist different empirical law describing this dependence for example steady flow of pastes can be described using viscoplastic constitutive models such as Bingham plastic or more general Herschel-Bulkley model [60]. Some of these laws are given in tab.5 and link the shear stress to the shear strain (velocity gradient).

Table.5 : Most often used equations to describe Non Newtonian behaviour of cements.

Power law	$\tau = K\left(\frac{du}{dy}\right)^n$	n flow behaviour index characterizing the behaviour of the fluid as n<1: Pseudoplastic, 1: Newtonian fluid, n>1 Dilatant. Easiest to use but describe only approximately the behaviour of a suspension mixture.
Bingham	$\tau = \tau_y + \mu_p \frac{du}{dy}$	Most often used in literature. Sum of a yielding term with a Newtonian-like term. Describe a material having a solid like behaviour at low stresses but flow as a viscous fluid at high stresses. But lack of physical sense, incapable of representing data within a shear rate range of several decades.
Herschel Bulkey [61]	$\tau = \tau_y + K\left(\frac{du}{dy}\right)^n$	n_1 and n_2 are fluid parameters which characterise the shear thinning or shear thickening behaviour of the fluid. It correspond to a generalized model for a non Newtonian fluid [62]

In reality models for cement flow rheology are numerous, here are a little compilation of the other less used models:

Table 6: Other equations describing Non-Newtonian behaviour of cement paste

Robertson stiff	$\tau = A.\left(B + \frac{du}{dy}\right)^n$
Casson [63]	$\tau^{1/2} = \tau_y^{1/2} + \left(\mu_p \frac{du}{dy}\right)^{n2}$
Sisko	$\tau \quad = \tau_\infty . \frac{du}{dy} + K\left(\frac{du}{dy}\right)^n$
Eyring	$\tau = A.\sinh^{-1}.\left(B.\frac{du}{dy}\right)$
Vom Berg [64]	$\tau \quad = \tau_y \; + B.\sinh^{-1}\left(\frac{\frac{du}{dy}}{C}\right)$
Yahia and Khayat [65]	$\tau \quad = \tau_y \; + \sqrt{\tau_y \mu_p \frac{du}{dy} e^{-A\frac{du}{dy}}}$
Quemada [66]	$\tau \quad = \left(\frac{1 + \sqrt{A\frac{du}{dy}}}{B + C\sqrt{\frac{du}{dy}}}\right)^2 . \frac{du}{dy}$
Modified Bingham [65]	$\tau = \tau_y + \mu_p \frac{du}{dy} + B\left(\frac{du}{dy}\right)^2$

Looking at the equations we can see similitude which exists between the models, for all of them A, B and C are constants, which can include materials parameters. τ_y represent the yield stress parameter when μ_p is a time dependent parameter. K represent the consistency and n is the power law index. Models are linked mainly by their power law index, indeed Robertson Stiff as well as Herschel-Bulkley models correspond to a Bingham model if n=1.

From these equation it is easy to define in a FEA code a material undergoing ram extrusion having such properties and study the evolution of its viscosity and extrusion force. Nevertheless even if sheared zone and basic extrusion data could be obtained from those simulations, no information concerning LPM nor jamming could be obtained from the

simulation results. Hence obtained results would help defining the rheological behaviour of the paste only.

1.6.2.3. Thermodynamic unification of jamming

In an effort to find an universal equation to define if a system is jammed or not Lu et al. [67] qualitatively described it in terms of pressure, packing fraction and effective temperature. Indeed since granular materials are metastable, any perturbation of the system in the direction of the applied stress (injection) will cause structural ageing during which particle rearrange through irreversible compaction. The term temperature refers here to the ageing of the system more than to the real temperature of the granular material.

The equation they proposed to define jamming is path dependent and is defined by the stationary observable pressure, packing density and shear rate. Here the external pressure P, is a function of shear rate $\dot{\gamma}$, and the free volume, ε and is presented in eq.[1.6].

$$P(\varepsilon, \dot{\gamma}) = \frac{1}{\kappa_1} ln\left[\frac{\varepsilon_0}{\varepsilon} \frac{1}{1 - C\ exp(-\kappa_2 \dot{\gamma})}\right] \qquad [1.6]$$

$\boldsymbol{\kappa_1}$& $\boldsymbol{\kappa_2}$ are experimental constant	$\boldsymbol{\varepsilon}$ is the free volume defined as $\varepsilon = V - V_{RCp}$
$\boldsymbol{V_{RCp}}$ being the dynamic close packing volume and V being the flowing shear band volume	$\boldsymbol{\varepsilon_0}$is the minimum free volume

As explained previously a fictive notion of temperature will explain a thermodynamic theory that governs the dynamic of reversible shear flow and irreversible compaction. In order to build a meaningful generalization of eq.6, the fictive temperature θ is incorporated into the Helmholtz free energy of flowing sand function, F_{sand}. Thermodynamic relation eq.[1.7], F_{sand} is derived and eq.8 is found.

$$P = -\left(\frac{dF}{d\varepsilon}\right) \qquad [1.7]$$

$$\frac{F_{sand}}{N\ \theta} = \ln\left(\frac{\varepsilon}{\varepsilon_0}\right) - 1 + ln\left[1 - C\ exp\left(-\frac{\xi}{\theta}\right)\right] \qquad [1.8]$$

$\boldsymbol{N = \frac{\varepsilon}{\nu}}$ could be thermodynamically interpreted as the number of grains $\boldsymbol{\theta = \frac{\nu}{\kappa_1}}$	$\boldsymbol{\xi = \kappa_2 \theta \dot{\gamma}}$ could be thermodynamically interpreted as the average dissipation per grain $\boldsymbol{\nu}$ is the grain volume

Thanks to this expression we can now write the constant $\kappa_1$and κ_2 in terms of material and problem constant.

$$\kappa_1 = \frac{\nu}{\theta}$$

$$\kappa_2 = \frac{\eta \nu}{\theta}$$

$\boldsymbol{\eta}$ being the effective viscosity of the granular system

It is now possible to replace $\kappa_1$and κ_2 in eq.[1.6] by their material and problem variable definitions. It is now possible to trace a surface corresponding to eq.[1.6] in a 3D space having as axis the normalized form of pressure, $\frac{P\nu}{\theta}$, shear rate $\frac{\xi}{\theta}$, and the free volume $\frac{\varepsilon}{\varepsilon_0}$.

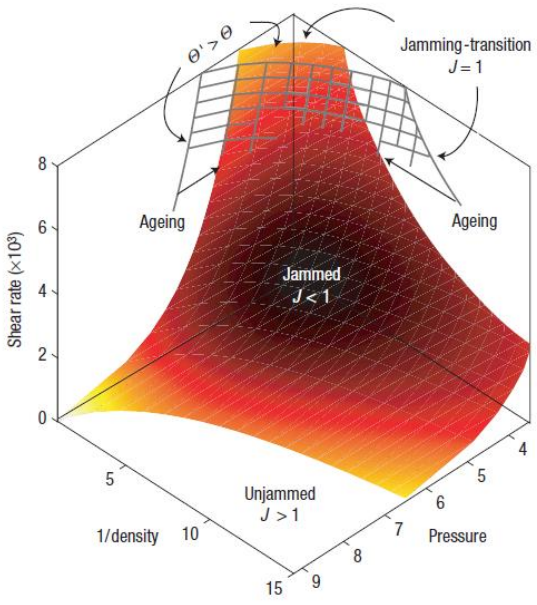

Figure 16 : Representation of J(P,ε,γ̇,θ) in a 3 dimensional space (Pressure, 1/density, Shear rate)

It is possible to define a jamming parameters that permits to define if a system is jammed or not. This parameter is defined as a ratio eq.[1.9] (with variable defined $\kappa_1$and κ_2) and $P(\varepsilon, \dot{\gamma})$.

$$J(P, \varepsilon, \dot{\gamma}, \theta) = \frac{\frac{\theta}{V} ln\left[\frac{\varepsilon_0}{\varepsilon} \frac{1}{1 - C\ exp\left(-\frac{\eta v}{\theta}\dot{\gamma}\right)}\right]}{P(\varepsilon, \dot{\gamma})} \quad [1.9]$$

The jamming transition occurs at J=1, when J<1 the system is also jammed and the system is considered unjammed for J>1.

1.6.2.4. Kinetic Monte Carlo simulations

We have seen that molecular dynamic simulations are not fitted to obtain results on macroscale injection modelisation, due to their relatively high numerical cost. On the other hand macroscopic model such as plastic one linking the evolution of viscosity with shear rate does not picture the hydrocluster formation, neither dilatant behaviour of the granular material. Model that can make the connection between molecular dynamic simulations and macroscopic ones are called mesoscopic models. They permit to access larger scales while retaining a description of the elementary processes characterizing jamming transition. From a general point of view four ingredients are required to build a mesoscopic model:

- A local yield criterion (occurrence of plastic rearrangements).
- An elastic coupling (elastic reaction of the granular matrix)
- An evolution rule for local yield criterion (plastic rearrangement change locally amorphous structures)
- A dynamical rule (take into account the time of the elementary process)

During extrusion of cement materials shear fractured band has been observed (same as the one observed in plastic deformation of amorphous metals). Indeed one explanation is that the solid present area of high stresses and a solution to minimize its energy is to deform

along specific surfaces which could be an explanation to fracture that has been observed [26] .

A numerical method allowing to study the time dependent deformation of amorphous materials is known as Kinetic Monte Carlo and have been used to study the deformation of glassy metals [68] [69] [70]. The main advantage of this method if applied to injection of cementitious material is that a settling rate law could be associated to the frictional plastic deformations of the material, allowing to picture the mechanical properties evolution with time as it is done for glasses.

A KMC algorithm could be used to model any process evolving with time, those process occurs with a known rate (plastic deformation of a granular material). An activation rate law has to be written to describe deformation of a group of granular materials, this activation rate is calculated based on the stress state. Then the Kinetic Monte-Carlo algorithm consist in generating a random number in order to define if the plastic deformation process of an element can occur or not and the other one permit to calculate the elapsed time for this process. Law specifying the deformation direction should be written and the stress and strain state evolution of the system as to be solved using an FEA code.

No paper have been found on the simulation of deformation of fresh cement materials via the use of KMC algorithm such as the one used for the deformation of glassy metals. Nevertheless it is trusted that an adaptation could be developed in order to picture both microscopic and macroscopic deformations.

Conclusion chapter I

Through this first part we have seen that cement paste rheological behaviour is influenced by a lot of parameters such as solid/liquid ratio, solid particle size and shape, liquid viscosity, etc. Moreover its processing (for instance injection in vertebrae) could lead to undesired phenomenon such as LPM and jamming. Thus the cement engineer will have to manipulate the formulation and processing conditions (ram velocity, syringe geometry) in order to lie within the window of acceptable product quality and easy process. Nevertheless, doing so could require a lot of trial and error tests, and standardised approach often fail to identify problems for these complex materials.

It would be naïve to think that there exists one universal equation to describe the deformation and flow of cementitious materials given their complexity. However, realisation of a wide range of tests and exploitation of the data can allow to set a number of predictive equations associated to certain families of cement. The use of deformation and flow measurement devices helps the cement engineer to define the phenomenon of jamming and LPM and identify their influencing parameters which we have been summarized in this first chapter.

It will be time before developing simulations capable of adequately represent individual particles of cement materials. Thus use representative equations, development of models and methods describing continuum mechanics are of interest in order to predict the occurrence of LPM or Jamming. We have seen that numerous theory derived from soil mechanics or plastic extrusion existed. Nevertheless, those theories still need to be developed, simplified, or include physical phenomena, this justify our work in the second chapter where we intended to meliorate the theory developed by Perrot, and we explained a multiphase flow modelisation approach within COMSOL® in order to study injection of cement in VP and KP processes. Finally the third chapter present experiments plans and methodology that should be employed in order to develop an optimum paste formulation and syringe geometry.

Bibliography chapter 1

[1] "Preliminary note on the treatment of vertebral angioma by percutaneous acrylic vertebroplasty" P.Galibert, H. Deramond, P. Rosat, Neurochirurgie,33, p166-168, 1987

[2] "Thermal analysis of bone cement polymerisation at the cement-bone interface."Stańczyk M, van Rietbergen B, J. Biomech, 37, p 1803-1810, Dec 2004

[3] "New developments in calcium phosphate bone cements: approaching spinal applications", M.D. Vlad, PhD thesis, Universitat Politècnica de Catalunya, 2008

[4] "Mechanisms underlying the limited injectability of hydraulic calcium phosphate paste" , Habib.M, Gamal.B, Gitzhofer.F, Bohnner.M, Acta Materialia Inc. April 2008

[5] "Injectability evalutation of tricalcium phosphate bone cement", H.L Rocha Alves, L.A dos Santos, C.P Bergmann, Journal material science, Mater Med, 2007.

[6] "Factors influencing paste extrusion pressure and liquid content of extrudate in freeze-form extrusion fabrication". H. Liu, J. Liu, M.C. Leu, R. Landers, T. Huang, Int J Adv Manuf Technol, vol 67, p899-906, 2013

[7] "Injectability of calcium phosphate pastes", M.Bohner, G.Baroud, Biomaterials 26, p 1553-1563, 2005

[8] "Liquid migration in paste extrusion: Advanced materials",A.S Burbidge, J. Bridgwater, Z. Saracevic, chem. eng. research & design, vol 73, p810-816, 1995

[9] "A brief update on biomechanisms underlying cement injection and leakage in Vertebroplasty", Gamal Baroud, 2005

[10] "Liquid phase migration in the extrusion and squeezing of Micro-Crystalline cellulose pastes", S. Mascia, M.J. Patel, S.L Rough, P.J. Martin D. I. Wilson, Eur. J. Pharm. Sci. vol 29, p22-34, 2006

[11] "Flow instabilities in capillary flow of concentrated suspensions", Rheol. Acta, vol 33, p48-59, 1994

[12] "Extrusion of pastes with a piston extruder for the determination of the local solid and fluid concentration, the local porosity and saturation and displacement profiles by means of NMR imaging",J. Götz, W. Kreibich, M.Peciar, Rheol Acta (2002), p134-143,

[13] "Mortar physical properties evolution in extrusion flow", A. Perrot, C. Lanos, Y. Melinge, P. Estellé,, Rheol. Acta 46, 8 , p1065-1073, 2007

[14] "Visualisation de la consolidation durant l'extrusion des matériaux à base cimentaire", A.Perrot, XXIVème rencontres universitaires de génie civil, 2006.

[15] "The squeezing test, a tool to identify firm cement based material rheological behaviour and evaluate their extrusion ability",Z. Toutou, N. Roussel, C. Lanos, Cement and concrete research, 2004

[16] "Effects of liquid phase migration on extrusion of microcrystalline cellulose pastes", S.L Rough, J. Bridgwater, D.I Wilson, Intl. J. of Pharm., vol 204, p117-126, 2000

[17] Terzaghi, Karl (1943), *Theoretical soil mechanics*, John Wiley&Sons, Inc., p. 265

[18] "Visualisation de la consolidation durant l'extrusion des matériaux à base cimentaire", A.Perrot, XXIVème rencontres universitaires de génie civil, 2006.

[19] "Extrusion of pastes with a piston extruder for the determination of the local solid and fluid concentration, the local porosity and saturation and displacement profiles by means of NMR imaging",J. Götz, W. Kreibich, M. Peciar, Rheol. Acta , 41: p134-143, 2002

[20] "Internal flow characteristics of a plastic Kaolin suspension during extrusion. "B.D. Rabideau, P. Moucheront, F. Bertrand, S. Rodts, Y. Mélinge, C. Lanos, P. Coussot, J. Am. Ceram. Soc., vol 95, p494-501.

[21] "Some factor controlling the injectability of calcium phosphate bone cements", I. Khairoun, M.G Boltong, F.C.M Driessens, J.A. Planell

[22] "Drainage phenomenon of pastes during extrusion", Z. Chen, K. Ikeda, T. Murakami, T. Takeda, Journal of material science 35, p 2517-2523, 2000

[23] "Un critère basé sur le temps de drainage pour l'extrusion des matériaux à base cimentaire", A. Perrot, D. Rangeard, Y. Mélinge, P. Estellé, C. Lanos, 25ème rencontre de l'AUGC, Bordeaux, 2007

[24] "Liquid phase migration in the extrusion of icing sugar", M.Bayfield, J.A Haggett, M.J Williamson, D.I. Wilson, A. Zargar, Trans IChemE, vol 76, Part C, 1998.

[25] "The rheology of wet powders: a measuring instrument, the compresso-rheometer", M. Delalonde, G. Baylac, B. Bataille, M. Jacob, A. Puech, Intl. J. of Pharm., vol 130, p147-151, 1996

[26] "Paste extrusion through non-axisymmetric geometries: Insights gained by application of a liquid phase drainage criterion", P.J. Martin, D.I Wilson, P.E. Bonnett, Powder Technology, vol 168, p64-73, 2006

[27] "Dilatancy of concentrated suspension with newtonian matrices", U. Yilmazer, D.M. Kalyon, Polymer composites,vol 12, p 226-232, 1991

[29] "Gelation, Shear-Thinning and Shear-Thickening in cement slurries" D.Lootens, P. Hébraud, E. Lécolier, H. Van Damme, Oil & Gas Science and Technology, Vol 59, p31-40, 2004

[30] "Giant stress fluctuations at the jamming transition", D. Lootens, H. Van Damme, P. Hébraud, Physical review letters, vol90,number 17, 2003

[31] "Orrifice jamming of fluid-driven granular flow", P.G. Lafond, M.W. Gilmer, C.A. Koh, E.D Sloan, D.T. Wu, Physical review E87, 2013

[32] "Shear thickening in concentrated suspensions: phenomenology, mechanisms, and relations to jamming", E. Brown, H.M. Jaeger, Journal of condensed matter, 2013

[33] "Flow behavior of concentrated (dilatant) suspension", A.B Metzner, M. Whitlock, Transaction of the society of rheology, p239-254, 1958

[34] "On the dilatancy of media composed of rigid particles", O. Reynolds, Phil. Mag. vol 20, 469, 1885

[35] "Rheological classification of concentrated suspensions and granular pastes", P.Coussot, C.Ancey, Physical review E, Vol59(4), 1999

[36] "Microstructural theory and the rheology of concentrated coilloidal suspensions", E. Nazockdast, J.Morris, Royal society of chemistry, 2012

[37] "Maldistribution of fluids in extrudates", M.J Patel, J. Wedderburn, S. Blackburn, D.I Wilson, J. of the Euro. Ceram. Soc., vol 29, p967-941, 2009.

[38] "Blockage of constriction by particles in fluid-solid transport", J. Dai, J.R. Grace, Intl. J. of. Multiphase Flow, 36, p78-87, 2009

[39] "Particle size and shape effects in medical syringe needles: experiments and simulations for polymer microparticle injection", M.A. Whitaker, P. Langston, A. Naylor, B.J. Azzopardi, S.M, Howdle, J Mater Sci: Mater Med 22, p 1975-1983, 2011

[40] "Effect of interparticle cohesive forces on the flow behaviour of Powder"O. Molerus, Pow. Tech, 20, p161-175, 1978

[41] "Capillary forces - modeling and application in particulate technology", H. Schubert, Pow. Tech vol37, p105-116, 1984

[42] "The effect of wall and rolling resistance on the couple stress of granular materials in vertical flow", Zhu, H.P and Yu, A,B, Physica A, 325, 347-360 2003

[43] "Steady state granular flow in a 3D cylindrical hopper with flat bottom using DEM simulation: Microscopic analysis", Zhu, H.P and Yu, A,B, J. Phys. D:Appl. Phys, 37, 1497-1508.

[44] "Jamming during the discharge of granular matter from a silo", I.Zuriguel, A. Garcimartín, D. Maza, L.A. Pugnaloni, J.M Pastor, Physical review E 71, 2005

[45] "Flow and jamming of granular materials in a two-dimensional hopper", Junyao Tang, Thesis Duke Univ, 2012

[46] Aproximación computacional al estudio de la inyectibilidad de cementos óseos. S. Laforgue, PFC UPC, 2008

[47] "Steady and transient flow behaviour of fresh cement pastes", N. Roussel, Cement and Concrete Research,35, p1656-1664, 2005

[48] "Rheology of fresh cement and concrete", P.F.G Banfill, Rheology reviews, p61-130, 2006

[49] "Rheology of semi-solid fresh cement pastes and mortars in orifice extrusion", X. Zhou, Z. Li, M. Fan, H. Chen, Cem and Concrete composites, 37, p304-311, 2013

[50] "A model describing liquid phase migration within an extruding microcrystalline cellulose paste", S.L Rough, D.I Wilson, J. Bridgwater, Trans IChemE, Vol 80, Part A, 2002

[51] "Prediction of extrusion load and liquid phase filtration during ram extrusion of high solid volume fraction pastes", H.Khelifi, A. Perrot, T. Lecompte, D. Rangeard, G Ausias, Powder Technology, vol 249,p258-268, 2013

[52] "Extrusion criterion for firm cement-based materials", A. Perrot, D. Rangeard, Y. Mélinge, P. Estellé, C. Lanos, Applied Rheology, 19, 2009

[53] "Ram extrusion force for a frictional plastic material: model prediction and application to cement paste", A. Perrot, C. Lanos, P. Estellé, Y. Melinge, Rheol Acta, vol 45, p457-467, 2006

[54] "Modelling of paste flows subject to liquid phase migration", M.J Patel, S. Blackburn, D.I Wilson, Intl, J for Num. Met. in Eng. vol 72, p1157-1180, 2007

[55] "Die entry pressure drops in paste extrusion", D.J Horrobin, R.M Nedderman, Chem. Engineering, vol53, p3215-3225, 1998

[56] "Properties of porous media affecting fluid flow", R.H Brooks, C.T Corey, J. Irrig Drain div am soc civ eng, vol 92, 1966

[57] Applications of soil mechanics theory to the processing of ceramics.C P Wroth; G T Houlsby; University of Oxford. Department of Engineering Science.

[58] Granular matter: a tentative view. De Genes, Rev. Mod. Phys, 71, p374-382, 1999

[59] "The granular silo as a continuum plastic flow: the hour-glass vs the clepsydra", L. Staron, P-Y Lagrée, S. Popinet, 2012

[60] "Paste engineering:Multi-phase materials and multi-phase flows", D.I Wilson, S.L Rough, The Can. J. of Chem. Eng., Vol 90, 2012

[61] "Consistency meaurements of rubber benzene solutions", W.H Herschel, R. Bulkley, Kolloid.Z, vol 39, p291-300, 1926

[62] "Rheological behaviour and concentration distribution of paraffin slurry in horizontal rectangular channel",M.N. El Boujaddaini, P. Haberschill, A. Mimet, Intl. J. of Dyn of Fluids, vol 6, p145-160

[63] "A flow equation for pigment- oil suspensions of the printing ink type", W.Casson, Rheology of disperse systems, Pergamon, London, 1959

[64] "Influence of specific surface and concentration of solids upon the flow behaviour of cement pastes", W. Vom berg, Mag. Concr. Res. 31, p211-216, 1979

[65] "Analytical models for estimating yield stress of high performance pseudoplastic grout", A. Yahia and Khayat K.H, Cem. Conc. Res. 31 , p731-738, 2001

[66] "Models for rheological behaviour of concentrated disperse media under shear", D.Quemada, Proc. of XIth Intl. cOngr. on Rheology, Acapulco, Mexico (1984)

[67] "A thermodynamic unification of jamming", K.Lu, E.E Brodsky, H.P Kavehpour, Nature, 2008

[68] "Kinetic Monte Carlo study of activated states and correlated shear-transformation zone activityduring the deformation of an amorphous metal" E.R Homer, D. Rodner, C. A Shuh, MIT Open access articles, 2010

[69] "Three-dimensional shear transformation zone dynamics model for amourphous metals", E.R Homer, C.A Shuh , Modelling and simulation in materials science and engineering, 2010

[70] "Modeling the mechanical behaviour of amorphous metals by shear transfortmation zone dynamics" E.Homer, 2010

2. Two new approaches for the modelisation of LPM and Jamming phenomenon

Introduction

In the first chapter we have seen that a lot of methods exist to model the behaviour or ceramic bone cements. Most of them are based on soil mechanics and use either mathematical description and user-built programs such as the work realized by Perrot et Al. or Benbow and Bridgwater or FEA software implementing material properties in pre-existing codes which use existing theories. In our thesis we tried to approach the problem of cement injection using the two approach in order to be familiarized with them, to feel their power and weaknesses. Nevertheless, even if the comprehension of the existing theory were itself demanding, we tried to either ameliorate existing methods or use new ones. For this we will see how we tried to adapt the work done by Perrot et al. [1] in order to take into account the migration of water forward the cement. In a second part we will present one of the module available in COMSOL® (Euler-Euler two phases laminar flow) as a possible methods to model cement injection, simply considering cement as a particle/fluid system and using existing theories pre-build in the software.

2.1. Mathematical modelisation :use of the QUICK scheme adapted on the work of Perrot et al.

Regarding the work realized by Perrot et al. [1] we realized that even if the model describing the evolution of extrusion force with the ram displacement were in accordance with the experimental results fig.10 nevertheless if we consider the evolution of the void ratio depending on the ram position fig.11 we can see that no migration of water can be observed, and that the model only consider a drying of the cement paste close to the ram. We have decided to numerically solve the void ratio migration occurring in the cement paste during the extrusion process. We consider this phenomenon to be driven by natural

diffusion[1] and non-linear convection[2] induced by pore pressure difference. We used Matlab® and an upper order finite volume differences scheme (QUICK) to solve the problem. Since the extrusion process we want to model is one dimensional we will derive the discretized equations from Navier-Stokes equation in 1D.

2.1.1. Approach of the problem

Based on the recent work realized by Perrot [1] where a drying of the paste near the ram has been considered (water were able to flow through the ram). We wanted to adapt his work to the injection of cements, considering the ram to be waterproof. It has been supposed that instead of observing a simple drying of our cement a liquid migration would be numerically observed. Indeed starting from an initial homogeneous system, the applied axial stress σ_z will induce a stress gradient in the paste, pore pressure gradient in other word, responsible for the fluid migration in the paste. Since the studied phenomena is the variation of water content in a given area of a syringe during the injection of cement we consider the problem as an unsteady convection diffusion problem applied to the void ratio (water content). The main goal were to build a numerical code adapted to our case taking in consideration the theoretical definition describing extrusion of cement described by Perrot [1]

In an effort to model the extrusion force and quantify the liquid phase migration, a 1D model based on consolidation theory developed by Terzaghi in 1943 [2] has been developed [1]. However even if similarities have been observed between experimental and numerical results on the extrusion force, it seems that the boundary condition used in this theory were responsible of an inaccurate description of liquid filtration occurring in the cementitious paste. Recent studies on cementitious paste linked the ability of a fluid to flow through the granular matrix to the permeability[3] of the paste. Permeability is itself strongly linked to the compactness of the packing (void ratio). Injection of cement could be assimilate to an extrusion process in which the cement undergoes compression, an analogy was made between consolidation theory developed by Terzaghi [2] and the compressed material.

[1] Spontaneous net movement of a quantity down its concentration gradient.
[2] Transfert of a property by matter movement in a middle.
[3] K capacity of a fluid to filtrate through a media

According to the Terzaghi consolidation theory the total axial pressure acting on a saturated layer could be divided between the effective stress $\sigma_z^{'}$ corresponding to the stress carried by the grains, and the pore pressure *u* corresponding to the stress carried by the fluid phase.

At the beginning of the process pore pressure carries the total stress, when volume fraction of grains is high enough contact between grains occurs and stress is transferred from liquid phase to the granular skeleton.

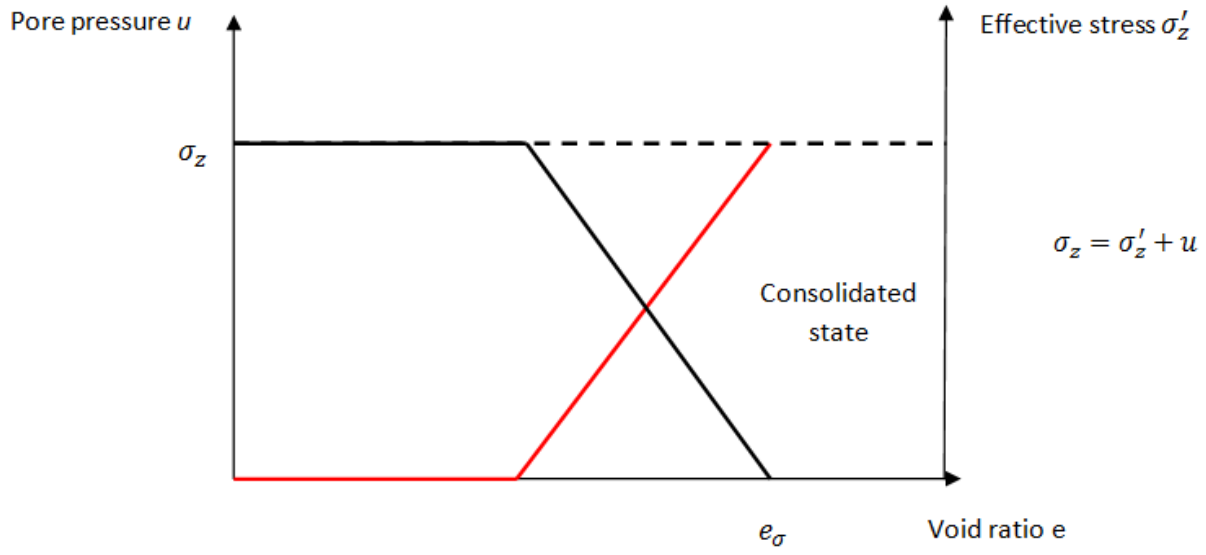

Figure 17: Evolution of pore pressure and effective stress as a function of void ratio during consolidation.

We consider our paste as a granular media filled with a liquid (water in our case), liquid phase flow is described by Darcy law which links the pore pressure gradient to the liquid flow rate:

$$Q_f = \frac{K(e)}{\rho_f g}\frac{d(\Delta u)}{dz} \qquad [2.1]$$

$\boldsymbol{Q_f}$: Volume flow rate $\boldsymbol{K(e)}$: Permeabilityof solid matrix $\boldsymbol{\Delta u}$: Pore pressure gradient

$\boldsymbol{g}$: Acceleration due to gravity $\boldsymbol{\rho_f}$: Interstitial fluid density

Cement paste is a granular media the permeability of it depends on the void ratio, to predict permeability Kozeny-Carman equation [4] is generally preferred, however we choose to use Taylor one eq.[2.2] for this case.

$$K(e) = 10^{\left(\frac{e-e_0}{C_k}\right)} + K_0 \qquad [2.2]$$

$\boldsymbol{K_0}$: Initial permeability of the granular matrix $\boldsymbol{C_k}$: Taylor fitting parameter

Rewriting Darcy's law in order to obtain the relationship between instantaneous variation of void ratio with time and spatial gradient of pore pressure we get eq.2.3:

$$\frac{de}{dt} = \frac{(1+e).K(e)}{\rho_f g}\frac{d^2u}{dz^2} \qquad [2.3]$$

Looking at the parameters defining eq.[2.3] we can see that our problem could be described as a function of time and space if we were able to link the void ration at a position *e(z)* to the pore pressure at this same position *u(z).*

We have seen on fig.17 that the stress were carried by the granular matrix of by the fluid depending on the void ratio in a slice of cement. Therefore in his work Terzaghi introduces a consolidation degree characterising the ratio between actual state of consolidation to the final theoretical state.

$$U(z) = \frac{e_0 - e(z)}{e_0 - e_\sigma(z)} \qquad [2.4]$$

According to Terzaghi theory consolidation degree can be expressed as a function of effective stress σ_z' or pore pressure *u.*

$$U(z) = \frac{\sigma_z'}{\sigma_z} = 1 - \frac{u}{\sigma_z} \qquad [2.5]$$

Relation between pore pressure and void ratio is then easily find and is written in eq.[2.6] :

$$u(z) = \sigma(z)\left[1 - \frac{e_0 - e(z)}{e_0 - e_\sigma(z)}\right] \quad [2.6]$$

Here $\sigma(z)$ represent the stress value at a position z in the syringe. Knowing the total stress distribution in the syringe would allow us to numerically solve the evolution of the system during extrusion.

2.1.2. Computation of the axial stress distribution along the syringe

As seen previously equations describing the axial stress distribution along the syringe has to be written in order to compute the evolution of the system. The description of this stress strongly depends on the rheological and tribological behaviour of a frictional plastic material.

For a cementitious pastes (concentrated granular paste) it has been shown that instantaneous shear resistance results of the combination of three mechanisms:

- Intergranular friction when solid volume fraction is higher than $0.8\phi_{cp}$, ϕ_{cp} being close packing volume fraction.
- Paste cohesion or yield stress $\tau_0(e)$ (dependent on the type of the soil, size of the soil grains and the packing of the soil grains and on the suction properties of the soil).
- Hydrodynamic contribution (not considered here because ram velocity is lower than ram velocity.

In 1773 Coulomb linked the intergranular friction to the normal stress acting on the surface of a slice and add it to the yield stress of the granular media in order to describe the shear resistance of a paste in his simple law eq.[2.7] :

$$\tau = \tau_0(e) + \tan\varphi(e).\sigma_N \quad [2.7]$$

$\boldsymbol{\tau_0}$: yield stress	$\boldsymbol{\varphi}$: Internal friction angle	$\boldsymbol{\sigma_N}$: Applied normal stress

Yield stress and internal friction angle are both functions of the solid volume fraction. At the initial state we consider the friction angle φ to be equal to 0 (solid particles are not in contact) and initial value of the Yield stress correspond to the target value defined by Toutou [7] ($\tau_0(e_0) = 20\text{kPa}$), it is also interesting to know the maximal value of these two parameters, meaning when sample if fully compacted and that $e = e_{min}$. It exists a lot of methods permitting to obtain yield stress, they will be described in chapter III.

Evolution of yield stress with void ratio follow an empirical power law permitting the use of a limited number of parameters.

$$\tau_0(e) = a.e^b \qquad [2.8]$$

a and *b* are constants that can be obtained using the initial yield stress and the final one and solving a system of two equations.

Concerning the evolution of the friction angle, a model has been developed to predict the evolution of φ, in this model a simple linear relationship was assumed between the increase of internal friction angle and the void ratio decrease. We consider e_0 to be the value where particles contact start to increase giving the following model.

$$\begin{cases} if\ e < e_0\ : \varphi(e) = 0 \\ else\ : \varphi(e) = \varphi_{max}.\dfrac{e_{min} - e}{e_{min} - e_0} \end{cases} \qquad [2.9]$$

This model is quite simple and has been given for other materials than biocements, future improvement on this model can be intended.

Since we have described theoretically the rheological behaviour of our granular material it is possible to study the stress distribution along the syringe axis. Indeed our we could consider two parts of our syringe, the first one being the barrel where simple plug flow with no internal strain occurs, and the second one being the die zone or shaping zone where the material is formed. The force needed to extrudate our material has two origins, the first one

is the force needed to give the material its shape, it is called plastic force and is noted F_{pl}this force is only dependent on the die geometry has it is assumed that void ratio remains constant in the shaping zone. The second origin comes from the fact that the force has to counter the friction occurring at the wall along the syringe plug area (over the length L1).

Since the shaping force is constant and does not depend on the void ratio, we consider frictional forces as the main parameters responsible for the required extrusion force increase when ram is pushed.

In order to estimate the frictional stress two assumptions have been made:

- Stresses are considered constant in an horizontal layer.

- Radial stress is proportional to the axial stress.

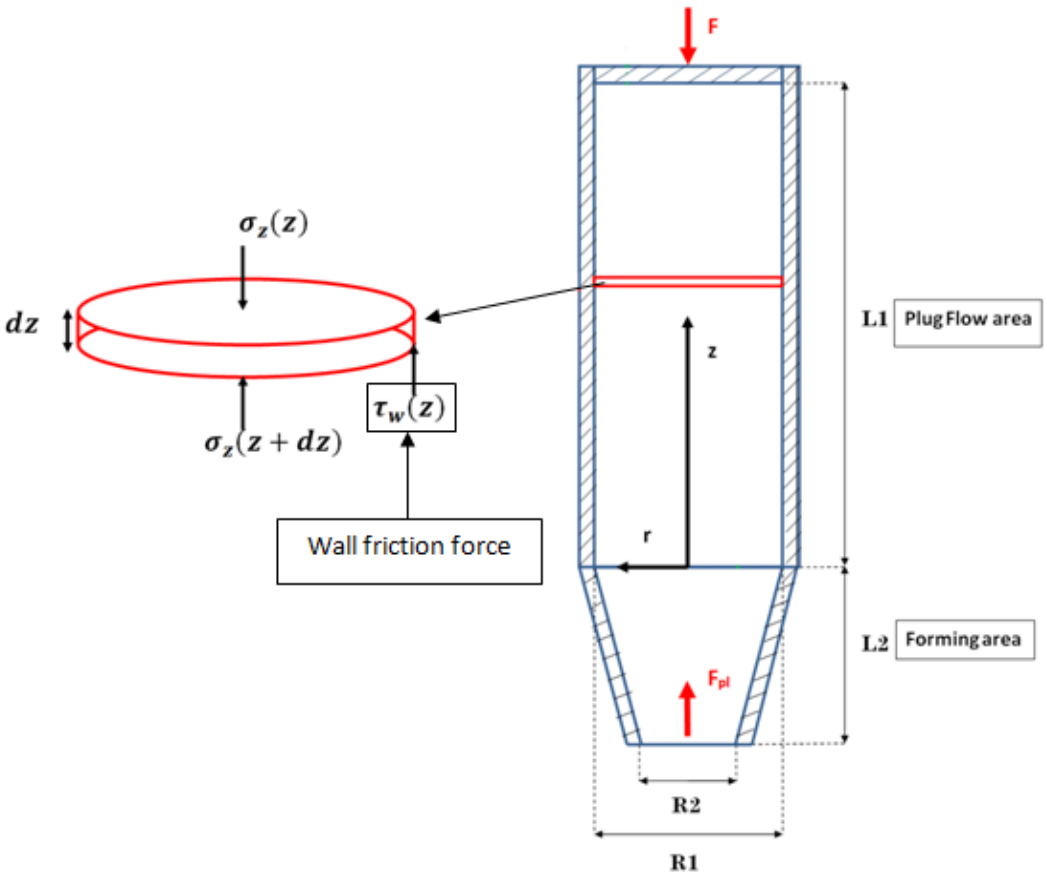

Figure 18:Mathematical solving of cement injection, representation of the space discretization of the syringe.

These two assumptions are the one developed by Janssen's to described granular flows in silos. The proportionality coefficient between radial and horizontal stress were taken from Jacky [8] for its dependence on the friction angle φ. This equivalence is written in eq.[2.10] :

$$\sigma_r(z) = [1 - \sin\varphi(e)].\sigma_z(z) \qquad [2.10]$$

We have now all the elements needed to write the stress equilibrium on an elementary layer. We consider that from a position z to a position z the only variable is the shear stress occurring at the wall. Thanks to eq.[2.7] and eq.[2.10] it is possible to write the stress acting at position *z+dz* as a function of the stress acting at position *z* and link it to the void ratio (see eq.[2.12]).

$$\sigma_Z(z + dz) = \sigma_z(z) + \frac{4dz}{mD1}[\tau_0(e) + \tan\varphi(e).(1 - \sin\varphi(e)).\sigma_z(z)] \qquad [2.11]$$

m : ratio between the wall shear stress and the internal shear

Now linking the stress to the void ratio directly we obtain eq.[12.2] :

$$\sigma_Z(z + dz) = \sigma_z(z) + \frac{4\Delta z}{mD1}\left[ae(z)^b + \tan\varphi_{max}\left(\frac{e_{min} - e(z)}{e_{min} - e_0}\right).\left(1 - \sin\varphi_{max}\left(\frac{e_{min} - e(z)}{e_{min} - e_0}\right)\right).\sigma_z(z)\right] \qquad [2.12]$$

In order to fully describe the axial stress along the syringe, boundary conditions are needed, we know that the required force needed to extrudate our material through the die is F_{pl}, then the stress acting at *z*=0 (at the die entrance) is:

$$\sigma_z(0) = \frac{4F_{pl}}{\pi D^2} \qquad [2.13]$$

The second boundary condition is given at the ram position and correspond to the total required force to extrudate our cement paste.

$$F = \frac{\pi D^2}{4}\sigma_z(z_{ram}) = F_{pl} + F_w \quad [2.14]$$

$\boldsymbol{F_{pl}}$ work of Deng and Liu [11]	$\boldsymbol{F_w}$ integration of the frictional force over L1

The frictional force is obtained summing stress differences over the entire plug zone :

$$F_W = \sum_{z=0}^{z=Ram} \sigma_Z(z+dz) - \sigma_z(z) = \sum_{z=0}^{z=Ram} \frac{4}{mD1}[\tau_0(e) + \tan\varphi(e).(1-\sin\varphi(e)).\sigma_z(z)]\,\Delta z \quad [2.15]$$

For the determination of the shaping force several assumption are made. First of all the material in the die land is supposed to have the same void ratio as at the plug zone exit, this void ratio remain constant in the die land. Moreover it is supposed that the material behaviour does not depend on the shear rate. Shaping force can be divided in two parts:

- The force needed to plastically form the material through a constriction F_{pl1}

- The force friction force acting on the conical die wall F_{pl2}

The summation of these two terms correspond to the shaping force F_{pl}.

$$F_{pl1} = \sqrt{3}\frac{\pi D^2}{2}\tau_0 ln\left(\frac{R1}{R2}\right) \quad [2.16]$$

$$F_{pl2} = \frac{\pi R1^2}{4} \times \left[\frac{4L_0}{R2}\tau_{w0}\left(\frac{R1}{R2}\right)^{2\left(\frac{1-sin\varphi_w}{m_c}-1\right)} + \frac{2\tau_{w0}cos\theta}{tan\theta(tan\varphi_w sin\theta)} ln\left(\frac{R2}{R1}\right)\right] \quad [2.17]$$

$\boldsymbol{m_c} = \tan\theta\dfrac{\cos\theta - \tan\varphi_w \sin\theta}{\tan\varphi_w + \tan\theta}$	$\boldsymbol{\theta}$ being the syringe conical exit angle

It is now possible to link the velocity of the fluid in a slice to the pore pressure dividing eq.[1.2] by the surface by which the fluid go through:

$$V_f = \frac{K(e)}{S\,\rho_f\,g}\frac{d^2u}{dz^2} \qquad [2.18]$$

Using a central differencing scheme to evaluate the second derivative of pore pressure regarding z:

$$\frac{d^2u}{dz^2} = \frac{u(z+dz) - 2u(z) + u(z-dz)}{(dz)^2} \qquad [2.19]$$

And replacing the pore pressure at position *z* by its expression in eq.[2.19]

$$\frac{d^2u}{dz^2} = \frac{\sigma_z(z+dz)\times\left(\frac{e_0 - e(z+dz)}{e_0 - e_\sigma(z+dz)}\right) - \sigma_z(z)\times\left(\frac{e_0 - e(z)}{e_0 - e_\sigma(z)}\right) + \sigma_z(z-dz)\times\left(\frac{e_0 - e(z-dz)}{e_0 - e_\sigma(z-dz)}\right)}{(dz)^2} \qquad [2.20]$$

$$\frac{d^2u}{dz^2} = \frac{\sigma_z(i+1)\times\left(\frac{e_0 - e(i+1)}{e_0 - e_\sigma(i+1)}\right) - 2\sigma_z(i)\times\left(\frac{e_0 - e(i)}{e_0 - e_\sigma(i)}\right) + \sigma_z(i-1)\times\left(\frac{e_0 - e(i-1)}{e_0 - e_\sigma(i-1)}\right)}{(dz)^2} \qquad [2.21]$$

2.1.3. Numerical scheme

We have now the expression of the velocity of the flow of water through a surface of our discretized domain. We have all the elements needed to solve our problem as a Convection-Diffusion problem since we have the velocity of the flow which is not constant in our case but depends on the permeability, the stress state and the void ratio content of the paste.

For this we should spatially and temporally discretize our problem. It has been reported that liquid phase migration principally occurs in the plug. Thus we choose to discretize only the plug area of our syringe. At t=0 void ratio is the same in every discretized element of the syringe. Thus permeability is also homogeneous in over the plug area. For numerical purpose discretization in space is represented by the letter i while discretization in time has been represented by the letter j. The plug zone of the syringe at t=0 can be represented as on fig.19.

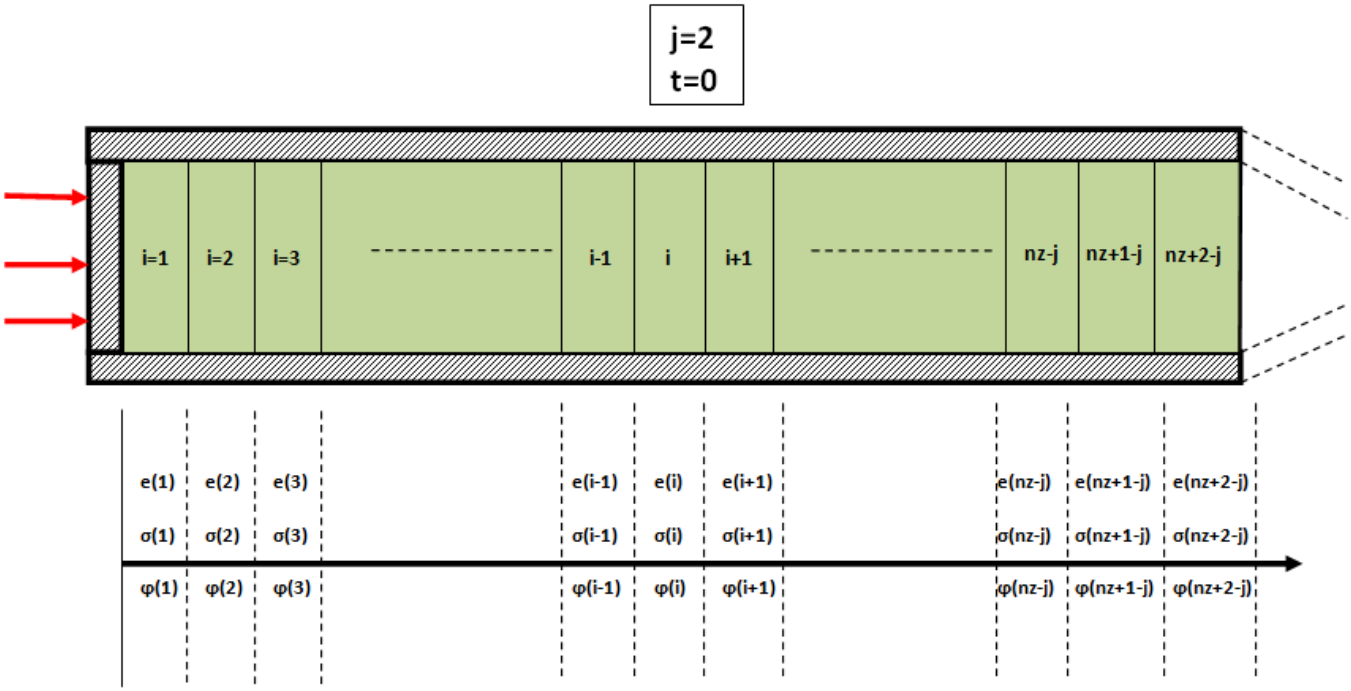

Figure 19: Numerical discretization of the syringe for t=0, cement is initially homogenised, void ratio is the same everywhere in the plug zone.

From this initial state several numerical steps will be realized at each ram advancement. And calculation will be realized based on the void ratio of the slice. If we describe the process in a simple manner it would be divided in 5 steps:

1. Void ratio in each slice at time t are used to calculate permeability and stress state in each slice at time t thanks to eq.[2.2] and eq.[2.12] respectively.

2. Stress state and permeability are used to compute velocity of void ratio in each slice at time t thanks to eq.[2.18]

3. Fluid velocity is used in the quadridiagonal matrix to solve flux problem, flux at time t is computed using flux at (t-1)

4. Void ratio at the end of Δt obtained by summing previous void ratio state with change rate of void ratio.

5. Time iteration and start of a new process similar to the previous one on a reduced domain.

All those steps have been summarized in the diagram presented on fig.20

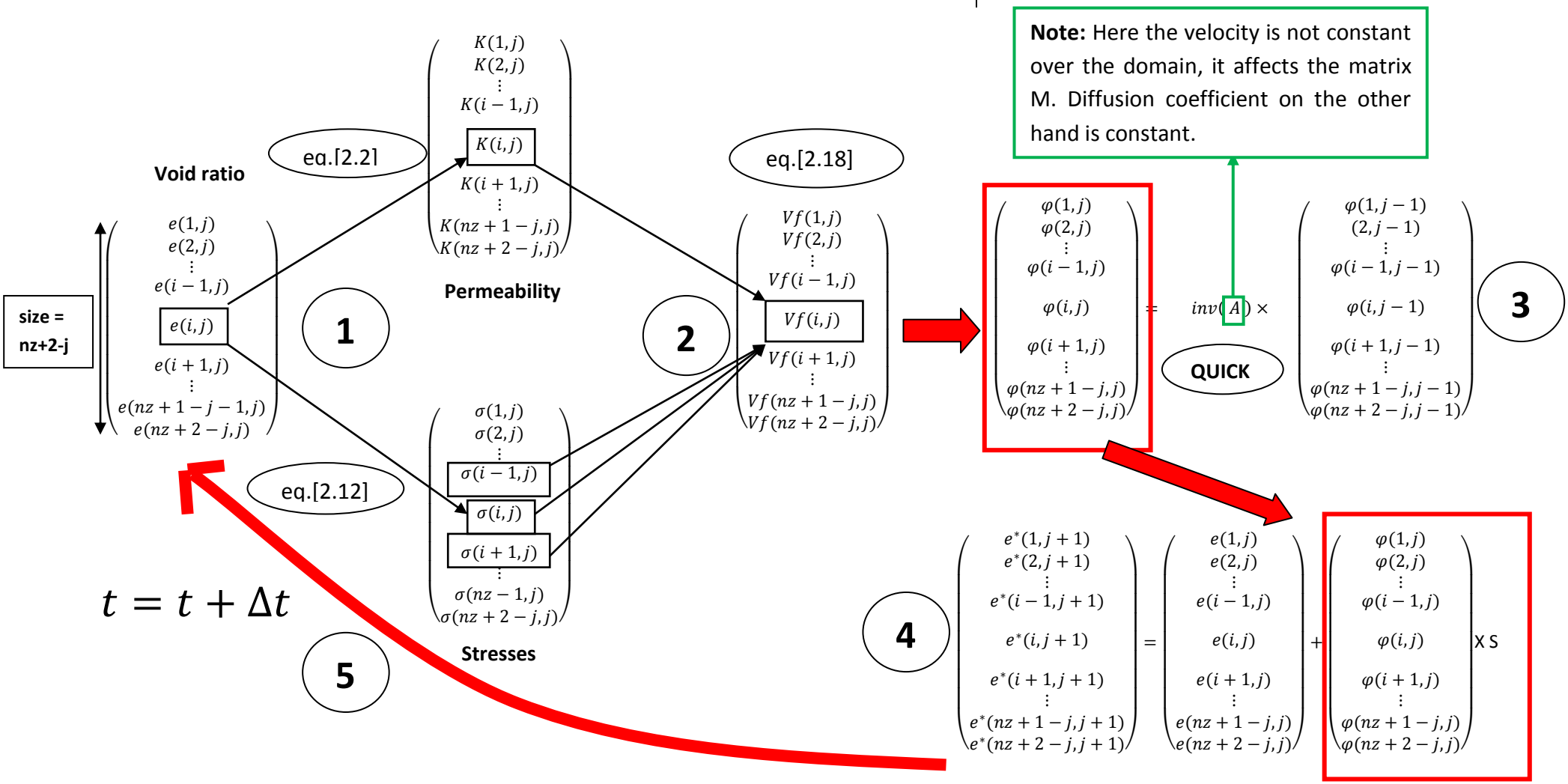

Figure 20: Diagram representing the numerical calculation realized during QUICK mathematical modelisation of cement injection.

After j steps the syringe present a new configuration where slice have been extruded. And where the value of void ratio (permeability, stress...) on each slice also changed consequently if ram velocity is sufficiently low. Indeed if injection velocity (Ram velocity) is high enough all the parameters remains constants during injection and we can consider the injection process to be a success.

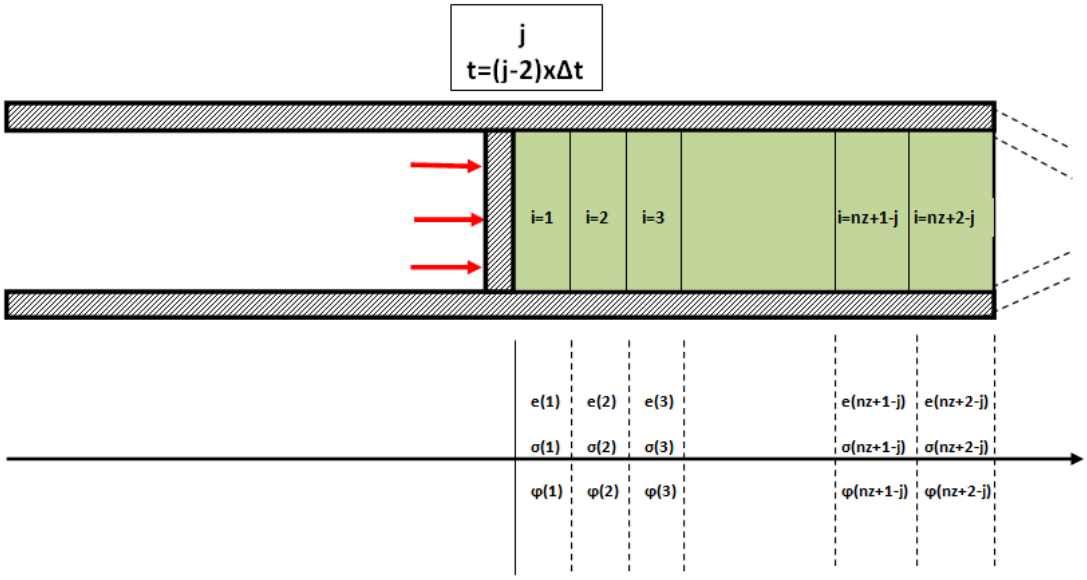

Figure 21: New numerical discretization of the syringe for a given time. Domain is reduced and properties such as void ratio have evolved

2.1.4. The finite volume element method - QUICK scheme.

In the theory developed by Perrot cement undergoes compaction and stress state linked to permeability evolution and void ratio describe the evolution of the system. We choose to focus on the migration of water in the paste in the plug area. Meaning that we had to adapt the problem in order to allow flux of water from one slice to another in our discretized syringe.

Computational fluid dynamics has been developed in order to solve the complex flows of fluid in or around given geometry, however the term fluid flow is a very general term it could include any kind of fluid, heat, persons or money by adjusting the definition of the fluid, the geometry of the problem and the definition of what drives it. In our case we study the flux of void in 1D, solving non-linear diffusion-convection problem.

A very general way to write a convection-diffusion problem is the following:

$$\frac{\partial}{\partial t}\int_{Vc} g\,dV + \int_{Sc} g\vec{V}.\vec{n}\,dS = \int_{Vc} q_f\,dV - \int_{Sc} \vec{q_S}.\vec{n}\,dS$$

Accumulation term	Entry-exit balance applied to convection of variable g	Volumic sources (production or sink)	Entry-exit balance of a surface flux of g (generally diffusion)

In our case there is no volumic sources since our problem is a simple extrusion of a fluid with no chemical reaction.

Due to the simple geometry of our problem we choose to solve it using volume differences method, once the domain has been discretized in space it is possible to write for a control volume that:

Void ratio in a control volume after a given time interval Δt = Void ratio in a control volume at the beginning of the time interval Δt + (Amount of e that flows into the control volume during Δt − Amount of e that flows out of the control volume during Δt)

→ Called φ in QUICK scheme

The strategy used to solve the ram advanced is similar to the one used by Rough et al. [8], [9], Perrot et al [1], Benbow et Bridgwater [10] and follows the scheme described in fig.9

When it comes to numerically solve partial differential equations several methods are generally used depending on the physic of the problem. While finite element method is preferred when the problem is solid mechanic. In computational fluid dynamics there are many methods for solving convection-diffusion problems (central differencing, upwind scheme, hybrid scheme, power law scheme and QUICK scheme). QUICK scheme is based on a quadratic interpolation on three points in an implicit scheme. It use finite differences at first and second order as well as Taylor series of our flux function.

In the finite difference scheme, first and second derivative of the flux are given by:

$$\frac{\varphi_{(i+1)} - \varphi_{(i-1)}}{2h} = \varphi'_{(i)} \qquad [2.22]$$

$$\frac{\varphi_{(i+1)} - 2\varphi_{(i)} + \varphi_{(i-1)}}{2h^2} = \varphi''_{(i)} \qquad [2.23]$$

If we write Taylor series of our flux at second order we have eq.[2.24]:

$$\varphi_{(i)} = \varphi_{(i)} + h \times \varphi'_{(i)} + h^2 \times \varphi''_{(i)} \qquad [2.24]$$

Replacing the first and second derivative by the one given by finite differences we obtain eq.[2.25]:

$$\varphi_{(i)} = \varphi_{(i)} + h \times \frac{\varphi_{(i+1)} - \varphi_{(i-1)}}{2h} + h^2 \times \frac{\varphi_{(i+1)} - 2\varphi_{(i)} + \varphi_{(i-1)}}{2h^2} \qquad [2.25]$$

Expressing eq.[2.25] as a function of z we have eq.[2.26]:

$$\varphi_{(z)} = \varphi_{(z)} + h \times \frac{\varphi_{(z+h)} - \varphi_{(z-h)}}{2h} + h^2 \times \frac{\varphi_{(z+h)} - 2\varphi_{(z)} + \varphi_{(z-h)}}{2h^2} \qquad [2.26]$$

Changing the variable by $Z = z + \frac{h}{2}$

$$\varphi_{(z)} = \varphi_{(z-\frac{h}{2})} + \frac{h}{2} \times \frac{\varphi_{\left(z+\frac{h}{2}\right)} - \varphi_{(z-\frac{3h}{2})}}{2h} + \frac{h^2}{4} \times \frac{\varphi_{(z+\frac{h}{2})} - 2\varphi_{(z)} + \varphi_{(z-\frac{3h}{2})}}{2h^2} \qquad [2.27]$$

$$\varphi_{(z)} = \varphi_{(z-\frac{h}{2})} + \frac{3\varphi_{(z+\frac{h}{2})} - 2\varphi_{(z-\frac{h}{2})} - \varphi_{(z-\frac{3h}{2})}}{8} \qquad [2.28]$$

In our case we will use this three points interpolation methods only to treat convective flux, indeed diffusion does not need any special consideration.

Convective flux is given as a function of φ_e et φ_w and φ_{ww}, *e,w* and *ww* stand for east, west and west-west.

EAST

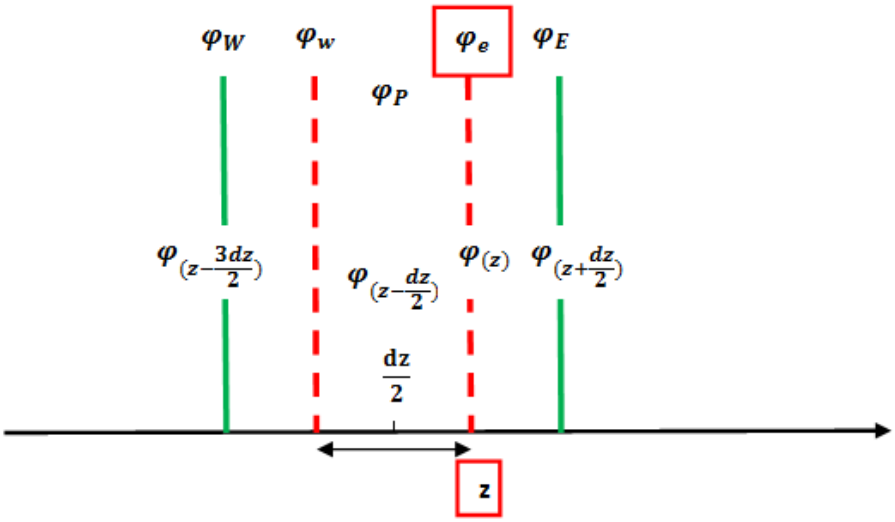

Figure 22: Discretization used for the calculation of the east flux

Applying eq.[2.28] on the east interface one can obtain:

$$\varphi_e = \varphi_P + \frac{1}{8} \times (3\varphi_E - 2\varphi_P + \varphi_W) \qquad [2.29]$$

WEST

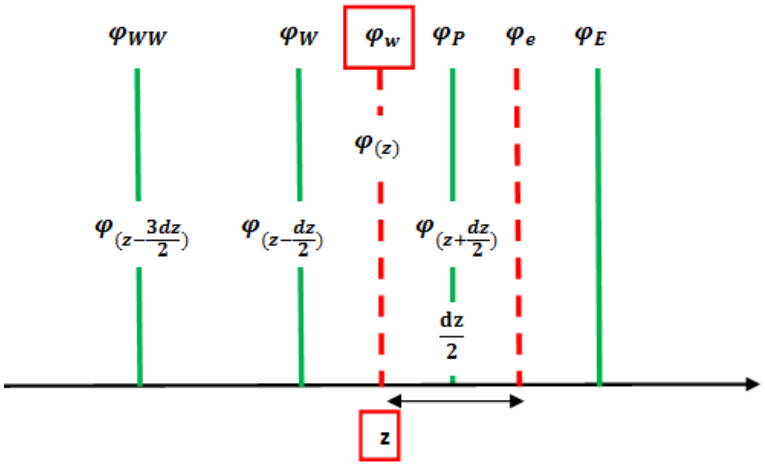

Figure 23: Discretization used for the calculation of the west flux.

Similarly applying eq.[2.28] on the west interface one can obtain:

$$\phi_w = \phi_W + \frac{1}{8} \times (3\phi_P - 2\phi_W + \phi_{WW}) \qquad [2.30]$$

We have now the two required expressions needed to estimate our flux.

The flux at an interface could be written in a more general form eq.[2.31]

$$\varphi_{face} = \frac{6}{8}\varphi_{i-1} + \frac{3}{8}\varphi_i - \frac{1}{8}\varphi_{i-2} \qquad [2.31]$$

2.1.4.1. Resolution of an equivalent advection diffusion problem.

In this part we will try to discretize the Navier Stokes equations associated with the problem in space and time. Starting from the general equation of Navier-Stokes:

$$\frac{\partial}{\partial t}\int_{Vc} g\, dV + \int_{Sc} g\,\vec{V}.\vec{n}\, dS = \int_{Vc} q_I\, dV - \int_{Sc} \overrightarrow{q_s}.\vec{n}\, d$$

Then integrating each terms of the equality in space (From west to east) and in time (from t to t+Δt. We can obtain:

$$\int_w^e \int_t^{t+\Delta t} \frac{\partial g}{\partial t} dt dV + \int_w^e \int_t^{t+\Delta t} g\vec{V}.\vec{n}\, dS = \int_w^e \int_t^{t+\Delta t} q_I\, dt dV + \int_w^e \int_t^{t+\Delta t} k\frac{dg}{dx}\,\vec{x}.\overrightarrow{n_{ext}}\, dt dS$$

1 2 3 4

Each of the number corresponding to:

- **1:** Accumulation term
- **2:** Entry-exit balance applied to convection of variable g
- **3:** Volumic sources (production or sink)
- **4:** Entry-exit balance of a surface flux of g (generally diffusion)

1

The accumulation term of our problem can be discretized as follow:

$$\int_w^e \int_t^{t+\Delta t} \frac{\partial g}{\partial t} dt dV = \rho(\varphi_p^1 - \varphi_p^0)\Delta x \qquad [2.32]$$

$$\int_w^e \int_t^{t+\Delta t} g\vec{V}.\vec{n}\, dS = (U_e\varphi_e - U_w\varphi_w)\Delta t \qquad [2.33]$$

2

Now, having introduced QUICK scheme we have seen that:

$$\varphi_e = \varphi_P^1 + \frac{1}{8}(3\varphi_E - 2\varphi_P^1 - \varphi_W)$$

$$\varphi_w = \varphi_W + \frac{1}{8}(3\varphi_P^1 - 2\varphi_W - \varphi_{WW})$$

Then rewriting eq.[2.33]:

$$\int_w^e \int_t^{t+\Delta t} \frac{\partial \varphi}{\partial t} dt dV = \left[U_e\left(\varphi_P^1 + \frac{1}{8}(3\varphi_E - 2\varphi_P^1 - \varphi_W)\right) - U_w\left(\varphi_W + \frac{1}{8}(3\varphi_P^1 - 2\varphi_W - \varphi_{WW})\right)\right]\Delta t \qquad [2.34]$$

This equation correspond to the convective term of our problem.

3

We consider our problem to have no source since the syringe is closed and the ram is simply pushing the cement, water will only flow in the barrel without being created or added.

4

We obtain the discretized expression of our diffusive term applying the centred difference method to the surface of our mesh. With $D = \frac{k}{\Delta x}$. k being the diffusion coefficient.

$$\int_w^e \int_t^{t+\Delta t} k\frac{dg}{dx}\vec{x}.\overrightarrow{n_{ext}}\, dt dS = [D_e(\varphi_E - \varphi_P^1) - D_w(\varphi_P^1 - \varphi_W)]\Delta t \qquad [2.35]$$

Finally if we write the discretized Navier-Stokes equation we obtain eq.[2.36]:

$$\rho\left(\varphi_p^1-\varphi_p^0\right)\frac{\Delta x}{\Delta t}+U_e\left(\varphi_P^1+\frac{1}{8}(3\varphi_E-2\varphi_P^1-\varphi_W)\right)-U_w\left(\varphi_W+\frac{1}{8}(3\varphi_P^1-2\varphi_W-\varphi_{WW})\right) = D_e(\varphi_E-\varphi_P^1)-D_w(\varphi_P^1-\varphi_W) \quad [2.36]$$

Rearranging the terms we obtain the discretized equation relative to our problem eq.[37.2]:

$$\varphi_p^0\frac{\Delta x}{\Delta t}\rho = \varphi_P^1\left(\frac{6}{8}U_e-\frac{3}{8}U_w+D_e+D_w+\rho\frac{\Delta x}{\Delta t}\right)+\varphi_E\left(\frac{3}{8}U_E-D_e\right)+\varphi_W\left(\frac{1}{8}(-U_e-6U_w)-D_W\right)-\varphi_{WW}\frac{U_W}{8} \quad [2.37]$$

For a better visibility we rewrite eq.[2.37] using coefficients eq.[2.38]

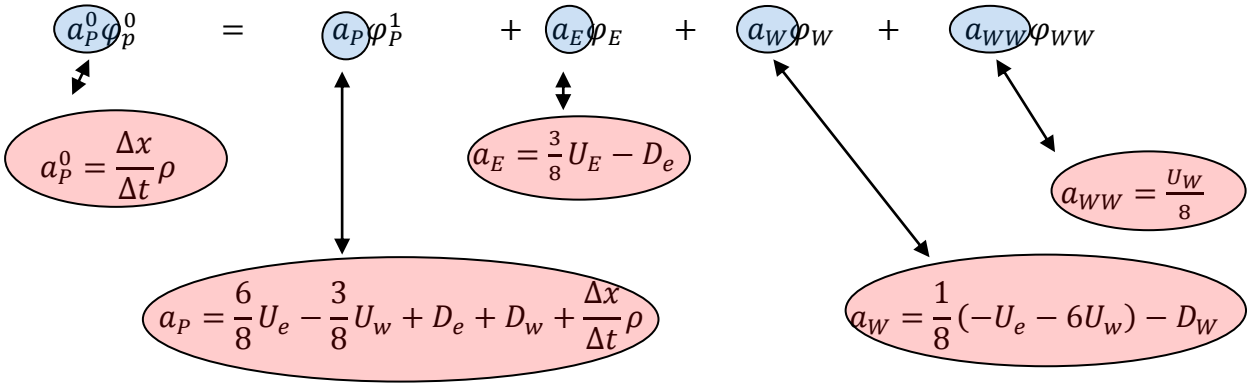

This discretized equation will be used to compute the flux of void over the entire domain, nevertheless, equation has to be modified on the boundary of the domain in z=0 and z=z(RAM) according to the boundary condition imposed by the physic of the problem.

At point z=z(RAM) no flux of void is permitted through the ram .

At point z=0 we consider the flux gradient to be 0, meaning that the flux of void from the barrel to the conical die does not change, it correspond to a Neumann boundary condition.

Balance for the 1st volume

The flux value on the interface of the first volume is given at the west by $\varphi_w = \varphi_A$, but there is no node on the west to evaluate the flux φ_e at east interface. Leonard suggest to use a mirror like linear extrapolation illustrated on fig.24

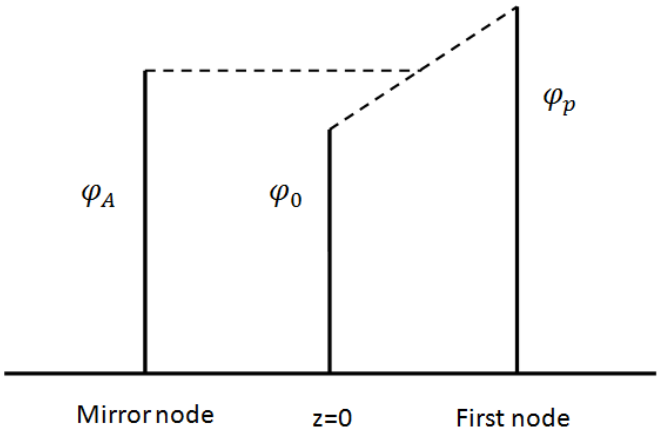

Figure 24: Representation of the mirror condition used at the first node.

According to fig.24 the flux φ_A correspond to the average of flux between φ_P et φ_0 meaning that $\varphi_A = \frac{\varphi_p + \varphi_w}{2}$. We have found the west flux (corresponding to φ_0) that were missing to calculate the east flux φ_e .

$$\varphi_e = \frac{6}{8}\varphi_P^1 + \frac{3}{8}\varphi_E - \frac{1}{8}(2\varphi_A - \varphi_P) \qquad [2.38]$$

$$\varphi_e = \frac{7}{8}\varphi_P^1 + \frac{3}{8}\varphi_E - \frac{2}{8}\varphi_A \qquad [2.39]$$

Using the mirror scheme we can write eq.[2.40] for the first volume:

$$k\frac{\partial\varphi}{\partial x}\Big|_A = \frac{D_A^*}{3}(9\varphi_P - 8\varphi_A - \varphi_E) \qquad [2.40]$$

With $D_A^* = \frac{k}{\Delta x}$ and k being the diffusion coefficient.

Using eq.[2.37] and eq.[2.39] in eq.[2.40] we can write the discretized equation for the first volume eq.[41.2]:

$$\rho\left(\varphi_p^1-\varphi_p^0\right)\frac{\Delta x}{\Delta t}+U_e\left(\varphi_P^1+\frac{1}{8}\left(3\varphi_E-\varphi_P^1\right)\right)-U_A\varphi_A \;= \\ D_e\left(\varphi_E-\varphi_P^1\right)-\frac{D_A^*}{3}\left(9\varphi_P-8\varphi_A-\varphi_E\right) \qquad [2.41]$$

Rearranging the terms we obtain eq.[2.42] :

$$\varphi_p^0\frac{\Delta x}{\Delta t}\rho=\varphi_P^1\left(\frac{7}{8}U_e+D_e+3D_A^*\right)+\varphi_E\left(\frac{3}{8}U_e-D_e-\frac{D_A^*}{3}\right)+\varphi_A\left(-U_A-\frac{8}{3}D_A^*\right) \qquad [2.42]$$

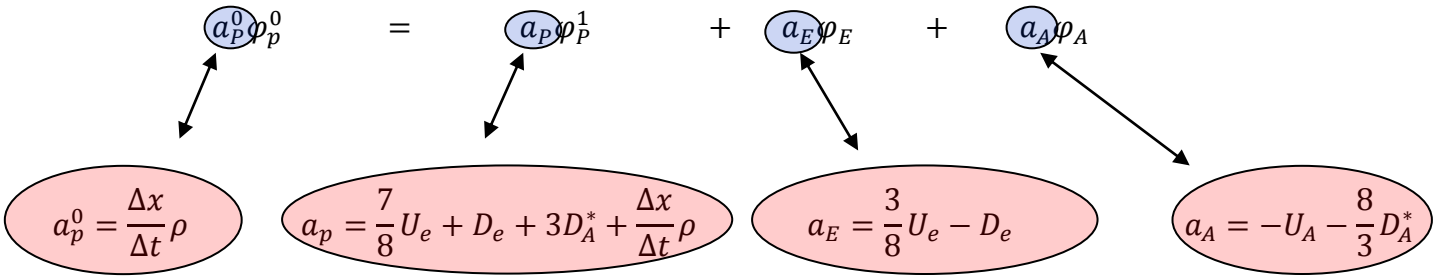

Balance for the 2nd volume

The discretization made on the second volume has to be adjusted to take into account the specific equations used to evaluate the convective flux through the shared interface between volume 1 and 2.

$$\rho\left(\varphi_p^1-\varphi_p^0\right)\frac{\Delta x}{\Delta t}+U_e\left(\varphi_P^1+\frac{1}{8}\left(3\varphi_E-2\varphi_P^1-\varphi_W\right)\right)-U_w\left(\varphi_W+\frac{1}{8}\left(3\varphi_P^1-2\varphi_W\right)\right) \\ =\; D_e\left(\varphi_E-\varphi_P^1\right)-D_w\left(\varphi_P^1-\varphi_W\right) \qquad [2.43]$$

$$\varphi_p^0\frac{\Delta x}{\Delta t}\rho=\varphi_P^1\left(\frac{6}{8}U_e-\frac{3}{8}U_w+D_e+D_w+\frac{\Delta x}{\Delta t}\rho\right)+\varphi_E\left(\frac{3}{8}U_E-D_e\right)+\varphi_W\left(\frac{1}{8}\left(U_e-7U_w\right)-D_W\right) \qquad [2.44]$$

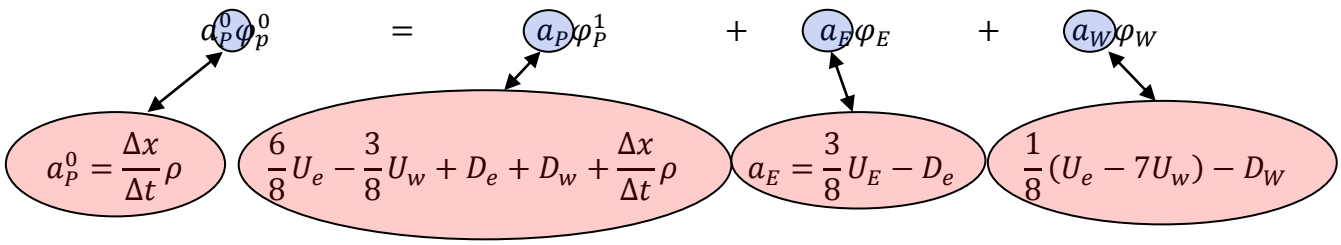

Balance for the last volume

Writing the balance equation for the last volume allow us to define the condition on the flux at z=0, we consider that $\varphi_{x=0} = 0$ meaning that the quantity of flux going to the east is 0. In other terms the value of flux φ at the interface of the last volume is equal to preceding volume, then $\varphi_B = \varphi_P$.

Giving if we take into account this condition in eq.[2.37]:

$$\rho\left(\varphi_p^1 - \varphi_p^0\right)\frac{\Delta x}{\Delta t} + U_e\varphi_P - U_w\left(\varphi_W + \frac{1}{8}(3\varphi_P^1 - 2\varphi_W - \varphi_{WW})\right) = \underbrace{D_e(\varphi_E - \varphi_P^1) - D_w(\varphi_P^1 - \varphi_W)}_{=0} \qquad [2.45]$$

Rearranging the terms we obtain the discretized eq.[2.46]:

$$\varphi_p^0\frac{\Delta x}{\Delta t}\rho = \varphi_P^1\left(-\frac{3}{8}U_w + D_w + \frac{9}{8}U_e + \frac{\Delta x}{\Delta t}\rho\right) + \varphi_W\left(-\frac{6}{8}U_W - D_w - U_e\right) + \varphi_{WW}\frac{U_w}{8} \qquad [2.46]$$

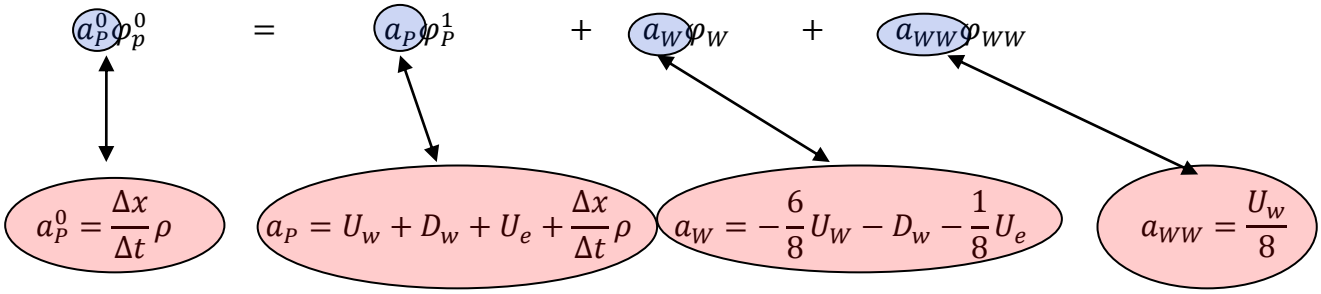

We have rearranged and expressed discretized equation of our problem for each node taking into account the boundary condition imposed by the problem at z=0 and z=z(RAM). We have rewritten all of the above results in tab.7.a and tab.7.b.

Table 7.a: Definition of $a_p^0, a_p, a_w, a_E, a_{WW}, a_A$ coefficient as a function of the discretized volume

Volume n°	a_p^0	a_p	a_W
i=1	$\frac{\Delta x}{\Delta t}\rho$	$\frac{7}{8}U_{(2)} + D_e + 3D_A^* + \frac{\Delta x}{\Delta t}\rho$	0
i=2	$\frac{\Delta x}{\Delta t}\rho$	$\frac{10}{8}U_{(3)} - \frac{3}{8}U_{(1)} + D_e + D_w + \frac{\Delta x}{\Delta t}\rho$	$\frac{1}{8}(U_{(3)} - 7U_{(1)}) - D_W$
3<i<nz	$\frac{\Delta x}{\Delta t}\rho$	$\frac{6}{8}U_{(i+1)} - \frac{3}{8}U_{(i-1)} + D_e + D_w + \rho\frac{\Delta x}{\Delta t}$	$\frac{1}{8}(-U_{(i+1)} - 6U_{(i-1)}) - D_W$
i=nz	$\frac{\Delta x}{\Delta t}\rho$	$-\frac{3}{8}U_{(nz+2-j)} + D_w + U_e + \frac{\Delta x}{\Delta t}\rho$	$-\frac{6}{8}U_{(nz+2-j)} - D_w - \frac{U_e}{8}$

Table 7.b : Definition of $a_p^0, a_p, a_w, a_E, a_{WW}, a_A$ coefficient as a function of the discretized volume

Volume n°	a_E	a_{WW}	a_A
i=1	$\frac{3}{8}U_{(2)} - D_e - \frac{D_A^*}{3}$	0	$-U_A - \frac{8}{3}D_A^*$
i=2	$-\frac{3}{8}U_{(3)} - D_e$	0	0
3<i<nz	$\frac{3}{8}U_{(i+1)} - D_e$	$\frac{U_{(i-1)}}{8}$	0
i=nz	0	$\frac{U_w}{8}$	0

Thanks to the determination of all the coefficient $a_p^0, a_p, a_w, a_E, a_{WW}, a_A$ it is possible to construct the matrix A that will permit to obtain the flux of void at iteration j from the previous flux of void at iteration j-1, as explicitly showed on fig.20, step 3.

$$nz+2-j \left\updownarrow \begin{pmatrix} \varphi(1,j) \\ \varphi(2,j) \\ \vdots \\ \varphi(1-j,j) \\ \varphi(i,j) \\ \varphi(1+j,j) \\ \vdots \\ \varphi(nz+1-j,j) \\ \varphi(nz+2-j,j) \end{pmatrix} \right. = inv(A) \times \left(\begin{matrix} \varphi(1,j-1) \\ \varphi(2,j-1) \\ \vdots \\ \varphi(i-1,j-1) \\ \varphi(i,j-1) \\ \varphi(i+1,j-1) \\ \vdots \\ \varphi(nz+1-j,j-1) \\ \varphi(nz+2-j,j-1) \end{matrix} \right) \left\updownarrow \right. nz+2-j$$

NB: *As explained in the first part we can see that both vectors and matrix size are dependent on the iteration, this to model the ram advancement and thus the reduction of the discretized model. In this approach extruded slices are suppressed and void ratio value of the extruded slice are stored. Meaning that the slice size remains the same.*

In order to build matrix A, 4 vectors corresponding to a_p, a_w, a_E, a_{WW} are created and placed on the diagonals of A as followed:

Table 8: Definition of the four vectors that will be put on the diagonal of A matrix

V1	Principal diagonal correspond to a_p
V2	Diagonal +1 correspond to a_E flux from east interface
V3	Diagonal -1 correspond to a_w flux from east interface
V4	Diagonal -2 correspond to a_{WW} flux from east interface

$$V1(i) = \frac{6}{8}U_{(i+1)} - \frac{3}{8}U_{(i-1)} + D_e + D_w + \rho\frac{\Delta x}{\Delta t} \quad [2.47]$$

$$V2(i) = \frac{3}{8}U_{(i+1)} - D_e \quad [2.48]$$

$$V3(i) = \frac{1}{8}\left(-U_{(i+1)} - 6U_{(i-1)}\right) - D_W \quad [2.49]$$

$$V4(i) = \frac{U_{(i-1)}}{8} \quad [2.50]$$

It should not be forget that the values of V1, V2, V3, V4, near the ram and the exit of the plug zone should be adapted to take into account the boundary conditions. Basically replacing the values of V1,2,3,4 (1,2,nz) by the values of $a_{p,E,W,WW}$ $(1,2,nz)$

Then matrix A is built as follow:

$$A = \begin{bmatrix} V1(1) & V2(1) & & & & & \\ V3(1) & V1(2) & \ddots & & & & \\ V4(1) & V3(2) & V2(i) & & & & \\ & V4(2) & V1(i) & \ddots & & & \\ & & V3(i) & \ddots & V2(nz+2-j) & & \\ & & & V3(nz+1-j) & V1(nz+2-j) & & \end{bmatrix}$$

$nz + 2 - j$ (horizontal) and $nz + 2 - j$ (vertical)

From the obtained value of "flux of void" it is now possible to compute the new value of void ratio after a ram advancement of Δz. This new void ratio values for each slice is used to compute the new permeability, extrusion force, pore pressure and flux of void and the process is repeated at each steps as explained previously on fig.20

2.1.5. Critical point of view on the code developed

Unfortunately, due to the amount of work to understand the subject, propose a relevant literature study that answer many of the initial questions asked and the documentation on the different tests that can be realized in future work to solve this problem of inhomogeneous injection. We were unable to have enough time and hindsight of this vast subject to develop a code taking into account all the parameters enounced. Even if the iteration of the code is realized, it seems that there is a problem of stability. We are aware that the Matlab® code written for this work is not complete and lack of specificity on certain parameters.

We will present in this part the weak point of the code and theory we developed based on the work realized by Perrot [1] .

- The function characterizing the evolution of the frictional angle φ with void ratio e is valid for a value of solid volume fraction superior to $0.8\phi_{max}$ in our case we consider that this function given in eq.[2.9] were always valid.

- No consistency study have been made, meaning that there is a divergence in results leading to velocity of the fluid going up to value of order 10^{200}. In his work and for consistency purpose Perrot include in his code a condition that step duration Δt was computed at each iteration steps in order to make a maximum variation of void ratio lower than 10^{-5}.

-Study the influence of different definition. Indeed in our work we mostly used the definition of Yield stress, Permeability and Frictional force presented by Perrot. All those definition were in accordance with his study which were more industrial oriented (extrusion of cement), and test have been realized on Kaolin pastes. Thus

the test we are presenting in Chapter three are supposed to give answer on the validity of equation used in our case of ceramic bone cement injection.

- Include the evolution of the shaping force required to plastically deform the material in the conical die of the syringe. Indeed void ratio is supposed to change in the die area of the syringe influencing the shaping force of cement material. Hence extrusion force should be modified and stress state of the cement too. The study of what is happening in the die area (jamming, dilatancy) should be investigated more in depth, by the use for example of FEA simulations that we will explain in the second part of this second chapter.

- Finally, we choose to solve this problem using QUICK simulations to study the variation of void during injection process. Is that path we choose to take valid? We cannot answer this questions yet since no exploitable results have been obtained and that we do not dispose of the right parameters neither experimental results to compare with numerical results. Nevertheless, motivated by the idea exposed in chapter 1 (fig.12) we choose this option to complete and adapt the work done by Perrot.

- Boundary conditions should be considered with more attention in order to avoid numerical errors, calculation problems and to model as accurately as possible the injection process. It should picture the complex flow occurring near the ram and eventually the flow occurring between the plug flow area and the die area. Such information can be obtained experimentally or using FEA simulations on the entire syringe geometry.

- An user friendly interface could be developed in order to visualize more easily the parameters used and the conditions imposed to the problem. It is sometimes considered as a sophistication of a code but it is necessary at one point in order not to get lost in the variable and to have a better readability of the results and the simulations.

Conclusion QUICK scheme

In this section we tried to adapt a numerical scheme usually used in computational fluid dynamic to solve flow of fluid or heat. In our case we consider void ratio *e* as flowing quantity. This flow were ruled by Darcy law, void ratio and pressure state void ratio dependent expressions and fitted in a spatially and temporally discretized Navier-Stokes equations. The whole flow has been solved using QUICK scheme.

Unfortunately, our dispersion and thirst to have a global view of the problems, did not allow us to finish to write a working and stable code able to compute evolution of void ratio during injection of cement. Nevertheless new perspectives have been given and we consider the idea of finding a way to accurately model the evolution of void ratio along the syringe during injection to be the next step after latest work done by Perrot et al. [1]

Another interesting part of the injection system that should be studied regarding LPM is the canula, indeed the smaller diameter of the canula give rise to more complex flow behavior (due to more complex stress state). It would be interesting in future work to study LPM occurring in the canula which no one up to now did.

2.2. Laminar Euler-Euler two phases flow modelisation with COMSOL®.

In an effort to find a way to study the injection of ceramic bone cement, it has been proposed to study this material as a suspension of spherical particles in a liquid. COMSOL® has been chosen to be the support of the simulations. In the optic of our study we wanted to simulate the injection of cement and use the power of finite element analysis in order to study the influence of particle size, inner syringe diameter, exit of die diameter, as well as the angle of aperture of the conical die. A literature study permit us to have a deeper understanding of the phenomenon leading to syringe blockage or liquid phase migration of interstitial liquid during injection. It also permit to obtain answers on the role of each parameters we wanted to control for an optimal injection of ceramic bone cement.

COMSOL® is a finite element analysis program (FEA) that can treats multiphysical problems, it is composed of several built-in sections able to solve problems ranging from solid mechanic, to heat transfer passing by electric fields problems. The first question we had to think of concerned the choice of a module including physically revealing modelisation of our problem. In a previous work [12] cement were chosen to be modelized as a Newtonian and Non-Newtonian fluid in order to study the pressure drop in different canula geometries, and even if the results permit to understand the influence of canula geometry on cement injection it didn't took into account neither LPM nor jamming which are of prime interest in our study. We tried to explore the software and to document ourself on the modelisation of cement rheology. Contrary to the mathematical modelling approach that we have tried to develop in this chapter we tried to base our approach on something that had never been used before in the modelisation of cement injection. Thus we excluded Cam-Clay model even if a module permits to use it in COMSOL®. We choose, amongst the large amount of model offered, to model injection of ceramic bone cements by using the Euler-Euler model, Laminar Flow (ee) for the few parameters required for modelisation and for the fact that it is close to the initial idea of cement we had (spherical particles in a liquid)

2.2.1. Laminar Euler-Euler Two-Phases Flow

The Euler-Euler two phase flow interface has been designed to handle different types of two phases flow. Indeed it permits to model both solid particles or droplets/bubbles as dispersed

phase. It can find applications in physical system such as fluidizided beds, spray or cyclone separator simulations. It can handle simulations ranging from low to high concentrations of dispersed phase. Moreover, Euler-Euler interface can handle large differences in density between the phases (example of solid particles in the air). In this model the different phases are mathematically treated as interpenetrating continua. Since the volume of a phase cannot be occupied by the other phases, the concept of phase volume fraction is introduced. These volume fractions are assumed to be continuous functions of space and time and their sum is equal to one. Conservation equations for each phase are derived to obtain a set of equations, which have similar structure for all phases. These equations are closed by providing constitutive relations that are obtained from empirical information, or, in the case of granular flows , by application of kinetic theory.

Concretely COMSOL® module will ask you to define the following parameters in order to run the simulations.

Table 9: Required parameters for Euler-Euler two phases laminar flow simulations.

Parameters	Choice proposed by COMSOL®
Continuous phase material	Needed to define its density and dynamic viscosity
Dispersed phase material	Needed to define its density and particle diameter
Density continuous phase ρ_c	Could be defined from material or user defined
Dynamic viscosity continuous phase μ_c	Could be defined from material or user defined
Density dispersed phase ρ_d	Could be defined from material or user defined
Diameter of particles d_d	User defined
Define a solid viscosity model	Calculated from mixture viscosity (Krieger Model) or user defined
Maximum packing concentration ϕ_{max}	User defined
Define drag model	Choice between Gidaspow, Schiller Naumann, Hadamard-Rybczynski or user defined models
Define solid pressure model	Choice between No solid pressure, Gidaspow-Ettehadieh, Gidaspow, Ettehadieh or user defined models.
Define behaviour of cement at the wall	Slip/No Slip

We have now a model with simple parameters to inform to the program. The goal now is to understand how the model works in order to prevent errors and ease interpretations of results.

First of all the nature of the model should be explained, three kinds of modelling approaches exists in the case of particulate modelling Langrangian ones, Eulerian ones and Lagrangian-Eulerian ones. The differences between them are explained in tab.10.

Table 10 : Treatment of particles and fluid motion for 3 different approaches

	Langrangian models	Lagrangian Eulerian models	Eulerian granular
Particle motion	Trajectories of individual particles	Trajectories of individual particles	Continuum model (multidimensional)
Fluid motion	Flow around individual particles or local averaging	Local averaging	Local averaging

Meaning that the model we are using cannot follow the motion of one particle and access features such as particle tracking. Nevertheless we don't trust particle tracking to be a good indicator for LPM or Jamming since the phenomenon are more complex and cannot be explained by particle trajectories. We will explain the constitutive equations that COMSOL® is solving in the case of Euler-Euler laminar two phases flow and discuss the different choices that can be done on the drag model, solid pressure, solid viscosity model as well as the virtual mass forces or lift forces that can be added to model indirect forces.

Constitutive equations

On particularity of COMSOL® is to indicate the equations associated to the model used, we can maybe reproach that documentation those equations, the manner the code is solving them and what they really represent is missing comparing to other more developed programs such as ANSYS®. Indeed even if equations are showed their implications are often occulted and it is to the scientist to make its own research to know if the use of one model or the other fits its modelisation requirements. For this reason we will quickly explain the Euler-Euler, two phases flow equations in order for the reader to make better choice or make its own opinion on the validity of the model.

We will start by explaining the equations given by COMSOL® and explain each terms of them, then we will explain solid viscosity model and solid pressure. Then explain what drag equations represents, and their domain of application. Finally we will talk about the virtual mass forces as well as lift forces to understand what they represent.

As explained previously, in EE models the two phases are treated as interpenetrating continua and conservation equations for each phase are derived from mass balance and continuity equations.

Equation derived for the continuous phase

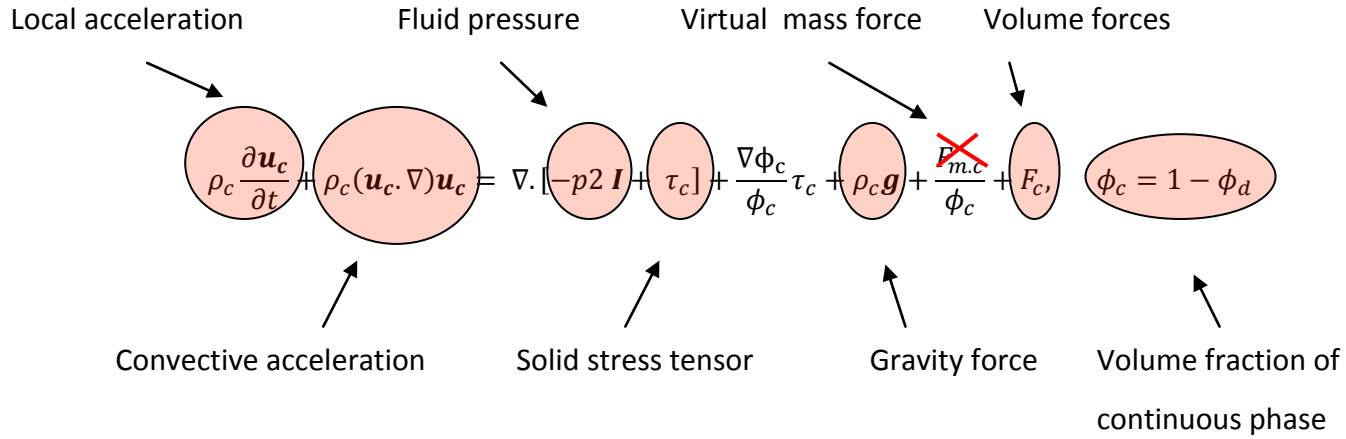

Granular phase momentum equation

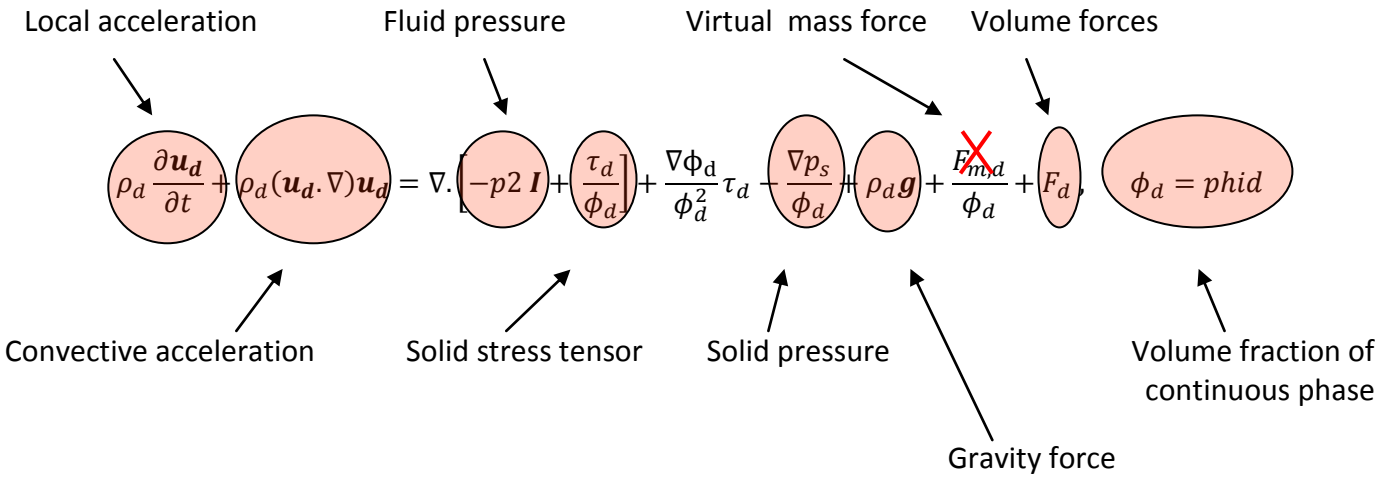

$\boldsymbol{u_c}$ and $\boldsymbol{u_c}$ Velocity vector	$\boldsymbol{F_{m,c}}$ and $\boldsymbol{F_{m,d}}$ Virtual forces f	$\boldsymbol{\tau_c}$and $\boldsymbol{\tau_d}$ viscous stress tensor
$\boldsymbol{\rho_c}$and $\boldsymbol{\rho_d}$ density	$\boldsymbol{F_c}$ and $\boldsymbol{F_d}$ Volume forces	$\boldsymbol{\phi_d}$ and$\boldsymbol{\phi_c}$ volume fraction

We can see that those two equations are pretty similar and regroup the same kind of terms but changing the domain of application (continuous (c) or granular phase (d for dispersed)).

The fluid phase in the above equations is assumed to be Newtonian and the viscous stress tensor is defined as:

$$\tau_c = \mu_c \left(\nabla \boldsymbol{u_c} + (\nabla \boldsymbol{u_c})^T - \frac{2}{3} (\nabla . \boldsymbol{u_c}) \boldsymbol{I} \right) \quad [2.51]$$

Where $\boldsymbol{\mu_c}$ (Pa.s^{-1}) is the dynamic viscosity of the liquid.

2.2.1.1. Dynamic viscosity

Empirical and analytical model for the dynamic viscosity of the two-phase mixture have been developed by a multitude of researchers. This dynamic viscosity is generally expressed as a function of the volume fraction of the dispersed phase. COMSOL® uses the simple Krieger model for mixture viscosity, its advantage is that it covers the entire range of particle concentration.

$$\mu = \mu_c \left(1 - \frac{\phi_d}{\phi_{d\,max}} \right)^{-2.5\phi_{d\,max}} \quad [2.52]$$

$\phi_{d\,max}$ being the maximum packing limit (0,62 by default)

Nevertheless other equations have been found to describe the evolution of dynamic viscosity, and can be implemented by the user in COMSOL®.

Table 11 : Other possible easy to implement models for dynamic viscosity

Liu's (for high solids concentrations)	$\mu = [a(\phi_{d\,max} - \phi_d)]^{-n}$
Chong et al.	$\mu = \left[1 + \frac{0.75 \left(\frac{\phi_d}{\phi_{d\,max}} \right)}{1 - \left(\frac{\phi_d}{\phi_{d\,max}} \right)} \right]^2$
Coefficient **a** and **n** are experimental parameters	

Other software such as ANSYS® propose to treat the solid viscosity term in a much more complex manner. Indeed in ANSYS® the solid viscosity arises due to kinetic motion and collisional interaction of particles.

$$\mu_d = \mu_{d,coll} + \mu_{d,kin} \quad [2.53]$$

When in plastic regime a frictional term is added and viscosity behave has:

$$\mu_d = max\left[\mu_{d,coll} + \mu_{d,kin}, \mu_{d,frict}\right] \quad [2.54]$$

Where $\mu_{d,coll}$ stands for the collisional part, $\mu_{d,kin}$ for the kinetic part and $\mu_{d,frict}$ for the frictional one.

Table 12: Dynamic viscosity collision contribution

Gidaspow and Syamlal models	$\mu_{d,coll} = \frac{8}{5}\phi_d\rho_d d_d g_{os}\eta\left(\frac{\theta_d}{\pi}\right)^{1/2}$
Sinclair model	$\mu_{d,coll} = \frac{5\rho_d d_d(\theta_d\pi)^{1/2}}{96\phi_d}\left(\left[\frac{8\phi_d}{5(2-\eta)}\right]\left[1+\frac{8}{5}\eta(3\eta-2)\phi_d g_{os}\right]+\frac{768}{25\pi}\eta{\phi_d}^2 g_{os}\right)$

Table 13: Dynamic viscosity kinetic contribution

Syamlal model	$\mu_{d,kin} = \frac{\phi_d\rho_d d_d(\theta_d\pi)^{1/2}}{12(2-\eta)}\left[1+\frac{8}{5}\eta(3\eta-2)\phi_d g_{os}\right]$
Gidaspow model	$\mu_{d,kin} = \frac{5\rho_d d_d(\theta_d\pi)^{1/2}}{96\eta g_{os}}\left[1+\frac{8}{5}\eta\phi_d g_{os}\right]$
Sinclair model	$\mu_{d,kin} = \frac{5\rho_d d_d(\theta_d\pi)^{1/2}}{96\phi_d\eta(2-\eta)g_{os}}\omega\left[1+\frac{8}{5}\eta(3\eta-2)\phi_d g_{os}\right]$

Table 14: Dynamic viscosity frictional contribution

$\mu_{d,frict} = \frac{p_s sin\Phi}{2\sqrt{I_2}}$

g_{os} radial distribution function, correction factor that modifies the probability for collision between grains for high concentration of solid grains. Adaptation of this function could take into account interparticle forces.

2.2.1.2. Drag model

Drag force is created by particle movement in the fluid, it influence both other particles and surrounding liquid. It is assumed in Euler-Euler model to be the main force and is defined as:

$$F_{drag,c} = -F_{drag,d} = \beta u_{slip} \quad [2.55]$$

$\boldsymbol{\beta}$ drag force coefficient	$\boldsymbol{u_{slip}} = u_d - u_c$

For dense flows with high concentration of dispersed phase, the Gidaspow model for the drag coefficient can be used. It combines the Wen and Yu drag model .Particles are assumed to be spherical, therefore, the total drag per unit volume on the liquid phase is given by:

$$\beta = \frac{3\phi_c\phi_d\rho_c C_D}{4d_p}\left|U_{slip}\right|{\phi_c}^{-2.65} \quad [2.56]$$

Gidaspow model

$\phi_d < 0.2$

$$C_D = \frac{24}{Re_p}\left(1 + 0.15{Re_p}^{0.687}\right) \quad [2.57]$$

$$Re_p = \frac{\phi_c d_d \rho_c \left|u_{slip}\right|}{\mu_c} \quad [2.58]$$

Gidaspow model

$\phi_d > 0.2$

$$\beta = 150\frac{\phi_d^2\mu_c}{(1-\phi_d)d_p^2} + \frac{1{,}75\rho_L|U_r|}{d_p} \quad [2.59]$$

Drag coefficient can also be computed using Hadamard-Rybczynski which is valid for Re<1.

$$C_d = \frac{24}{Re_p}\left(\frac{1 + \frac{2}{3}\frac{\mu_c}{\mu_d}}{1 + \frac{\mu_c}{\mu_d}}\right) \quad [2.60]$$

The last model proposed by COMSOL®(Schillller-Naumann) stands for liquid-liquid mixture.

2.2.1.3. Solid pressure

For fluid solid mixture such as cement, a model of the solid pressure is needed. Solid pressure is introduced to model the particle interaction due to collisions and friction between particles. COMSOL® use a gradient diffusion based assumption presented in eq.[2.61]:

$$\nabla p_s = -G(\phi_c)\nabla\phi_c \qquad [2.61]$$

Where G is an empirical function that is proposed under three forms in COMSOL.

Table 14 : Empirical models proposed by COMSOL for solid pressure.

Gidaspow and Ettehadieh	$G(\phi_c) = 10^{-8.76\phi_c+5.43}$
Ettehadieh	$G(\phi_c) = 10^{-10.46\phi_c+6.57}$
Gidaspow	$G(\phi_c) = 10^{-10.5\phi_c+9.0}$

While COMSOL® choose to describe solid pressure from simple function of volume fraction of liquid. Other software such as ANSYS® propose a more complex definition of solid pressure, where it is composed of a kinetic term and a second term due to particle collisions.

$$p_s = \phi_d\rho_d\theta_d + 2\rho_d(1+e_{ss})\phi_d{}^2 g_{0s}\theta_d \qquad [2.62]$$

$\boldsymbol{g_{os}}$ radial distribution function, correction factor that modifies the probability for collision between grains for high concentration of solid grains. Adaptation of this function could take into account interparticle forces.

$\boldsymbol{\theta_d}$granular temperature

$\boldsymbol{e_{ss}}$ coefficient of restitution for particle collision

We can see that COMSOL® offers simple models in comparison with other more advanced code. It can be of great help for a lambda user willing to use pre-existing semi-empirical model. Nevertheless we can regret the lack of parameterisation of the program for those who wants to design their model as close as possible to their case. Other programs propose to have a full control of the behaviour of its particle-fluid system, nevertheless more knowledge and interrogations are needed to use them intelligently.

2.2.1.4. Virtual mass force

Virtual mass effect is cause by the relative acceleration between phases, it is significant when the second phase density is much smaller than the primary phase density (i.e., bubble column). Thus in our case they are pretty irrelevant.

2.2.1.5. Lift force

Lift force are cause by the shearing effect of the fluid onto the particle, they are usually insignificant compared to drag force except when the phases separate quickly and near boundaries.

2.2.2. Practical simulations with Euler-Euler two phases flow module

Concerning the modelisation itself we have tried to run several simulations in order to feel the power and weakness of such method. For this we choose the Euler-Euler Model, laminar flow with the following configuration:

Table 15: Summarization of the parameters chosen for simulations - A fork of values is given for each parameters

$L1$ [m]	[6cm-12cm]
$L2$[m]	[1cm-4cm]
$R1$ [m]	[2cm-4cm]
$R2$ [m]	[0.5cm-1,5cm]
d_d [m]	[1µm-40µm]
ϕ_{max} [1]	[0,54-0,62]
Injection time t1 [s]	[360s-600s]
Inlet fluid velocity V1 [m.s^{-1}]	V1=t1/L1
Dynamic viscosity: Krieger model	$\mu = \mu_c \left(1 - \frac{\phi_d}{\phi_{d\,max}}\right)^{-2.5\phi_{d\,max}}$
Drag model: Gidaspow	$\beta = 150\frac{\phi_d^2 \mu_c}{(1-\phi_d)d_p^2} + \frac{1{,}75\rho_L\lvert U_r\rvert}{d_p}$
Solid pressure model: Gidaspow	$G(\phi_c) = 10^{-10.5\phi_c + 9.0}$

Fig.25 represents the geometry of the problem as it has been modelled.

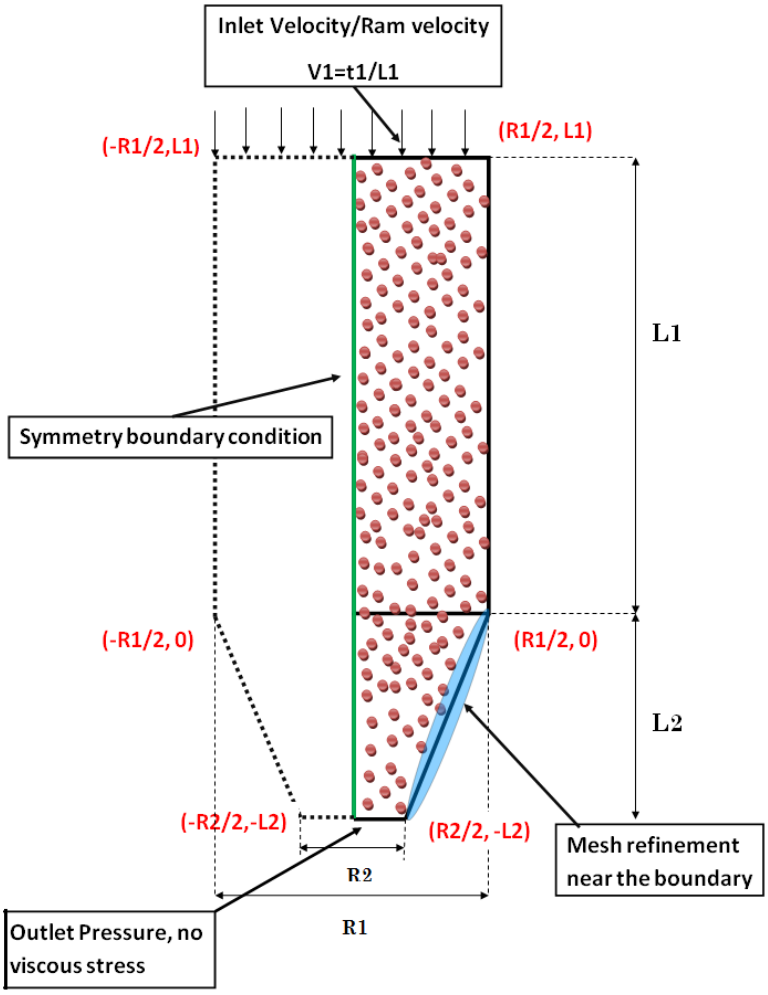

Figure 25: Representation of the geometry and parameters used for simulation with COMSOL

2.2.2.1. Meshing

During our first simulations we found out that it was not possible to access results depending on the mesh chosen, or sometimes computation time were too long and the fact that we were not sure of the final results and their validity made us to stop them. In an effort to reduce computation time to access more rapidly to results, an efforts has been made on mesh generation. COMSOL® detects automatically the physic and the geometry of the model and propose a corresponding mesh. A good meshing has a significant impact on the rate of convergence, the solution accuracy, CPU time required.

2.2.2.1.1. Mesh refinement

It is trusted that in the die area, particle contact with the wall and the conical constriction shape are responsible for more computation, since the mesh density should be high enough to capture all relevant flow features, mesh is refined at die wall.

Another mesh refinement is executed at the flow inlet in order to let the flow to be fully developed in the syringe.

2.2.2.1.2. Boundary layer

Added to that the mesh adjacent to the wall should be fine enough to resolve the boundary layer flow. Thus at the syringe wall two boundary layers has been defined in order to avoid computation errors.

2.2.2.1.3. Filet

In order to avoid sharp angle, responsible for computational errors in fluid flow simulations the angle forming the passage from the plug area to the die area has to be filleted.

2.2.3. Problems encountered

Several problems have been encountered during simulations resulting in no results to present and analyse. We will summarize these problems in order to draw a map of what should be investigated and modified in the future if this way is chosen to continue studies.

2.2.3.1. Accumulation of particles near the die exit:

Particles do not seems to exit from the syringe, we thought it was due to the jamming phenomena forming an arch at die exit but this phenomena appears during the first seconds of injection showing that the particle aggregates quickly at die exit.

Added to that, depending on the boundary condition at the wall (slip or not) particles aggregation takes different form, from uniform aggregation similar to the formation of a particle floor. To aggregation near the angle formed at die exit, the problem being that they don't aggregate on the wall but in the cement. Same phenomena is observed when the syringe geometry is cut in two, spherical high solid volume fraction zone appears at the angle between exit and cutting line. We suspect this behaviour to be caused by meshing issues, the mesh design causing the particles to preferentially aggregates near the angle.

2.2.3.2. Computation time

Injection process last minimum 360s leading to large computation time. Simulations done on 10s injection at relatively high speed lasts from 1hours to 16hours depending on the initial volume fraction. Nevertheless 6 minutes injections leads to long computation time and often computation even stops after a certain time due to divergence of results, certainly due to instabilities at high solid volume fraction.

2.2.3.3. Computational instabilities at high solid volume fraction

Instabilities have been observed when solid volume fraction reach high values around 0.60, indeed when volume fraction are this high particles are not able to rearrange, high frictional forces exists between them, and since the simulation are Eulerian and treat the phases globally it cannot pictures what occurs locally in the paste. Practically such solid volume fraction are never reached in cements since it corresponds to a nearly close packed state. Simulation can be run at much lower volume fraction, and we can consider that if the system reach a close packed state it is jammed, which is not desired. Simulations we be considered relevant if solid volume fraction only vary of several percent.

2.2.3.4. Flow of particles in constriction vs ram displacement

We were simulating the flow of a particle/fluid in a syringe shaped pipe, instead injection process should be represented by a solid moving part, compressing the system and hence expulsing the cement out of the syringe. Nevertheless it seems that this features needs another kind of physical description, using Arbitrary Langrangian Eulerian module (moving mesh module). Indeed the domain during injection will be strongly deformed and constant remeshing is needed. Unfortunately our efforts to model injection instead of flow are solved by a failure.

Conclusion COMSOL® simulations

We have seen that FEA software are a powerful tool to model physical behaviour or phenomena. Nevertheless if someone wants to access accurate results, it requires deep knowledge in the field of what has to be studied and in the field of computer modelisation. Indeed one can blindly trust the calculation made by an user friendly software, but reality can be that this apparent facility could reveals an unfriendly problems, being the one of not modelling the system we want to model but model something similar (but false) instead. For this purpose, we needed to understand what were the multiple options proposed by COMSOL® for the modelisation of Eulerian Eulerian ,two phases laminar flow as well as the cement rheology.

Also it has to be kept in mind that computer simulations alone cannot be considered as scientific results and universal truth if not validated by experiences. It should be seen as an help to access at lower material, human and time cost results, but the model used should be put to the test many times to be trusted (nearly) blindly. The phase in which we are located is a phase of understanding, and planning for future experiments having as goal to obtain an optimum injection of ceramic bone cement during the process of VP and KP.

For this purpose chapter 3 is dedicated to in our sense what should be done in the future and how it can be achieved in order to obtain scientifically relevant results and conclusion that we weren't able to obtain here.

Conclusion on Euler-Euler two phases laminar flow module proposed by COMSOL

We have seen that thanks to a basic description of the particle/fluid (particle diameter, density and viscosity of fluid) and the use of existing models directly implemented in COMSOL® it was easy to model flow of two phases medium.

Nevertheless, the models implemented in COMSOL® might be too simple for an accurate description of injection of cementitious paste. Added to the fact that they are based on existing models that might not be adapted to cement. Thus the need of experiments in order to decide if yes or no a model can be used.

Other software propose an Euler-Euler description of particle fluid flow in a more sophisticated way allowing the user to play on interparticle forces. The model design is more parametrable but requires more parameters definition and study. Moreover, these models are also based on other work and the same validation by experiment of them have to be done.

Finally, more difficult doesn't mean more accurate, it exists in physics simple laws which are beautiful in there simplicity and accuracy. Sometimes the use of more difficult model, even if it brings us closer to the reality, is computationally too expensive and requires a great number of constant which make the process of modelisation too complex. Nowadays industrial tends to use more simple model perfectly knowing the margin of errors they can introduce. In our case, we think that the use of models proposed by COMSOL® are more than enough for our study, nevertheless they should be fully understood and comparison with experimental results on the chosen cement should be conducted in order to conclude on the truthfulness of a model regarding another.

Bibliography Chapter 2

[1] "Prediction of extrusion load and liquid phase filtration during ram extrusion of high solid volume fraction pastes", A.Perrot, H.Khelifi, T.Lecompte, D. Rangeard, G. Ausias, Powder Technology 249, p258-268,2013

[2] Theoretical Soil Mechanic, K.Terzaghi , New York, 1943

[3] "Extrusion criterion for firm cement-based materials" Perrot A. , Rangeard D., Mélinge Y., Estellé P, Lanos C., Applied Rheology Vol 19,Issue 5, 2009

[4] "Permeability of satured sands and clays" Carman, P. C., The Journal of Agricultural Science, 29 (02), p.262, Apr 1939

[5] Fundamentals of Soil Mechanics, D.W Taylor, New York, 1948.

[7] "The squeezing test: a tool to identify firm cement-based material's rheological behaviour and evaluate their extrusion ability", Zahia Toutou, Nicolas Roussel, Christophe Lanos, Cement and concrete research, vol 35, p 1891-1899, 2005

[8] "Effects of liquid phase migration on extrusion of microcrystalline cellulose pastes", S.L Rough, J. Bridgwater, D.I Wilson, Intl. jrnl. of pharmaceutics, 204, p117-126, 2000

[9] "A model describing liquid phase migration within an extruding microcristalline cellulose paste" S.L Rough, J. Bridgwater, D.I Wilson, Trans IchemE, vol. 80 Part A, 2002.

[10] Paste Flow and Extrusion, Benbow, J.J. & Bridgwater, J. (1993), Clarendon Press, Oxford, 25-44.

[11] "Analysis of coal log ram extrusion",Q.Deng, H.Liu, Powder Technology, vol91, p31-41, 1997

[12] "Aproximación al estudio de la inyectibilidad de cementos óseos", Solenn Laforgue ,PFC UPC, 2008

3. Experiments and future work

Introduction

This work first objective were to provide an insight in what are LPM and jamming phenomena, understand what parameters influence their behaviour and try to model them upgrading existing methods or exploring new ways to do so. Nevertheless, simulations are useless without experiment, they need to be designed from experimental data and understanding of the phenomenon. As we have seen, parameters and observations come from experiments. It is then an obligation to use experimental techniques in order to get those parameters and validate the obtained results, it is better to build a numerical model from physical occurrence than trying to simulate a complex process from what appears to be physically relevant.

In this optic to pursue with research in this domain and to develop an adapted syringe and cement, we decided to dedicate this third chapter to the design of experiments and existing resources allowing the scientific to have an idea of the path to follow in order to obtain an optimum or at least improvement in injection of ceramic bone cements. Experimental methods used to obtain the materials properties required for simulations will be presented and explained.

We have seen in chapter one that two approach have been used by scientific community in order to avoid LPM and jamming. One of them rely on the cement formulation (particle size, distribution, solid volume fraction, interparticle forces, use of adjuvant or nanoparticles) in order to make the cement easier to inject (less viscous) and less subject to jamming. The other approach is to change the syringe design for a better injectability.

Given the aim of VP and KP which is the restoration of the vertebrae and its mechanical properties, also we have seen that the advantages of ceramic bone cements to be biocompatible and even bone conductor. Since the cement formulation establish its properties and is trusted to give advantages to ceramic bone cements over polymeric bones cements. We think it is important not to change the formulation of the cement. It is easier for the scientist to control the syringe design than the paste formulation. Nevertheless

rheological properties of the paste has to be investigated in order to run the simulations and influences of paste formulation parameters can also be investigated as it is of interest in ceramic industry. Moreover, occulting a field of research while doing investigations could lead to tremendous errors or misunderstanding of the physics of the process. If no solutions is found modifying the syringe design or the process parameters, then efforts can be done on the cement formulation by identifying the most relevant parameters, that both have an influence on LPM and jamming, and do not influence dramatically the cement properties once injected (mechanical properties, toxicity, setting time).

This chapter will be axed on three parts, the first one states on the philosophy that could be considered to investigate injectability of ceramic bone cement, experiment design will be proposed to orient future work and research. The second part will regroup and explain the existing experiments that permits to characterize cement rheology, and physical properties evolution during extrusion, methods used to visualize and characterize LPM and jamming will also be reported. Finally a discussion on the possible modifications to the injection system will be presented as motivated ideas for pattern development and lever of innovation in that field.

3.1. Experiment design and research orientation.

This part will be dedicated to a reflection to the design of experiment, and research orientation for future work on the injectability of ceramic cement paste. It does not have to be read as universal truth on how to conduct the experiments or to be strictly followed. It does not comes from scientifically developed experiment design but more from literature studies and personal thought.

Experiments that will be presented correspond to the one permitting to describe cement rheology and to model phenomena such as LPM and Jamming. It exists a lot different ways to study those phenomena and comment cement injectability. And it is difficult to claim that one path is "better" than another one. It strongly depends on the scientific believes and experience. Meaning that some person thanks to their experience in a domain decide to investigate a particular properties of a process thinking it is the key to all the problems encountered (and sometimes occulting all the other relevant parameters).

Nevertheless, thanks to the literature study realized in the first chapter, we have seen that cement injectability, LPM and Jamming phenomena can be controlled via many ways, and that its perfect control rely more on finding optimum of multivariable functions than finding the best configuration regarding only one parameter.

All the difficulty for the scientist will be to adjust parameters that will enhance cement injectability (homogenized injection at acceptable injection pressure), without affecting other properties such as mechanical, setting temperature, or toxicity ones. Another kind of properties that have to be conserved (if not enhanced) is the one of resorbability or osteoconductivity, those properties are one of the main interest to choose ceramic bone cements over polymer ones. Thus (without reinventing ceramic bone cements) many experiments have to be conducted in order to study the multiple variable that have to be controlled. Maybe the best start would be to work with existing ceramic bone cement [1] company (for financial support), and make change to their products, or to keep on studying injectability in a more fundamental way (particle size, shape, interparticle forces).

We think that studying fundamental physic of the phenomena would be interesting since it touch many industrial process (cement, food, and any kind of granular materials workability, and extrusion). Thus knowing a bit more on the basic physic of those kind of materials would be of great interest for the industrial world. Nevertheless, it seems easier on a practical and financial plan to start with an existing product (or several) and study the influence of the modification of parameters on cement injectability and on cement properties once injected. The following diagram (fig.26) represent a possible path that could be followed to obtain relevant and useful results on cement injection.

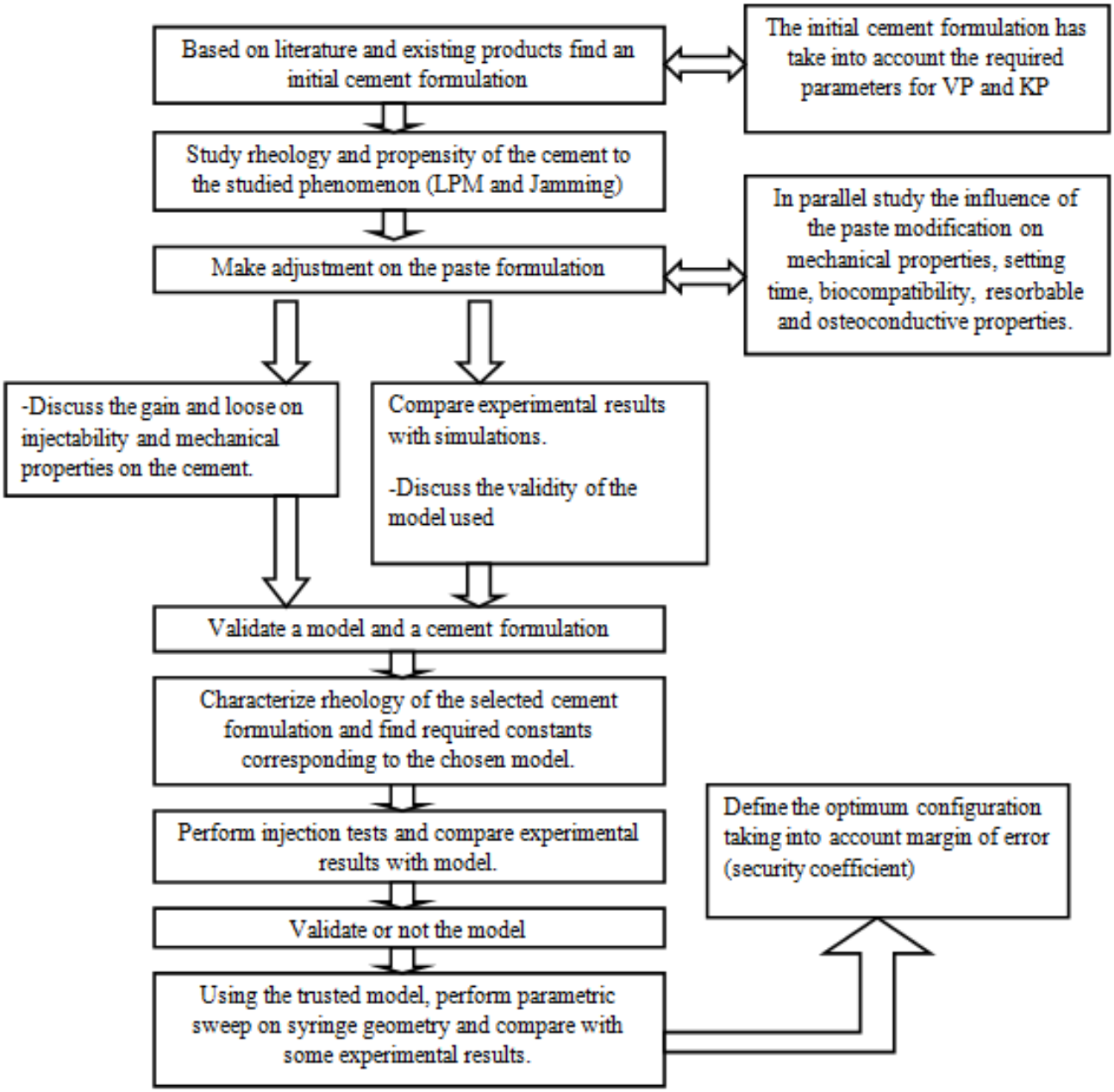

Figure 26: Possible experiment design that can be used for injectability study of ceramic bone cements.

The diagram presented on fig.1 is more cement design oriented. Considering that efforts should be done on cement more than on syringe. Nevertheless one can choose to only study syringe design influence on LPM and Jamming and compare injectability of different brand of cement paste. It strongly depends on the motivations of the scientists and on the financial helps accorded to his research. Indeed comparing different bone cement brand [1] and syringe design regarding injectability could constitute a market study interesting both cement and syringe manufacturer as well as surgeon community. A diagram describing experiment design could be drawn in that way the one given here is very general and can be modified according to the future decision taken in that field.

3.1.1. Parameters to control

We have seen in the first chapter of this work that several parameters have an influence on cement injectability. One of the main objective of future works will be to play on those parameters in order adjust cement properties and enhance cement injectability. It is then important before starting investigations and experiment, to have an overview of what parameters should be modified and how. The following tables (Tab.16 & Tab.17) will summarize the ameliorations that has to be done on the different injection parameters and how they can be achieved.

Table 16: Example of parameters that should be controlled and how to control them in order to obtain better cement injectability. Case of the syringe and process design.

Parameters	Ameliorations	How it can be achieved.
LPM	Decrease forces due to plastic shaping at the die. Reduce frictional forces at the wall	- Use a large exit die diameter - Die having smooth change in cross section. - Keep wall roughness low.
Jamming	Die geometry optimization	- Set up a relation between an adequate particle size and a minimal die exit aperture avoiding jamming. - Use squared shaped die instead of conical ones. - Find optimum aperture angle for conical die
	Favour particle slip at wall cement interface.	Make the wall of the syringe as smooth as possible.

Table 17: Example of parameters that should be controlled and how to control them in order to obtain better cement injectability. Case of the cement.

Parameters	Ameliorations	How it can be achieved.
Viscosity	Lower viscosity for ease of injection	-Increase liquid volume fraction - Increase particle size - Decrease particle interaction
	Higher viscosity to avoid leakage of the cement out of the vertebrae	- Inverse of the parameters indicated before. An equilibrium has to be found.
Cohesiveness	Increase of Van der Waals interaction	-Smaller particle size - Shorter distance between the particles (higher solid volume fraction)
	Decrease of electrostatic interactions	- Shift of pH to a value near isoelectric point. - Desorption of charged molecules - Increase of the ionic strength of the interstitial liquid.
	Decrease of osmotic pressure	- Decrease concentration of dissolved species in the interstitial liquid.
	Decrease of steric interactions	-Removal of all the polymeric molecules present in the cement
LPM	Permits the particle to move in the cement	- Low particle roughness - Appropriate solid volume fraction - Low interstitial viscosity - Adequate interparticle forces. - Broad particle size distribution. -Smaller particle size
Jamming	Allow particle to flow out of the syringe	-Limit size of particles - Define exit diameter at which cement cannot be fully injected anymore
	Allow the particle to move in the cement.	-Use spherical particles - Keep particle roughness low - Keep interparticle forces low

3.1.2. Injection tests

We cannot study injectability of ceramic bone cement without making injection test and controlling the different parameters that would permit to determine if the injection is successful or not. This injection test can be seen with two angles. From one side it can be used to study cement behaviour during injection, and from the other side it can be seen as the main test used for syringe design.

Injection test is pretty simple to realize since it consists in mounting the syringe in a tensile test machine (Fig.27) and controlling both injection speed and force. Before realizing this test every parameters have to be known, meaning the geometry of the syringe as well as the cement rheological properties and extrusion behaviour.

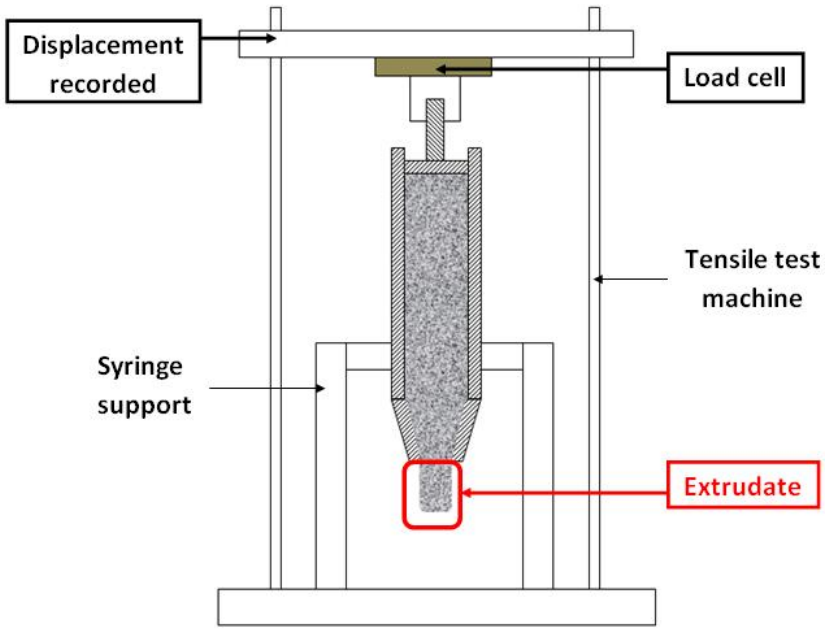

Figure 27: Configuration used for injection test. The syringe is mounted in a tensile test machine where the ram will be pushed at constant force or velocity and extrusion pressure or flow of cement will be recorded.

Then once the cements behaviour is characterized, understood and accurately modelized, the scientist can process to the injection test using a simple tensile test machine. The tensile test machine will permit to inject the cement at a certain velocity rate or force and to record data on extrusion force or ram displacement. In parallel to that, the operators will have to

control the extrudate flowing out of the syringe, this in order to detect potential heterogeneity in solid volume fraction or particle size distribution.

For this, the scientist will collect extrudate every X seconds, will weigh it before and after drying in order to obtain flow rate and liquid volume fraction. Granulometry can be obtain thanks to different methods (image processing being the easiest one). The obtained results will be compared with extrusion force in order to trace extrusion force or liquid volume fraction in the extrudate as a function of ram velocity. Tab.18 regroups the different diagram and comparisons that can be drawn in order to conclude on the success of the injection process or not.

Table 18: Possible plot permitting to characterize injectability of ceramic cement regarding syringe geometry.

At different ram velocities for a given paste formulation compare different:	**And plot**	
	Y- axis	**X-axis**
-Angle of the conical shaped die -Die exit size -Inner syringe barrel diameter	- Liquid volume fraction - Mean diameter of particle - Particle size distribution - Injection force	Ram advancement

The easiest way to control if injection is successful and suits VP and KP requirements is to look at the injection force as a function of ram advancement, indeed this one must remains constant and even slightly decrease during cement injection.

Since ram velocity is trusted to be one of the major parameters controlling LPM it would be optimal to find an injection time ranging from 6 to 10 minutes with no heterogeneity in the cement formulation, both in terms of particle size distribution and liquid concentration.

3.2. Rheology study of cement

More than 100 empirical tests for concrete, mortar, grout and cement slurry (see fig.28) have been developed and many have been standardised by international institutions (ASTM). All of them have been developed attempting to model practical conditions and involve flow, compaction, deformation, extrusion, penetration of a probe in order to characterize rheology of hydrated granular materials. Nevertheless most of them have been used only by their inventor and can be used only for specific kind of materials. We have seen through this work that several methods can be used in order to model injection of cement during VP and KP processes. All of these methods needed materials and process parameters that are general parameters commonly used for rheology description or specific parameters to a modelisation method. We will try to summarize the required constant and their determination methods needed for a better understanding, design and modelisation of cement behaviour undergoing injection.

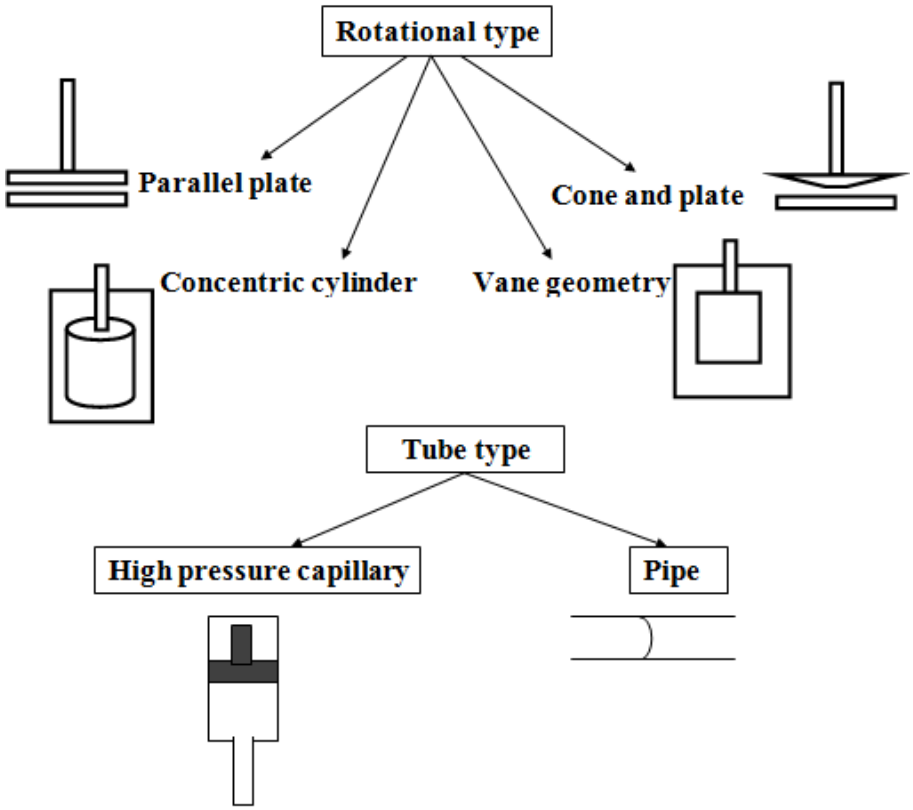

Figure 28: Different test geometry generally used to characterize Non-Newtonian fluid (such as granular pastes).

3.2.1. Parameters to control and corresponding experiments

In order to know which test should be performed scientist need to know what parameters or phenomena he wants to measure or observe. In the first and second chapter we have seen several modelisation method, that required several parameters, thus it could be an option for the scientist to measure those parameters in order to run simulation and try to find the best way to study cement during extrusion. Tab.19 regroup the constants needed for the several modelisation methods. Nevertheless, tests can be realized for other purpose than to simply find parameters for modelisation, they can be used to study cement behaviour and to find optimum in the adjustments.

Table 19 : Table constants used in the different models presented in chapter 1

Modelisation method	Constant	Experiment
Mathematical method	Yield stress τ_0	Rheometer [2] YODEL [3]
	Maximum yield stress	Rheometer [2]
	Initial void ratio e_0	Liquid volume fraction measurements
	Minimum void ratio e_{min}	Liquid volume fraction coefficient
	Compressibility coefficient C_c	Consolidation test
	Fitting parameters describing τ_0 vs e, a and b.	Can be computed from τ_{0i} and τ_{0max}
	Initial permeability K_0	Permeability test [4]
	Taylor fitting parameter C_k	Permeability test [4]
	Maximum angle of friction φ_{max}	Shear test
	Wall friction/internal friction ratio m	Coal extrusion
Cam-Clay	Elastic modulus κ	Consolidation test
	Shear modulus of the granular media G	Direct shear box Parallel disk rotational rheometer
	Slope of the normal compression line λ	Consolidation test
	Preconsolidation pressure p_0	Consolidation test
	Slope of the critical state line M	Shear test

COMSOL® two phases Euler-Euler	Particle mean diameter	Granulometry
	Material density	Weight and volume of solid particle only
	Liquid density	Simple density measurements
	Maximum packing concentration	Hu and de Larrard [5]
Plastic modelisation	Relation shear stress and shear rate	Rotational two parallel disk rheometer Simple shear box

3.2.2. Tests permitting to study rheology and cement behaviour

This part regroup different methods commonly used in the study of cement rheology, it does not constitute a complete list but the main tests are simply explained so it can be seen what information they can bring. Of course new tests can be designed from existing one it only depends on the scientists imagination and resources. Thanks to the little review done in this part, new tests can be thought more adapted to our case of injection of ceramic bone cement.

3.2.2.1. Void ratio measurements

First of all we recall that void ratio correspond to the ratio of liquid volume to solid volume. It is written as a function of solid volume fraction ϕ_s.

$$e = \frac{1}{\phi_s} - 1 \qquad [3.1]$$

It is possible to simply access void ratio by measuring the solid volume fraction of cement. This is achieved by weighting a sample of cement before and after drying it in an oven. And using the mass solid fraction with the density of cement and interstitial liquid to access solid volume fraction.

3.2.2.2. Particle size distribution

It could be of certain interest to study the particle size distribution in a sample of extrudate, indeed even if solid volume fraction remains the same, we can imagine an easier migration of small particles in the cement during injection , resulting of injection of small particles in a first time and then, injection of bigger ones. We haven't seen such phenomena occurring during injection in literature, however it is of common sense that smaller particles move with more ease than larger one.

In order to access the particle size distribution simple measurements techniques can be used such as ultrasound attenuation spectroscopy which employs ultrasound to collect information on particle dispersed in a fluid. Similarly to laser diffraction methods used for dry granular materials, dispersed particles will absorbed and scatter ultrasound the same way they do it with light. Signal is then recorded and analysed to obtain particle size distribution.

3.2.2.3. Yield stress

Thanks to granulometric measurements we have seen that one can access particle size distribution as well, as mean particle size. This can be used to study extrudate composition or influence of particle size distribution on injectability. Nevertheless knowing perfectly the granulometry of cement particle and information related to its solid volume fraction, one can predict Yield Stress of a particulate suspension. Indeed Flatt [3] proposed an adaptation of YODEL (Yield stress mODEL) to multimodal particle size to predict Yield Stress.

$$\tau_0 \cong \frac{A_0 a^*}{d^2 H^2} f_\sigma^* \frac{\phi^2(\phi - \phi_{perc})}{\phi_{max}(\phi_{max} - \phi)} \qquad [3.2]$$

d is the median cement particle diameter	f_σ^* particle size distribution function equal to 1 for monodisperse system	A_0 Hamaker constant
H minimum separation distance between particles	ϕ_{perc} solid volume fraction, percolation threshold.	a^* radius of curvature of contact point between particles

We will see that Yield stress of cement paste can be accessed by multiple test more or less difficult. It represent one of the most studied parameter in granular system rheology.

3.2.2.4. Maximum packing fraction

In the case of a stable packing of rigid particle it is relatively easy to access the maximum packing volume fraction of particle (usually considered to be of order 0.64 for identical spheres). Nevertheless cement materials particle diameter is polydispersed making the prediction of maximum packing fraction more difficult. Hu and De Larrard proposed a semi-empirical relation which predicts this value (eq.[3.3]) in the case of polydispersed granular system.

$$\phi_{max} = 1 - 0.45\left(\frac{d_{min}}{d_{max}}\right)^{0.19} \quad [3.3]$$

$\boldsymbol{\phi_{max}}$ maximum packing volume fraction	$\boldsymbol{d_{min/max}}$ Minimum and maximum diameter of particles

This value of the maximum packing fraction will be used for the Krieger Model proposed by COMSOL®.

3.2.2.5. Vane geometry rheometer

Vane geometry tests exists under various forms and has grown in popularity for their simple but effective means of measuring properties of very Non-Newtonian fluids. Nevertheless concentrated suspension and granular pastes are the most difficult systems to study with rheometers. Various disturbing effects may develop during tests, such as wall slip, fracture, sedimentation, migration, evaporation, edge effects. Which could lead to serious misinterpretation of rheometrical data. Meaning that even if they appear relatively simple vane geometry tests should be realized with care.

Rheometer vane test can be used to find the yield stress value of cement which is one of the most relevant parameters to study cement injection process. Test are performed in

order to obtain torque-displacement curve at different rotational speed. If the curve are the same it can be assumed that shear stress does not depends on shear rate and that consequently the materials behaviour is mainly plastic.

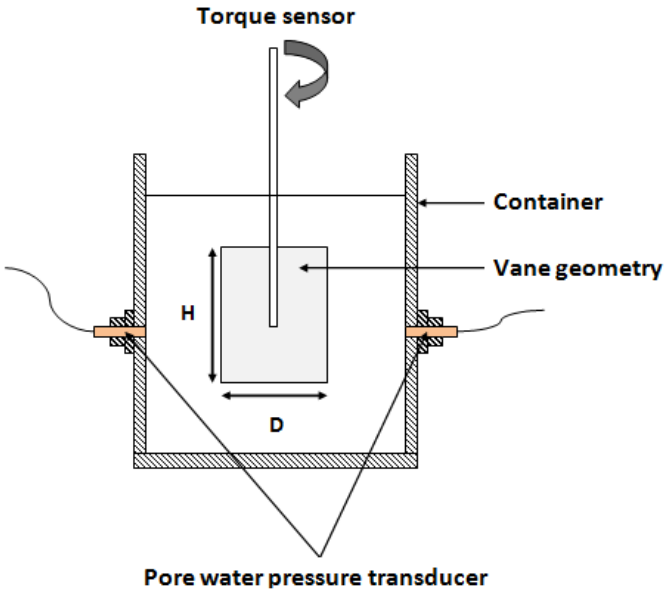

Figure 29: Schematic representation of a vane geometry rheometer

The rheometer geometry consist in a cylindrical container in which cement is placed fig.X. Then a rotating vane of given geometry is introduced in the cement mix and torque is recorded with rotational speed. The yield stress for a 4 bladed vane can be measured thanks to eq.[3.4].

$$\tau_0 = \frac{M}{\frac{\pi D^2}{2}\left(H + \frac{D}{3}\right)} \qquad [3.4]$$

M maximal torque	**H** height of blade	D diameter of blade

Using such test on mixture presenting different water to cement ratio, yield stress can be studied as a function of void ratio. Legrand proposed an empirical relation linking both (eq.[3.5]) where a and b are experimental parameters.

$$\tau_0 = a.exp\left(0.5b\frac{1-e}{1+e}\right) \qquad [3.5]$$

Of course other empirical relations can be found linking for example ageing of fresh cement, mean particle size, or even pH to cement yield stress. It can be interesting to measure the validity of such empirical relation in order to model cement mechanical properties thanks to easier to access parameters.

3.2.2.6. Permeability

We have seen in the description of the mathematical approach to model LPM (chapter II) that cement permeability represents a key parameter in the understanding of hydro-mechanical behaviour of cement during injection.

Two methods to measure evolution of permeability can be used as described in [4], both are based on consolidation kind of test. The aim being to find a relationship between permeability and void ratio that will be used in Darcy's law to quantify flow of water, thus homogeneity of material during injection strongly depends on permeability.

Parameters influencing permeability are particles size distribution, specific surface area or particle packing. Those parameters will influence water adsorption forces or interstitial liquid flow path and velocity.

We will quickly summarized the main idea of the two methods presented in [4], this in order for the reader to understand the philosophy of permeability measurement and make its own choice in his research. Prior to any performed permeability measurements cement should be characterized in terms of particle size distribution, and initial solid volume fraction (or void ratio).

3.2.2.6.1. Filtration test

This relatively simple method is based on percolation and consolidation of cement under a constant hydraulic head. Test is realized using a configuration such as the one represented on fig.30. The main goal of this test is to measure both consolidation under a given pressure, and water flow through the cement under a hydraulic head.

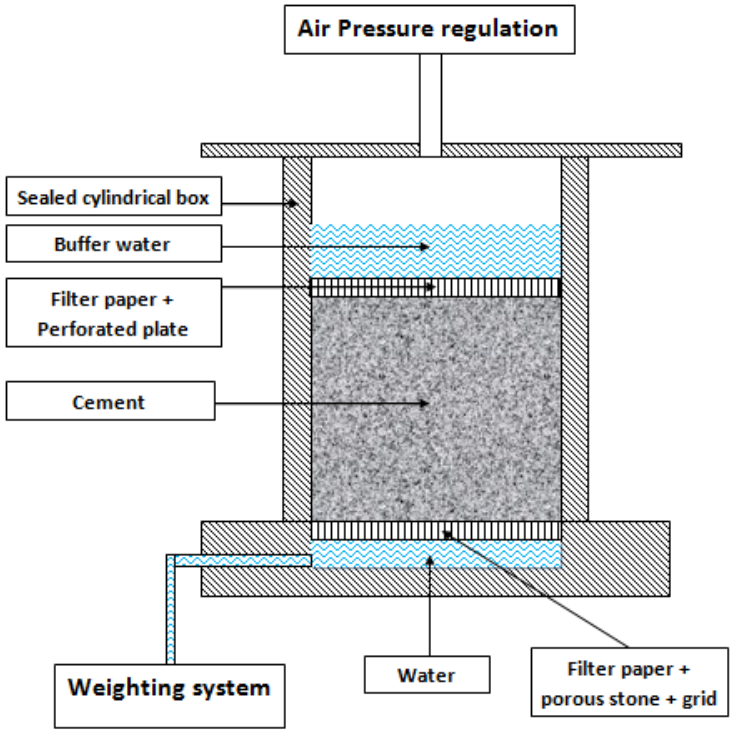

Figure 30: Scheme of the material used to realize simple filtration test.

In a first step pressure is applied via the air pressure regulator located on top, while the outflow of water is blocked by a valve located before the weighting system. Permeability K ($m.s^{-1}$) is deduced from the measured percolating flow rate Q ($m^3.s^{-1}$) through a specimen section S (m^2).

$$\frac{Q}{S} = -K\frac{dH_w}{dz} \qquad [3.6]$$

$\frac{dH_w}{dz}$ Represents the hydraulic gradient

Thus measured parameter will be the evolution over time of percolated water volume. And the kind of curve that should be observed is presented fig.31. Permeability measurements

will be realized on the right part of the curve where the flow of water through the cement paste reach a steady state. And permeability can be measured from the linear part of the curve. The relative decrease of permeability observed during the first minutes of the test is due to the decrease in void ratio induced by consolidation of the cement.

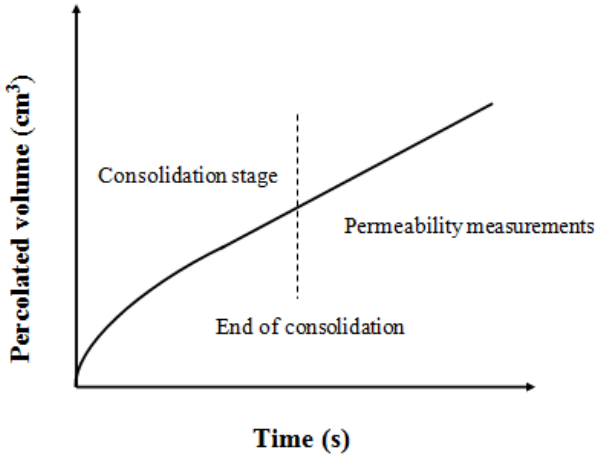

Figure 31: Evolution of the percolated volume of water as a function of time during filtration test.

This kind of curve can be traced for cement having different water to cement mass ration and hence different void ratio according to eq.[3.7] linking the two.

$$e = \frac{W}{C}\frac{\gamma_c}{\gamma_w} \qquad [3.7]$$

(W/C) water to cement mass ratio γ_c Specific unit weight of cement particle (kN.m^{-3})

γ_c Specific unit weight of interstitial liquid at 20^{0}C (kN.m^{-3})

It is then necessary to know the initial W/C ratio and to take into account the settlement of the global height of the sample that will decrease the void ratio e of the tested material. The variation in void ratio Δe is given by eq.[3.8] as a function of the variation in height of the sample.

$$\Delta e = \frac{\Delta h}{h_0}(1 + e_0) \qquad [3.8]$$

Realizing several measurements at different W/C ratio it is possible to determine permeability of the cement as a function of void ratio.

3.2.2.6.2. Controlled Oedometer

In the second test proposed in [4] consist in inducing water percolation (same as before). But it is considered more accurate and many permeability measurements can be obtained from the same fresh cement paste simply changing the compaction state between the different measurements. An oedometer is placed under a compression press as shown on fig.32 thus force and displacement can be obtained as well as pore water pressure. The flow of water will be induced by hydraulic head difference between hydraulic head at top and bottom specimen. And flow of water will occur from the Mariotte bottle to the recipient.

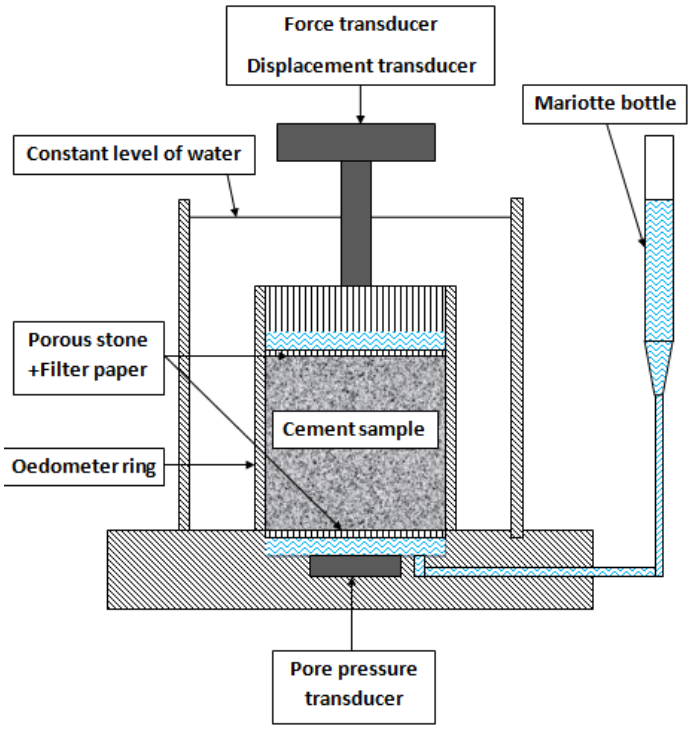

Figure 32: Scheme of the controlled oedometer used to measure fresh cement permeability.

Thus two kind of test stages are performed: classical one dimensional compression test consisting in changing the height of specimen in the oedometer cell. Then the permeability measurement is performed at fixed height, the flow of water is bottom-up, permeability is calculated as before from Darcy's law from the rate of inlet water volume $\Delta V/\Delta t$. And can be written as in eq.[3.9]

$$K = \frac{\Delta V h_i}{\Delta t \, S \Delta H_w} \qquad [3.9]$$

$\boldsymbol{h_i}$: height of speciment during permeability measurement	$\boldsymbol{\Delta H_w}$ Applied hydraulic head, difference between hydraulic head at top and bottom surface of specimen

Thus from these two experiments curves linking permeability to void ratio can be obtained and empirical linear relation can be drawn such as the one used in our model (eq.[2.2])

3.2.2.7. Simple Consolidation test

The time dependent process during which a soil specimen responds to compression is commonly called the process of consolidation. Compression of cement can be conducted either in a consolidometer (oedometer) or in an axial compression cell (usually called triaxial cell). As already mentioned in chapter two, the stress acting on a cementitious paste can be divided in two contributions, being the effective stress (σ') and the excess pore pressure (u).

$$\sigma' = \frac{P_s}{A} = effective\ stress$$

$$u = \frac{P_w}{A} = excess\ pore\ pressure$$

$$\sigma = \sigma' + u = \frac{P}{A} = Total\ applied\ stress$$

The main goal of consolidation test will be to determine the evolution of void ratio at a given stress state. The determination of such will permit to draw a diagram similar to the one presented on fig.X and thus it will be possible to determine λ and κ parameters that are needed for Cam-Clay simulations. For this a sample of cement will be placed in a consolidometer (or equivalent) and will undergoes a series of loading and unloading process. While lost of water and pressure will be recorded in order to link void ratio to pressure state.

The process of consolidation is time dependent, meaning that a certain time is required in order to reach an equilibrium state for the settlement of the piston at a given load.

Loading process

When valve is closed at t=0. We got σ'=0, $u = \sigma = \frac{P}{A}$

When valve is opened we can observe that the water flows out of the cylinder into the reservoir and we got $\sigma' = \sigma - u$

Rate of flow of water will decay with time, and eventually after an infinite time all excess of pore-pressure will have dissipated and the load will be carried by the cement.

At $t = \infty$ we got $\sigma' = \sigma = \frac{P}{A}$, and $u = 0$.

Unloading process

When the total applied stress *P* is removed water is immediately sucked back into the cylinder and the free piston move up. Since the total load is zero the force acting on the free piston and responsible for its movement is "negative"

$$\sigma' = \frac{P}{A}; u = -\sigma'; \sigma = u + \sigma' = 0$$

Water is then sucked from the reservoir into the cylinder and we got a stress state where σ' decrease with time an where pore pressure u increase with time.

And after infinite time the system will reach an equilibrium state where $\sigma' = u = 0$.

From a series of load-increment it is possible to obtain the virgin compression line eq.[1.4] as described in first chapter for Cam-Clay model. And each swelling and recompression line will be described by eq.[1.5]. Thus One-dimensional consolidation permits to access λ and κ parameters by looking at the slope of virgin compression and swelling line. Those parameters were needed for Cam-Clay model simulations in COMSOL®.

3.2.2.8. Squeezing test

Cement behaviour can be investigated using a range of compression tests which are reviewed by Kretser et al. [6]. The approach in compressive rheology are relatively identical, in every cases the cement sample is place between two parallel disks, either both or one plates moves at a given velocity or squeeze the sample under a known applied pressure. The disks can be transparent so we can record LPM phenomena during squeezing if it occurs. A lot of parameters can be derived for this relatively simple kind of test.

Squeezing test is a tool used to identificate rheological behaviour of cement materials in order to evaluate their extrusion ability [7]. It can also picture the rheological behaviour at low compression speed of cement, when they undergoes fluid drainage through the granular skeleton. It appears as a relatively good methods to study cement design and to draw and extrusion criteria based on rheological behaviour of cement.

Squeezing test consist in a compression of a cement cylinder between two coaxial circular and parallel plates fixed on a tensile test machine (see fig.33). The upper disc can be controlled at constant velocity displacement of force while the lower one is kept at its initial position. When compressed the cement presents an essentially radial flow and at low velocity drainage phenomena can be easily observed (drier part near the centre of the discus) and studied (easier sampling of the squeezed material than material undergoing extrusion).

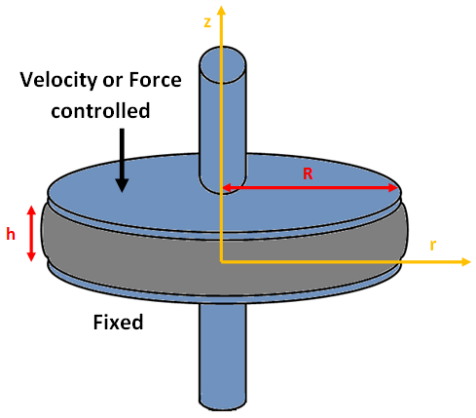

Figure 33: Parallel plate rheometer used for squeezing test.

Then two interpretations of the experimental data can be done. Depending if drainage occurred or not during the squeezing test. When no drainage occurs perfect yield plastic behaviour analytical solutions [8] are used to identify the material plastic yield value. In the case where drainage occurs instantaneously, frictional plastic theory (Coulomb frictional law and Drucker-Prager plastic criterion) [9] is used in order to determine materials yield stress, cohesion, bulk and apparent friction factors.

Squeezing test procedure and data interpretation is described by Toutou et al[4]. [7] and Estellé [10] it permits to ease the design of cement for the study of extrusion ability and represent a relatively low-cost experimental technique since it only requires a simple tensile test machine and adapted circular plates. Moreover coupled to the squeezing test it is possible to compute liquid migration from Darcy's law, material properties and squeezing test setting [11].

3.2.2.9. Rotating disk rheometer

Another test that can be performed using two parallel circular plates is the test of rotational rheometry in which a cement sample is placed between the two plates, and where the shear stress is measured via the torque measurements and angular velocity following eq.[3.11]

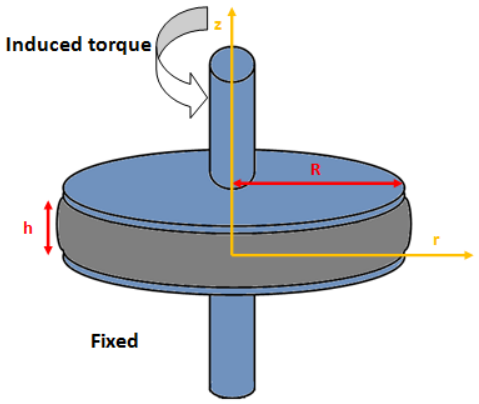

Figure 34: Parallel plate rheometer used for shearing test.

[4] Method described by Toutou is given for particularly firm cement pastes, it could be adapted to more fluidified pastes.

$$\tau = \frac{M}{2\pi R^3}\left(3 + \frac{h\ ln\ M}{h \ln \dot{\gamma}}\right) \quad [3.11]$$

M is the torque **R** is the radius of the plate

$$\dot{\gamma} = \frac{R}{h}\omega \quad [3.12]$$

h is the value of the gap between the two plates $\boldsymbol{\omega}$ is the angular velocity

This would help to obtain the shear stress as a function of the shear rate, thus determine what kind of Non-Newtonian model would fit more the cement behaviour and use it in eventual FEM calculation as it was done in previous UPC PFC [12]

***NB**: Many other kind of rotational rheometer can be used, such as coaxial cylinder, or replacing the upper flat disc by a cone shaped disc. The main idea being to link shear stress to shear rate.*

3.2.2.10. Simple shearing test (ASTM D 3080)

Shear tests are used in order to determine the shear strength, cohesion and internal angle of friction of soils, they can be adapted to cement which present a relatively similar kind of behaviour.

Determination of shear strength parameters are generally obtained from either, direct shear test or Triaxial Shear test (Casagrande shear test). Direct shear test is quick and inexpensive, the test equipment consists in a metal box in which the specimen is placed, this box is split into two halves and normal force is applied at constant rate of displacement while shear force is recorded as it is shown on fig.35.

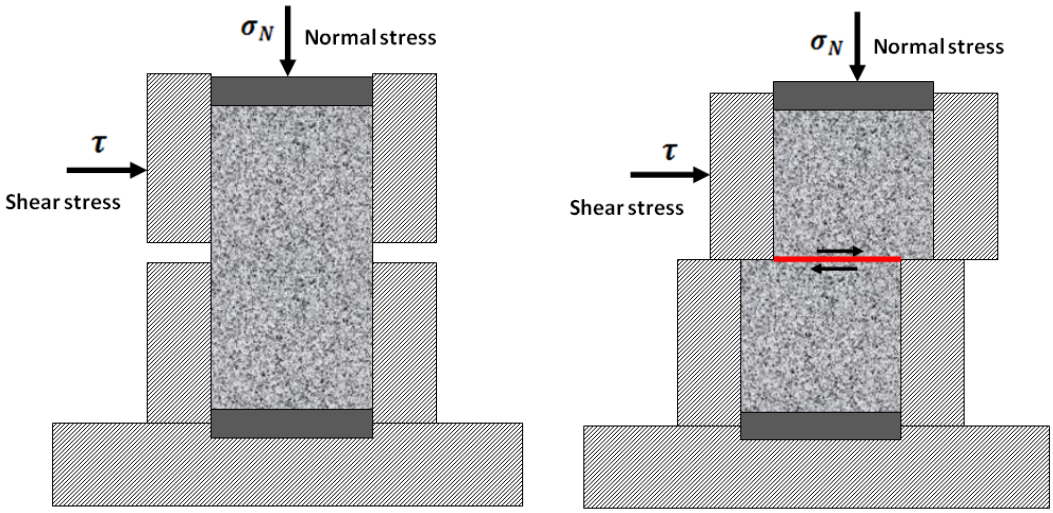

Figure 35: Scheme of the simple shearing test used to study fresh cement paste.

The box can be circular and similar to an oedometer cell, or rectangular, this will influence on the sheared surface area. In order to obtain material parameters such as cohesion, shear strength angle of internal friction or coefficient of friction test are conducted under a given normal force and constant displacement, is recorded the shear stress. The obtain curve should have the same behaviour as on Fig.36.

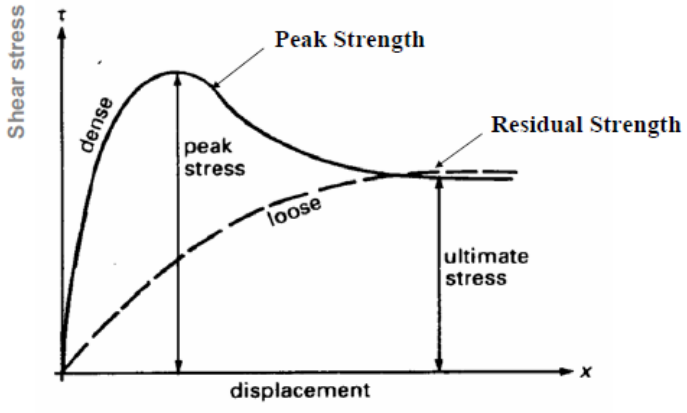

Figure 36: Evolution of the shear stress as a function of lateral displacement during simple shear stress.

If this test is conducted at different normal stress for a same cement composition it is possible to obtain curve such as the one presented on fig.37 simply drawing the shear strength as a function of the normal applied stress.

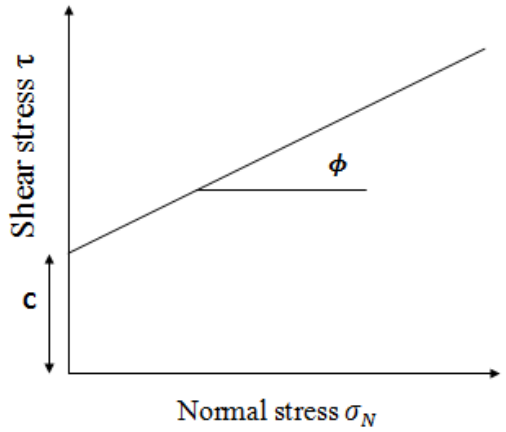

Figure 37: Evolution of the peak shear stress value as a function of normal stress applied.

From this simple curve it is possible to draw a linear relation eq.[3.10] between shear strength and normal stress and to identify parameters C (cohesion), ϕ (angle of internal friction) and μ (coefficient of friction).

$$\tau_f = C + \sigma_n tan\phi = C + \mu\sigma_n \quad [3.10]$$

τ_f: Shear strength	C: Cohesion	$\sigma_n$normal stress
ϕ: angle of internal friction		μ: coefficient of friction

In addition to the fact that several material parameters can be obtained from direct shear test, other material behaviour such as dilatancy can be investigated. In the shear box device, two displacement sensors are placed at both ends of the box to quantify the dilatancy. Then volume change is recorded with displacement, dilatation is observed in the case of dense system, while contraction will be observed in the case of loose system. Thus if large dilatation of the cement under shear is observed, jamming phenomena can more likely appears during injection.

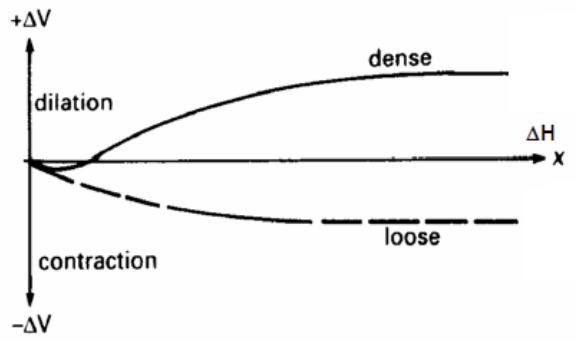

Figure 38: Volume variation recorded as a function of lateral displacement during simple shearing tests.

3.2.2.11. Syringe wall frictional coefficient

We have seen that the wall friction coefficient of the syringe is an important parameter for both jamming and LPM phenomena. Thus wall of the syringe should be smooth and a way to control it is to measure the wall friction coefficient. In order to measure this value a cement sample is placed in the syringe between two ram, the upper one is controlled by a tensile test machine while the lower one is fixed. Force and displacement are recorder on the upper and lower ram.

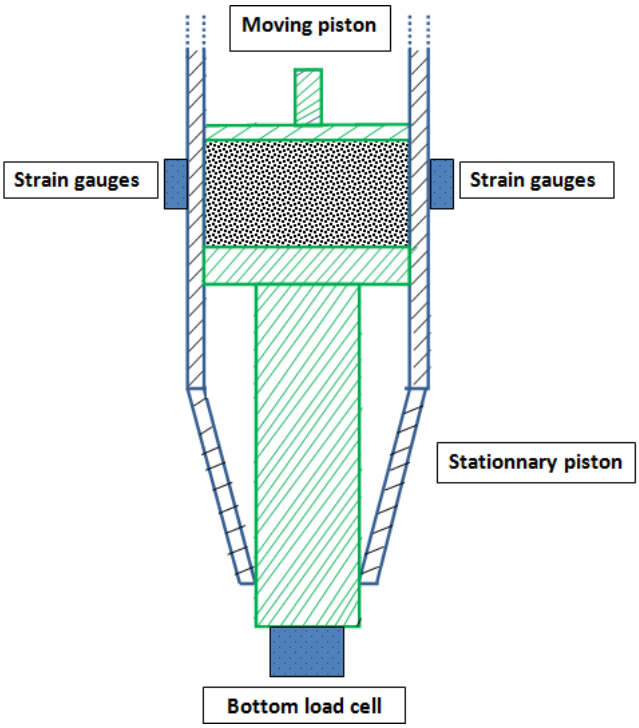

Figure 39: Test used to study wall friction coefficient of the syringe. The syringe is mounted on a tensile test machine the ram is controlled by the machine while the bottom ram is keep fixed.

Relation between the moving-piston pressure P_m and the stationary piston pressure P_s is given by:

$$F_S = F_m \exp\left(-\frac{4m\eta}{d}H\right) \quad [3.13]$$

m radial to axial stress ratio	$\boldsymbol{F_s}$ exerted force on the stationary piston	$\boldsymbol{F_m}$ exerted force on the moving piston
D is the diameter of the plug		**H** length of the compressed plug

Radial-to axial stress ratio can be measured thanks to the strain gauges located on the outside syringe wall, thus radial stress can be obtained as well as axial stress thanks to a load cell located at the bottom fixed piston. Thus radial to axial stress ratio m can be easily calculated.

The contact frictional coefficient η is calculated via eq.[3.14].

$$\eta = -\frac{d}{4mH} ln\left(\frac{F_s}{F_m}\right) \quad [3.14]$$

In the mathematical model developed by Perrot and al. [13] and used in this work. We have seen that the parameter m (ratio between the wall shear stress and the internal shear stress) should be found in order to compute the axial stress distribution along the syringe. It can be measured using the method described in [14] where m is assumed to be equal to:

$$m = \frac{K_W(Barrel\ zone\ wall\ surface)}{K_W(Die\ zone\ wall\ surface)} = \frac{K_{W0}}{\tau_0} \quad [3.15]$$

$\boldsymbol{K_W}$: Wall friction stress	$\boldsymbol{K_{W0}}$: Wall friction yield stress	$\boldsymbol{\tau_0}$: Bulk shear yield stress

3.2.2.12. Critical angle of syringe die

The critical angle can be seen as the angle under which no dead zone appear in the die during injection. It is of prime interest to find an optimum angle where all the cement is in motion and that no dead zones are formed in the die (fig.40). It could be interesting to verify the relation given in [15] for extrusion of hydrated coal through a cone shaped cylindrical die.

$$\theta_c = tan^{-1}\left(\frac{1}{\eta}\right) \qquad [3.16]$$

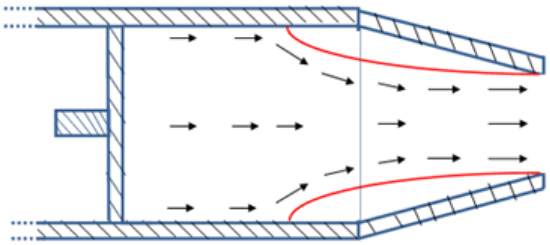

Figure 40: Schematic representation of the formation of dead zone on the wall of syringe die.

3.2.2.13. Visualisation of flow

In the case we fail in obtaining homogeneous and accessible injection of ceramic bone cements. It could be interesting to visualize what occurs in the paste during injection regarding water concentration variation. The problem is that cement is not a transparent materials meaning that we cannot use light and methods such as spectrophotometry to study the different water concentration in the cement during injection. Nevertheless it exists similar methods using different kind of energy beam capable of detecting water variation in a system. For example NMR (Nuclear magnetic resonance) has been used [16] in order to study extrusion behaviour of PTFE pastes. In the same way it is possible to study the injection behaviour of ceramic bone cement and the eventual variations of fluid concentration. And this without affecting the cement nor the syringe. Nevertheless injection process cannot be followed in live due to the special design of equipment that would be required to perform both injection and NMR images.

Another method would be to use Neutron imaging facility to study water concentration of cement during injection. Nevertheless since Neutrons are absorbed by water this experiment should be done on a system such as the canula which present a smaller diameter or on a thin bone sample in which we would inject the cement. Finally Neutron imaging can be used to obtain tomography of the vertebrae before and after cement injection in order to study if the filling process were successful or not. Nevertheless the equipment required to form a Neutron beam having a sufficiently high intensity is big and can be encountered in only several particle accelerator research centre. Hence the reservation of such a beam would cost a lot and they are generally used for industry having a lot of financial resources (fuel cell research, automobile industry), it is particularly appreciated as a non-destructive investigation method to see through metallic materials (which cannot be done using X-Rays). Nevertheless the cost of such experiments would need financial support and great motivations from the industrial community. Both of these options have to be considered if no solutions have been found and that the problems of LPM and jamming persists, ideally the pre-design of cement would permit to obtain the required configuration to access a successful injection in terms of cement homogeneity and injection pressure.

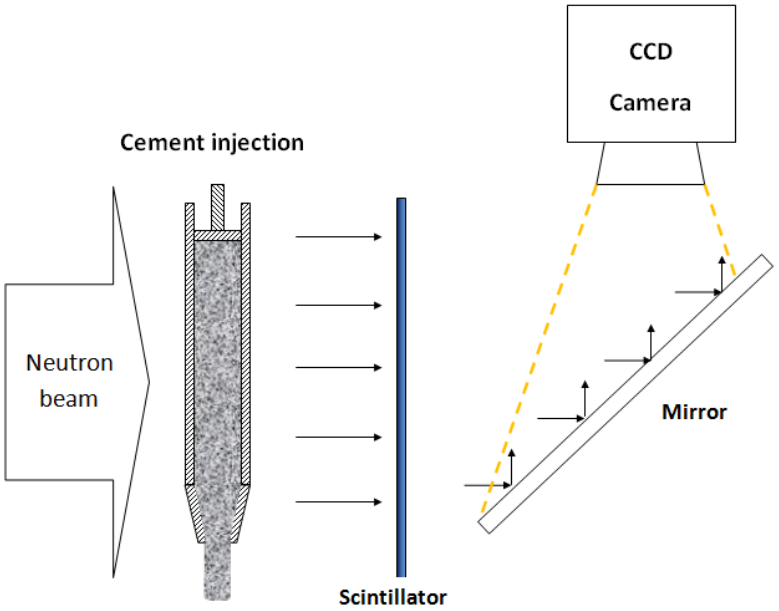

Figure 41: Configuration required to record image from Neutron beam. LPM investigation in canula.

Conclusion characterization methods

We have seen that the number of characterization methods has as limit the imagination of the scientist. Indeed, tests can be declined in many ways in order to study one parameters or phenomena in particular. What seems important to us at this point is to study the different properties of cement such as friction coefficient, yield stress, Non-Newtonian behaviour, and evolution of permeability as well as void ratio under imposed stress. As explained it does not exists an universal method permitting to a scientist to solve the problem of LPM and Jamming during injection of ceramic bone cement. Nevertheless thanks to a deep reflexion and previous literature study it is possible to draw a path to follow that would help to enhance cement injectability without affecting its properties in-vivo.

Aware that the experimentation explanation presented in chapter 3 will not lead the scientist to the direct solution, we hope that it will at least motivate to continue investigation in that field and that it lights up some idea in the readers head for future work.

3.3. Motivated ideas of pattern development.

3.3.1. Ram shape

Since it has been observed that when LPM occurs cement dries near the ram and form an arch on the syringe wall. An idea, to prevent the formation of this arch which increase considerably injection pressure, would be to use a ram having a dome form, it is believed that the dry zone if formed would be located in the dome, and would not influence injection pressure. Similarly recessed shaped ram allowing the dry cement to be formed "in" the ram instead of on the wall would decrease extrusion pressure. This ram design would be responsible for cement loss, indeed using such a shape do not allow the injection of the whole cement. Moreover, in a optimum design of the cement paste and the syringe, LPM is not supposed to occurs making this design obsolete.

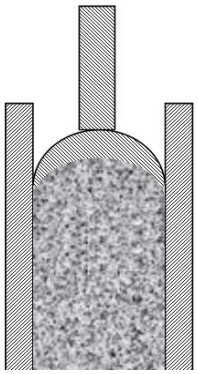

Figure 42: New RAM geometry expected to reduce LPM probability.

3.3.2. Use of ultrasonic waves

Friction and difficulty for cement particles to move in the paste are trusted to be one of the reason for the occurrence of both particle jamming and LPM. Hence the use of ultrasonic wave would reduce interparticle friction by inducing micro-movement at the particle-particle interface, reducing probability for particle to block one on each other. Added to that if particle came to a jammed state, the vibrations produced could unjammed the system in the same way as the vibration you are giving to pour salt or sugar [17].

Nevertheless, this vibration has to be controlled in order not to form particle-rich zone and water rich ones. Also, ultrasonic wave influence on VP and KP (contact of canula

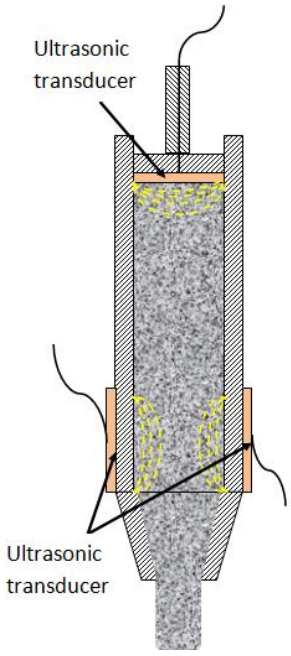

Figure 43: Ultrasound waves system mounted on a syringe to prevent jamming and reduce interparticle friction (hence LPM)

with bone, electric device and syringe complexity) could be prejudicial for the surgery and for the surgeon comfort.

3.3.3. Use of an obstacle in the syringe

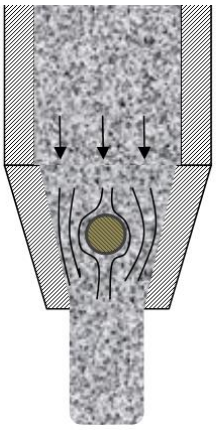

Figure 44: Syringe presenting an obstacle in its die area.

Since the 1960's obstacles has been used before outlet opening of silo in order to enlarge mass flow rate , reduce stresses in the silo as well as mixing and homogenization of the grains. When obstacle is placed at an optimal height it disturb the formation of an arch responsible for jamming. It has been shown that an obstacle placed in an hourglass (similar to the conical shape of our die) can increase flow rate by up to 16% [18]. Indeed an optimized obstacle such as the one presented on fig.44 splits the flow into two less convergent hopper flows.

Bibliography Chapter 3

[1] "Design of ceramic -based cements and putties for bone graft substitution" M.Bohner, European cells and Materials vol20, p1-12, 2010

[2] "Cement-based mixes: Shearing properties and pore pressure", T.Lecompte, A.Perrot, V.Picandet, H. Bellegou, S.Amziane, Cement and concrete reseach, vol 42, p139-147, 2012

[3] "Yield stress of multimodal powder suspension: an extension of the YODEL (Yield stress mODEL), R.J. Flatt, P Bowen, J. Am. Ceram Soc., vol 90, p1038-1044, 2007

[4] "Permeability measurement of fresh cement paste", V.Picandet, D.Rangeard, A.Perrot, T.Lecompte, Cement and Concrete research, vol 41, p330-338, 2011

[5] "The rheology of fresh high performance concrete" C.Hu, F. de Larrard, Cem. Concr. Res, vol 26, p283-294, 1996

[6] "Compressive rheology; an overview", De Kretser, R.G Boger, D.V and Scales P.J, Rheology reviews, p125-165, 2003

[7]"The squeezing test: a tool to identify firm cement-based material's rheological behaviour and evaluate their extrusion ability", Z.Toutout, N. Roussel, C. Lanos, Cement and concrete research 35, p1891-1899, 2005

[8] "Mechanik der plastichen Formänderung von Kristallen", R. Von Mises, Z. Angew. Math. Mech., 1928

[9] "A model for recombining clay aste plastic flow in dies",F.X Mortreuil, C.Lanos, M.Laquerbe XIIIth internationa congress on rheology, vol3, British Society of Rheology, Cambridge, p400-402, 2000

[10] "Méthodes d'analyse inverse des données d'écoulement de compression de fluides complexes homogènes" Patrice Estellé, PhD thesis, INSA Rennes.

[11] "Liquid-solid relative motion during squeeze flow of pastes", J.D Sherwood, J. Non-Newtonian FLuid Mech. vol 104, p1-32, 2002

[12] "Aproximación computacional al estudio de la inyectabilidad de cementos óseos" Solenn Laforgue, PFC-UPC, 2008

[13] "Prediction of extrusion load and liquid phase filtration during ram extrusion of high solid volume fraction pastes", A.Perrot, H.Khelifi, T.Lecompte, D. Rangeard, G. Ausias, Powder Technology 249, p258-268

[14] "Use of ram extruder as a combined rheo-tribometer to study the behaviour of high yield stress fluids at low strain rate". A.Perrot, ,Y. Mélinge, ,D. Rangeard, ,F. Micaelli, P.Estellé, C. Lanos

[15] "Analysis of coal log ram extrusion", Q. Deng, H. Liu, Powder Technology, vol 91, p 31-41, 1997

[16] "Extrusion of pastes with a piston extruder for the determination of the local solid and fluid concentration, the local porosity and saturation and displacement profiles by means of NMR imaging", J. Götz, W. Kreibich, M. Peciar, Rheologica Acta, 41, p 134-143, 2002

[17] "Role of vibrations in the jamming and unjamming of grains discharging from a silo", C. Mankoc, A. Garcimartín, Iker Zuriguel, Diego Maza, Physical review, vol 80, 2009

[18] "Bottlenecks in granular flow: When does an obstacle increase the flow rate in an hour glass?", F.A. Marroquin, S.I Azeezullah, S.A Galindo-Torres, L.M Olsen-Kettle

Cost of the project

The main goal of this part of the report is to make a reflexion on the costs such a project can lead to. This in order for the student to see the financial part of research and to realize that efforts should be done to find motivations to do such research and receive financial support. Meaning that research are not financially supported if they do not represent any interest for governmental authorities or industry.

This project has been realized between the 16th of September and the 18th of February for a period of 5 months of effective work. And 6 Months in the city of Barcelona in the context of an obligatory laboratory work to obtain EEIGM engineering diploma.

The calculus made to estimate the costs of the project are not precise as it should be done if the project was a long term industry financed project for example. In our case the project were not restricted by any initial budget, which does not mean that it was an unrestricted project, but that its form (mostly literature and numerical study) did not imply material costs and the resource used were included in UPC budget (access to online specialized literature).

Costs will be divided in 3 categories:

- Human costs
- Material costs (Specialized literature-Simulation software)
- Material costs (Physical material)

Human costs

A project cannot exist if there is not at least 1 person doing it. And since everyone deserve a salary, the first cost associated with a project are human ones. We will see that human costs can be pretty elevated in such a project.

First of all we should define an hourly salary for every person involved in the project. Considering that I have been paid as an "engineer".

Table 20: Estimation of costs related to salaries.

	Salary per hours of work	Hours of work during the project	Subtotal
Engineer	25€	750	18 750€
Doctoral student	20€	0	0 €
Professor	40€	15	600 €
Technical Personal	15€	3	45 €
		Total	**19 395€**

Material costs (Specialized literature-Simulation software)

Second of all in a project, especially research project, a part of the budget should be dedicated to literature study. Indeed, even if internet has a ridiculous price compared to the price of a project, all the information that can be found on it are not free. In the field of science internet can be seen as a huge library, and as in every library, books, journals, or articles have a price. Access to an article or a journal can be bought for a year, a month, a week or even a day.

In our case the literature study done, has been based on publications in journals, all of them were paying. But other more general information have been gleaned freely on internet.

For information a yearly subscription to a scientific journal costs between 150 and 2000€. Price of a single article range from 30 to 40€.

Since the project we had to treat is cross-disciplinary we can consider that a subscription to at least 10 journals would be necessary, since literature study were pretty important. Considering that around 250 articles have been consulted during this project (giving useful or not information). It seems irresponsible to buy articles of interest one by one.

In this sense research team associated to a big university have a certain advantage since the subscription to most of the scientific (and other) journals is included in the global budget of the university. In our case we will consider that a yearly subscription to 10 journals were necessary in order to have a relevant literature study.

We can estimate the price of a complete literature study to 10 times the price of one subscription that we can estimate to 8000€. Of course when a team is working in an area there is several searcher and subscription cost can be split between at least 6 persons. Also, many laboratories depends on university institution which generally buy a global licence to access all (or nearly all) the biggest scientific publication editors. It is more difficult for a company for example that wants do develop a new technology and needs a literature study. In that case Journals should be chosen with care.

Other materials costs that should be considered in such a project are related to the software licences. For this project we used three software being , COMSOL®, Matlab®, and Microsoft works student version.

Table 21 : Estimation of costs related to software

COMSOL®	**Matlab®**	**Microsoft office**	Total
8000 €	500 €	139 €	8639 €

Nevertheless, we cannot consider all these costs to be for one person only that would be irrelevant. Generally the most expensive software are installed on a workstation accessible by all the member of the team by remote desktop. Permitting to pay the price for only one licence.

Material costs (Physical material)

Due to the fact that our research work have been done using only computer and software the list of physical material is pretty restricted and includes only computers, notebook and pencils.

Table 22 : Estimation of costs related to material used

	Quantity	Price	Subtotal
Workstation	1	1300€	1300€
Computer ASUS	1	910€	910€
Notebook	1	2,5€	2,5€
Pencil	3	0,50€	1,50€
Paper costs	5	0,05€	0,25€
Thesis impression	1	130€	130€
		Total	2344.25

Nevertheless, in chapter 3 we explained several tests that have to be realized in laboratory. If we consider that a complete study should be realized in this field, subvention for a Doctoral Thesis should be found for a period of 3 years of work. This could be included in the research team budget or supported financially by a company interested in the answers that can be found. Of course, the realisation of such a Thesis would involve more physical material costs, such as the cement, testing machine, syringe, mixer, paper... as well as a subscription to a Matlab® or COMSOL® for at least a year to run the simulations.

Thus the need to define clearly the experiment that should be realized in a plan of experiment. Nevertheless it seems impossible to clearly define a budget at the beginning of a doctoral thesis since the obtained results or reflexions will make it evolves in time. Constraining the doctoral student or allowing him/her to realize more test.

Total costs of the project

Considering this project would have been realized by a paid engineer working in a team of about 10 searcher working in an university we could draw a table summarizing the price of the project such as:

Table 22 : Estimation of the total cost of the project

Type of cost	What they include	Price
Human costs	Regrouping salary of the personal involved in this project	19 395€
Specialized literature and simulation software	Considering that the subscription to specialized journal and licence for COMSOL cost are divided between the 10 members of the team but that MATLAB and office one are personal.	1439€
Material costs	Considering that every piece of material have been paid by UPC.	2344.25€
	Total	23178.25€

We can see that even a small 6 months project could lead to high costs for the laboratory**.** Nevertheless in our simulations I have been considered as a paid employee (18750€) and I include the material I used as paid by the university (laptop, papers) . The costs of my project itself is then lowered comparing to the one obtained here.

Environmental impact

Apart from the impression of 5 pages of administrative document and the impression of the thesis itself, the environmental impact produced by those 6 months of work in Barcelona are only related to the electricity consumption of the office light, my computer and air conditioning during the first month of work. Otherwise I choose to live at a reasonable distance of the university allowing me to come every day walking instead of taking the metro. In other word the impact of this work on the ecosystem is the same as a normal human living in a west European country. I can't see any solution to make this project more "eco-friendly" than it is already.

Conclusion

In this work we have been asked to study the different parameters influencing liquid phase migration and jamming phenomena occurring during the cement injection phase of Vertebroplasty and Kyphoplasty by mean of FEA analysis. The initial idea were to consider cement as a two phases (solid/liquid) granular material. The interrogation we had concerned the influence of the particle size, the syringe design and the injection velocity on injection of cement. All this interrogation have been answered partially or totally thanks to a preliminar literature study on the phenomenon of LPM and Jamming. Nevertheless, this same literature study give rise to other interrogations and thought on how to control those undesired phenomenon.

In an effort to push reflexion forward, we tried to understand, and build two models never used before for injection of ceramic bone cement. The first one is being a mathematical description of LPM phenomena occurring in the plug zone, based on a previous work proposed by Perrot et al. we tried to propose a solution to the apparent problem noticed in his work (No higher water content forward the plug). For this we used a QUICK scheme to model the "flow" of void in the syringe during injection. The second model used Euler-Euler Two phases laminar flow module proposed by COMSOL®, we choose to understand and work with this model because it corresponded to the initial idea of modelling cement as a particle/fluid granular media. Nevertheless, studying literature on the subject we have seen that this idealisation were maybe a little bit too simple to be accurate. Thus we choose to describe more in detail the theory used by COMSOL® and to understand more in depth the physic behind this user friendly designed module. Indeed it is believed that even if not capturing all the complexity of ceramic bone cement injection such method of modelisation can picture complex phenomena occurring in the die land where cement is plastically deformed and is more subjected to jamming due to the contraction of the die.

Nevertheless due to a lack of time and a desire to build this thesis in a useful way for future work, no interpretable or physically relevant results have been obtained for both of those methods of simulations. It has been decided not to present them in this work since they were incomplete.

In order motivate future investigation in this field we choose to dedicate the third chapter to the design of experiment and existing test that could be used to characterize cement injectability. It should be used as a source of ideas, to innovate and propose solution to the problems encountered during injection of ceramic bone cement in vertebrae.

Finally, a small reflection on the costs of such a project and on any kind of research project have been realized in order to realize that one of the most difficult part of scientific work is to motivate industrial or public authorities to invest in your work and help you to realize investigations.

The construction of this project correspond to a tree starting from a very general problem, we tried to summarize the knowledge in that field in a very wide way, then we tried to propose solutions or ameliorations in order to push the reflexion forward, and finally we choose to present the possibilities offered for future work in that field as a source of ideas and motivation for the reader.